UNIVERSITY OF OKLAHOMA

GRADUATE COLLEGE

DESIGN OF PRECAST POST-TENSIONED SLABS USING LIGHTWEIGHT CONCRETE FOR RESIDENTIAL FOUNDATIONS

A THESIS

SUBMITTED TO THE GRADUATE FACULTY

in partial fulfillment of the requirements for the

Degree of

MASTER OF SCIENCE

By

BRUNO NICOLAS SIRI

Norman, Oklahoma

2024

DESIGN OF PRECAST POST-TENSIONED SLABS USING LIGHTWEIGHT CONCRETE FOR RESIDENTIAL FOUNDATIONS

A THESIS APPROVED FOR THE SCHOOL OF CIVIL ENGINEERING AND ENVIRONMENTAL SCIENCE

BY THE COMMITTEE CONSISTING OF

Dr. Royce W. Floyd, Chair

Dr. P. Scott Harvey

Dr. Jeffery S. Volz

Acknowledgments

There are many people without whom this project would not have been possible. First, I would like to extend my deepest gratitude to my advisor and professor, Dr. Royce W. Floyd, whose support throughout the last year and half in this research has been invaluable. His willingness to answer every single one of my questions, no matter how unreasonable or unintelligent these might have been, has been instrumental in shaping my knowledge as a researcher and engineer. I would also like to express my gratitude to my committee members, Dr. Jeffery S. Volz and Dr. P. Scott Harvey. They took the time to review my research and attended my defense, providing me with valuable feedback on my submissions.

Second, I would like to express my deep appreciation towards Lance Windel, who has been an instrumental figure in helping me achieve this significant milestone. Throughout my research journey, and college career, Lance has been a constant source of support and motivation, always pushing me to strive for excellence. His unwavering trust in my abilities and his eagerness to see me grow and expand my knowledge has been a driving force behind my success.

Third, I need to thank John Bullock, Fears Lab manager, without whose help this project would not have been accomplished on time. His constant encouragement and motivation to get the job done were instrumental in pushing me towards the finish line. Although I still struggle to measure twice and cut once, and my cuts are often an inch too short or too long, John's guidance has made me a little better.

Fourth, this journey would not have been the same without the support and help of my lab mates that after long hours in the lab I am happy to call now, friends. I want to extend a special thank you to Omar Yadak, Cade Harris, Mutjaba Ahmadi, Jake Choate, and Courtney Dawson for taking the time out of their busy schedules to assist me and answer my doubts.

It is important to acknowledge the help and support provided by my family, even though they were located over 5,400 miles away. They were always a phone call away to listen to me, calm me down and offer me their guidance.

Last but certainly not least, I would like to extend a special thanks to all the sponsors who made this project possible; Daron Brown and David Perez from Arcosa Aggregates, Dan Mayen from Dolese Bros. Co., Matthew R. Barlow from Post-Tension Services (PTS) of Oklahoma, and Teresa, Carlos, Cherish, Denton, and Natalia from The House Factory.

Abstract

The use of precast concrete in construction is highly favored due to its many benefits, including improved quality control, reduced construction time, increased durability, and sustainability. In Oklahoma, post-tensioned slabs are commonly utilized in construction projects due to their resilience and capacity to withstand expansive soil movement. Nevertheless, when it comes to residential foundations, precast post-tensioned concrete slabs may present some limitations, such as challenges related to their transportation and installation due to their weight.

The use of lightweight concrete (LWC) for precast slabs and structural elements has become increasingly popular due to its lower concrete density resulting from use of lightweight aggregates. This not only makes transportation and installation more manageable but also enhances insulation. However, the use of lightweight concrete may result in reduced tension and shear strength, which could be addressed by incorporating post-tensioning. This research was conducted to identify the key factor in designing and producing a precast post-tensioned slab using LWC. The goal was to create a slab that can be manufactured off-site, transported to the job site with the first-floor structure already constructed, and positioned using a crane for lifting and a leveling mechanism for attachment to the foundation on site. This study consisted of four phases; the first phase involved reviewing previous research conducted on precast post-tensioned slabs made with LWC. In the second phase, a LWC mix was developed that could be used for the precast post-tensioned slabs cast in this project. The third phase focused on designing the

slab using various methods and software. Finally, in the fourth and last phase of the research project tests were carried out on medium and large-scale specimens of the slab design developed in Phase 3, using the mix developed in Phase 2.

Valuable insights were gained from the research study results. First, it was confirmed that the final mix design developed during the study was feasible, performed as intended, and yielded positive results. Secondly, it was noted that while design software can be used to design structural elements, it is important to double-check reinforcement details for the sake of construction. Third, a preliminary design for precast post-tensioned slabs was carried out, and the medium specimen responded as expected without showing any cracks or excessive deflections, indicating the feasibility of this structural element. Finally, inadequate rigging led to inconclusive results for the large-scale specimen.

Table of Contents

List of Figures

List of Tables

Chapter 1: Introduction

1.1 Background

Precast concrete has been popular for decades as a construction technique due to the advantages it possesses. Some of these advantages are better quality control, reduced construction time, and greater durability, as well as being a more sustainable and environmentally friendly construction method (Gomez et al., 2017). Precast concrete slabs have been used in a variety of construction projects (Graybeal, 2006). In Oklahoma, traditional reinforced concrete slabs on grade are used for residential foundations frequently crack because of expansive soil movement. Post-tensioned slabs are reinforced with high-strength steel cables that are tensioned after the concrete is poured and cured. This process puts the concrete under an initial precompression making the slabs stronger and more durable, allowing them to withstand the forces caused by soil movement. As a result, post-tensioned slabs have become a popular choice for construction projects in Oklahoma, especially in areas where soil conditions are a concern (Phang et al., 2014). However, the use of precast post-tensioned concrete slabs for residential foundations has been limited by several issues, such as their weight, which can make transportation and installation difficult.

To overcome this challenge, there has been significant interest in using lightweight concrete (LWC) in precast slabs (Naaman, 2002), as well as in a broad selection of structural elements, such as, double T beams, and bridge girders. LWC is a type of concrete that incorporates lightweight aggregates (LWA), such as expanded shale, clay,

and slate, to reduce the density of the concrete. LWA is a type of aggregate that undergoes a manufacturing process. Initially, the raw material is mined or quarried and then crushed. The crushed material is then fed into a rotary kiln where it is heated up to temperatures of about 2200°F. As a result of the heat, the material turns into liquid and carbonaceous compounds form gas bubbles that expand the material and leave a porous structure in the finished product. Once the aggregate has cooled down, it can be resized, reshaped, and shipped to distribution plants (US EPA, 1993).

This approach offers several advantages, such as reduced structural loads, easier transportation and installation, and improved thermal insulation. However, a downside of this approach is the tension and shear strength reduction.

1.2 Purpose & Goal of This Research

This specific research was conducted to identify the key design and production considerations for developing a post-tensioned precast slab using LWC that can be manufactured off-site, transported to the job site, and positioned using a crane for lifting and a leveling mechanism for attachment to the foundation on site (Gannon et al., 2000). It also examined how these considerations will impact the slab's structural integrity. The slab is intended to serve as foundation for a two-story townhome. The slab is intended to carry the first-floor module, including the finishes and walls for the first floor of a townhome unit, which will be constructed on the factory and transported with the slab to the site. The complete townhome unit will be a two-story residential structure with the

precast slab intended to be used to transport the completed first floor to the site and be placed on a pre-built foundation.

This study will close the gap identified in the literature review on the production of precast post-tensioned slabs using LWC, that can be attached to pier foundations through the utilization of individual supports.

To identify the key design and production considerations the research examined the following hypotheses.

i. LWC using aggregates available in Oklahoma can be formulated to meet the compressive strength, tension strength, modulus of elasticity, and density requirements for precast post-tensioned slabs.
ii. It is possible to design an approximately 500 ft^2 precast post-tensioned slab using LWC to keep the slab's weight under the limit for truck transportation.
iii. Precast post-tensioned slabs cast in a factory are a more efficient alternative compared to slabs poured on-site.

The purpose of this research was to create a two-way precast post-tensioned slab using LWC that can be transported from the factory to a construction site while remaining under the weight allowed for truck loads (Ahmad et al., 2008). Furthermore, this study proposes various designs and alternatives for two-way slabs to withstand the stresses of lifting and transporting as well as service loads. Finally, the selected designs were analyzed for all loading stages (lifting, transport, and service). To achieve all these steps a series of the following objectives were pursued.

i. Analyze and design a precast post-tensioned two-way slab using LWC.

ii. Develop a mix design using LWC able to meet the requirements for precast post-tensioned elements.

iii. Experimentally evaluate the performance of the slab design during casting, under lifting and transportation loads, and under service loads.

iv. Compare the quality and determine advantages and disadvantages of using precast post-tensioned slabs compared to traditional on-site pouring.

By achieving the proposed objectives and testing the hypotheses of this study, significant improvements could be made. These being the enhancement of the construction process for precast post-tensioned two-way slabs in residential construction. The use of LWC in precast post-tensioned slabs offers a promising alternative to traditional on-site pouring methods.

Chapter 2: Literature Review

Over the years, significant research has been conducted on the use of precast post-tensioned slabs made of LWC, with numerous studies investigating various aspects such as structural behavior, design methods, and material properties.

2.1 Lightweight Concrete

The first use of LWC dates back over 2000 years and it has been used in numerous structures. This type of concrete is specifically engineered to have a lower density than traditional concrete. It achieves this reduced weight by incorporating lightweight aggregates or other lightweight materials while maintaining the essential properties and characteristics of conventional concrete (Ahmad et al., 2008). The aggregates used in LWC can be lightweight coarse aggregates made up of materials like expanded shale, clay or slate, or lightweight fine aggregates made from the same materials. These aggregates have a low particle relative density because of their cellular pore system. Therefore, pockets of air are allowed to remain in the composition of the structure and thus, reduce its weight (ACI 213r-14). The possibility of reducing the weight of concrete structures is one of the main reasons for its use.

This cellular pore system results in a high absorption capacity of the aggregate compared to normal weight coarse aggregate. If the LWA is not presoaked, this would result in water being absorbed from the mix during mixing, an incorrect water-cement ratio, and consequently a different strength results from what was expected. On the other

hand, prewetted lightweight aggregate (PLWA) is effective in aiding concrete hydration during the 7-day to 28-day period due to internal curing provided by the water stored in the cellular pore system and drawn-out during cement hydration. This would also contribute to a delay in the growth of compressive strength, while at the same time reducing shrinkage due to the internal curing (Wang et al., 2017).

Thienel et al. (2020) drew on 25 years of practical and theoretical experience to address challenges in designing LWC, emphasizing the need to adapt design, production, and execution rules distinct from normal weight concrete (NWC). Despite this article being written in Europe it provides a detailed approach to the basics of LWC as well as different mix designs, and shows interesting information on how the internal curing of LWC, might affect its strength compared to NWC.

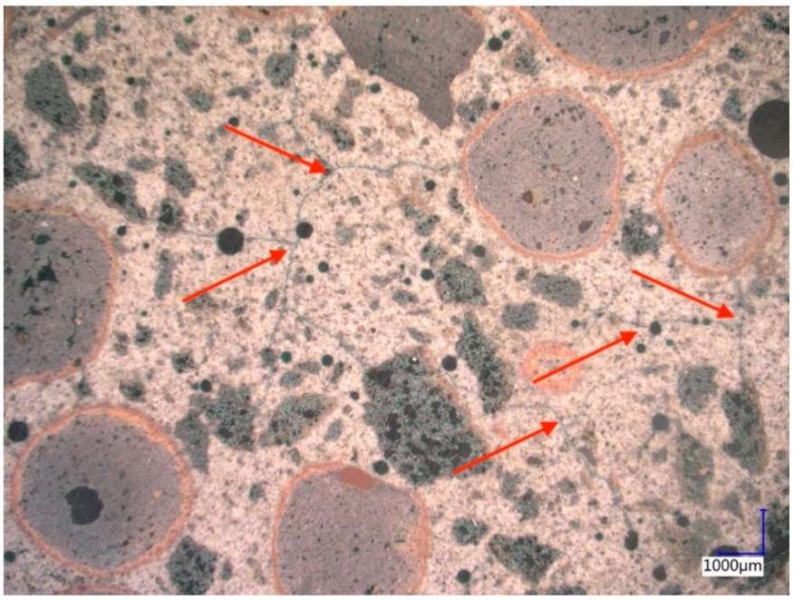

Figure 1 - Severe formation of microcracks in the matrix (marked with red arrows) of a high strength LWC due to water absorption of fine and coarse LWA. Source: Thienel et al. (2020).

Figure 1, from Thienel et al. (2020), shows how micro cracks are formed inside the matrix after hardening due to the high levels of absorption of lightweight aggregates, both fine and coarse. Microcracks can contribute to improved thermal insulation and reduced weight of concrete but may have detrimental effects. Gao et al. (2002) conducted a study on the performance of these microcracks and the microstructure of high-performance LWC. Their conclusions focused more on the negative aspects of these cracks in the cement interface. One of the drawbacks is related to the service life of concrete when exposed to freeze-thaw cycles. Moisture can collect in some of these microcracks, which may freeze and expand at low temperatures. As a result, the service life of the concrete is shortened (Gao et al., 2002).

Additionally, Thienel et al. (2020) provided valuable information on how the aggregates affect the strength of the concrete, since LWAs tend to be weaker in strength than normal weight aggregates. Therefore, it becomes necessary to significantly boost the strength of the concrete matrix for further strength improvement. When dealing with LWC, there is a practical limit to increase the strength since LWAs strength controls at certain limit. Increasing the matrix strength is not always economically viable and it is more practical to opt for a stronger lightweight aggregate instead (Thienel et al., 2020).

Lightweight self-consolidating concrete (LWSCC) is a LWC that can consolidate under its own weight, which is beneficial for precast concrete applications. Wendling et al. (2018) studied and compared the creep and shrinkage behavior, as well as the

prestress losses for LWSCC and normal weight self-consolidating concrete (SCC). Figure 2 shows the two different concretes' strengths at different testing ages up to 275 days.

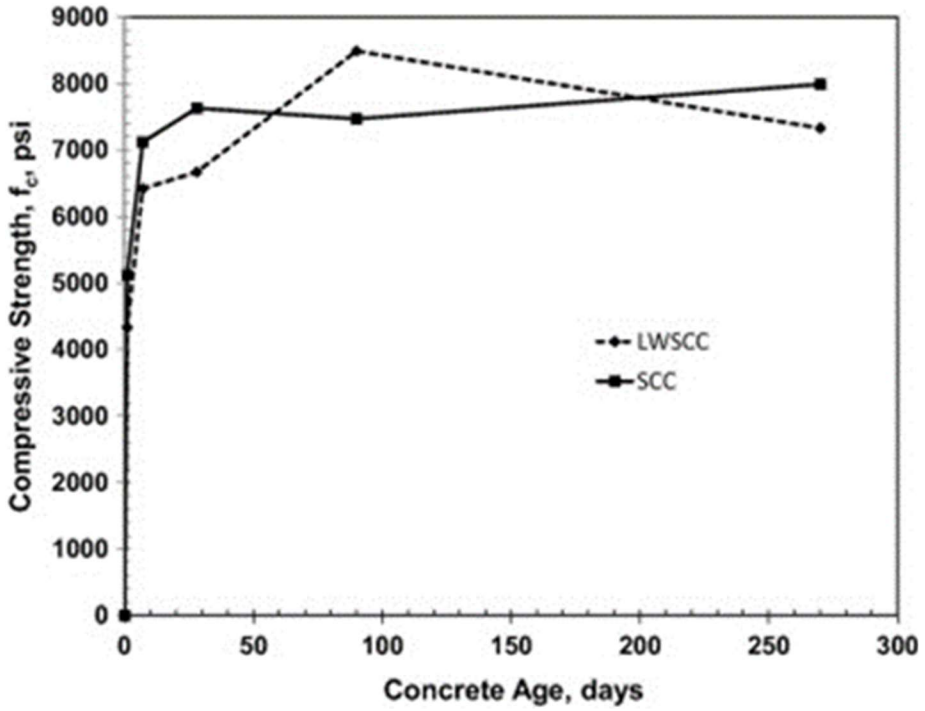

Figure 2 - Compressive Strength at Different Testing Ages. Source: Wendling et al. (2018).

This study investigated how the use of lightweight aggregates in SCC affects creep and shrinkage behavior. The findings revealed that SCC had higher compressive strength and elastic modulus compared to LWSCC. LWSCC initially expanded and exhibited slower shrinkage over time, resulting in less overall shrinkage when measured from the time of casting. However, when measurements began one day after casting, LWSCC showed 50% more final shrinkage than conventional SCC (Wendling et al., 2018).

In terms of creep behavior, LWSCC showed slightly higher creep strain than SCC for specimens loaded after one day and significantly more creep for specimens loaded after 28 days. The one-year creep coefficient was lower for LWSCC when loaded after one

day but similar when loaded after 28 days. Measured prestress losses were greater than predicted values, suggesting the potential need for modifications to account for creep and shrinkage in SCC and LWSCC (Wendling et al., 2018).

2.2 LWC in Structures

LWC is an efficient solution for structural elements where weight is a concern and multiple studies have been conducted on this topic. Szydłowski and Mieszcak (2017) focused on the application of lightweight aggregate concrete (LWAC) in the construction of post-tensioned long-span slabs. They tested in two full-scale long-span slab specimens in the elastic range using a uniform load. They identified the benefits of using LWAC in concrete structures, including reduced weight, improved thermal insulation, and lower transportation costs (Szydłowski et al., 2017). Table 1 shows the cross-section bending moment and concrete stresses at mid-span due to the prestress.

Table 1 - Middle-span cross-section bending moment and concrete stress values. Source: Szydłowski et al. (2017).

	M [kN-m]		Prestress force – P [kN]	Prestress eccentricity – e [mm]	Stress σ [Mpa]	
	Self-weight	Prestressing			Top layer	Bottom layer
Conventional Concrete	51.1	-42.6	840	70	2.6	4.1
Lightweight concrete	34.0	-42.3	832	70	-3.1	9.7

The load test results showed that the LWAC slabs had high load-carrying capacity and stiffness and that the use of post-tensioning in the slabs contributed to their overall strength and durability (Szydłowski et al., 2017). Another article by the same authors presents a study on the properties of LWAC containing sintered fly ash. The study focused on the evaluation of shrinkage, creep, and prestress losses in concrete, with the objective of evaluating its behavior for use in post-tensioned concrete structures. In this study, Szydłowski also mentioned a very important characteristic of LWC. In NWC, the weakest point is the interface zone between the aggregate and cement matrix. Stress concentration in this zone causes cracking due to the difference in modulus of elasticity. LWAC has a more similar modulus of elasticity, between cement paste and aggregates, resulting in less stress concentration and cracking, as shown in Figure 3 (Szydłowski et al., 2021).

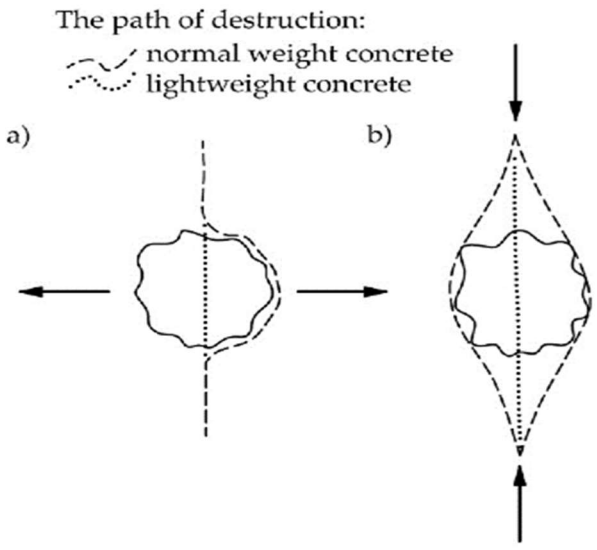

Figure 3 - Scheme of destruction of lightweight and normal weight concrete in (a) tension and (b) splitting. Source: Szydłowski et al. (2021).

The experimental results showed that the use of sintered fly ash in LWAC had a significant effect on concrete shrinkage, creep, and prestress losses. The study revealed that as the proportion of sintered fly ash increased, concrete shrinkage and creep decreased, while prestress losses also were reduced (Szydłowski et al., 2021).

Furthermore, another structural element where LWC can be used is composite slabs. Skrupien (2019) investigated the use of precast, pre-tensioned concrete planks in combination with LWC to create composite slabs, as shown in Figure 4. This construction technique results in high load-carrying capacity and stiffness (Skrupien, 2019). The study objective was to determine the suitability of the composite slab in building construction by assessing its structural behavior, mechanical properties, and durability. The composite slab was made by casting a LWC layer on top of precast, pre-tensioned concrete planks. The LWC used in the study incorporated expanded clay aggregates and had a density of 1500 kg/m^3 (around 93 lb/ft^3). The precast concrete planks were 30 cm wide with two prestressing strands and an initial prestressing force applied to the cross section of 275 kN. Skrupien suggests that the precast composite slab made of pre-tensioned concrete planks, as shown in Figure 4, and LWC is a viable option for building construction, offering

benefits over traditional concrete slabs like speed of construction and quality control of the precast planks (Skrupien 2019).

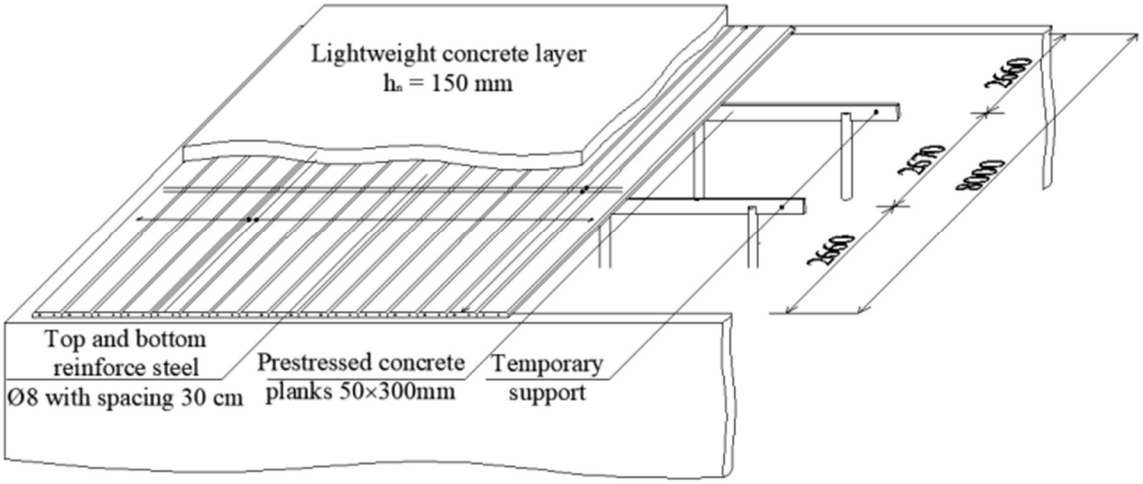

Figure 4 - Precast composite slab with prestress concrete planks studied by Skrupien (2019).

The author of the study concluded that the construction method, which involves using a semi-prefabricated solid light slab, could be a viable and effective alternative to existing methods. The results of the study showed that their design met the deflection limit, and no cracking was observed in any of the planks. In the context of using lightweight materials in this construction technique, Skrupien (2019) identified several benefits:

- Geometric reduction of the cross-section.
- Increased span length of the structure.
- Good resistance to fatigue and dynamic loads.
- The possibility of increasing the imposed loads.
- Better thermal insulation.

Yang et al. (2013) investigated the flexural behavior of post-tensioned normal-strength lightweight concrete (NSLWC) one-way slabs. The authors highlight this concrete mix as an increasingly popular construction material thanks to its low density and high strength-to-weight ratio, making it easier to handle and transport while reducing structural loads. The experimental study utilized six post-tensioned NSLWC one-way slab specimens, each measuring 1200mm x 1200mm x 100mm (4 ft x 4 ft x 4 in.). These specimens were designed with varying post-tensioning forces and reinforcement ratios. The flexural behavior of the slabs was evaluated using mid-span deflection measurements and cracking patterns. The specimens were tested under a symmetrical top one-point loading and a symmetrical top two-point loading, according to Yang et al., (2013).

The study concluded that post-tensioning significantly improved the flexural behavior of the NSLWC one-way slabs compared to the design values, reducing deflection and delaying the onset of cracking. Additionally, the amount of post-tensioning force and the reinforcement ratio affected the behavior of the slabs, with higher levels of each resulting in increased stiffness and reduced deflection. Interestingly, the study found that the use of NSLWC did not significantly affect the flexural behavior of the post-tensioned slabs. This result indicates that NSLWC can be a viable alternative to conventional concrete in post-tensioned one-way slab systems (Yang et al., 2013).

Furthermore, research done by Moldovan et al. (2018) focus on two-way post-tensioned concrete waffle slabs. This study was key to evaluate the possibility of designing waffle slabs as opposed to flat plates, reducing the structure's weight even more.

Moldovan et al. (2018) found in their research that having concrete ribs in two orthogonal directions help reducing torsion inside the structural element. This is a reason why the study focused on two-way post-tensioned waffle slabs. In their design, the post-tensioned cables were found in these concrete ribs as indicated in Figure 5.

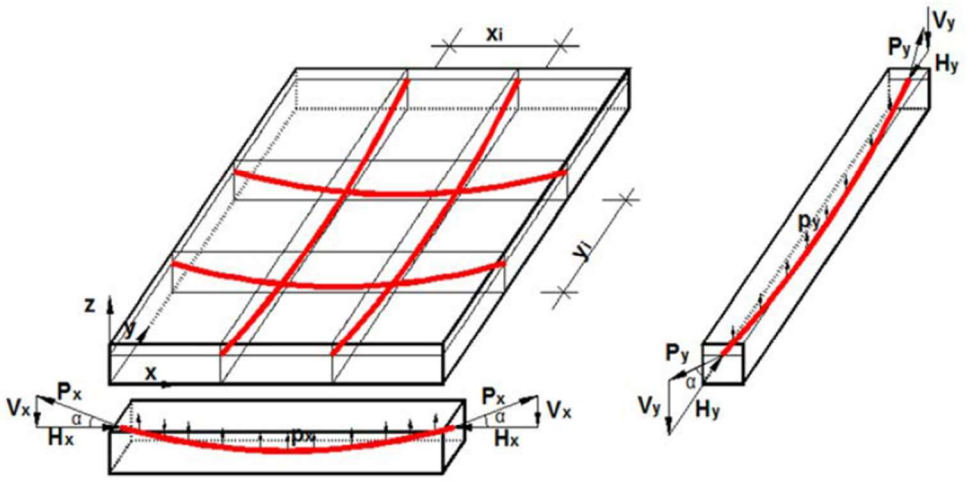

Figure 5 - Post-tensioned cables in ribs and moment diagrams indicated by Moldovan et al. (2018).

Also, Figure 5 shows how the border elements act like simply supported beams because, as Moldovan et al. (2018) explained in their research, the slab is only supported in the corners as analyzed. Moreover, it is possible to see in the figure the individual deflection of each strip and, how the two-way slab deflects acting as a "bowl". This research also provided significant insight into how to build the inserts in the formwork. The study utilized concrete-made inserts which are great for preventing shrinkage or expansion of concrete, making its extraction a concern.

Furthermore, Moldovan et al. (2018) described how the tendons were stressed following a particular sequence. This would allow distribution of the precompression

uniformly across the slab, control cracking, and minimize the deflection that the slab is put under during the pre-stressing process. Figure 6 shows the sequence in which the tendons were stressed in the research by Moldovan et al. (2018).

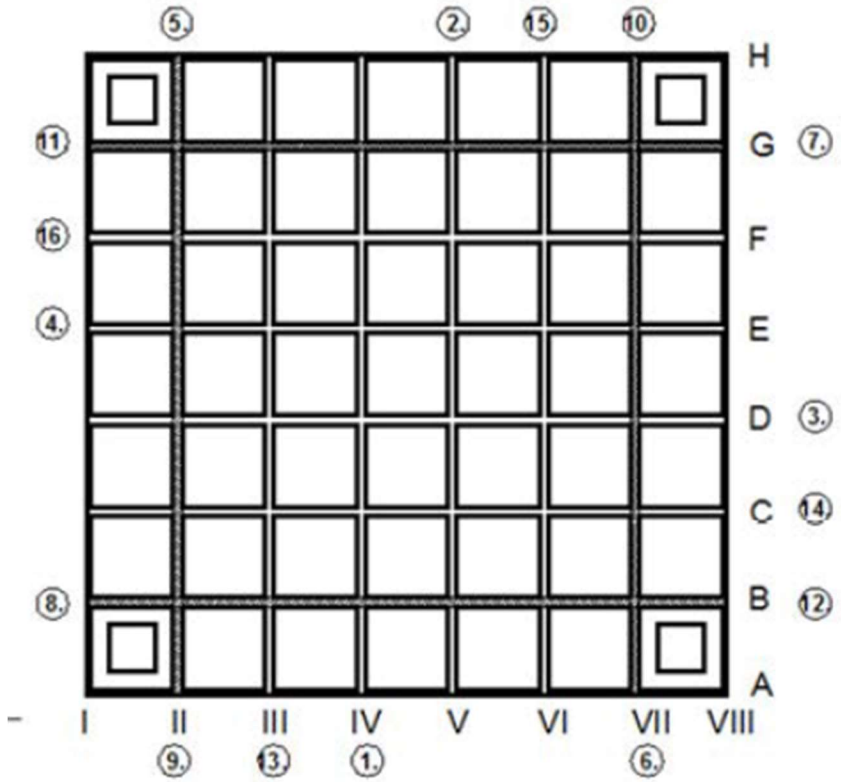

Figure 6 - Sequence of post-tensioning in Moldovan et al. (2018)

In conclusion, numerous research studies have been carried out globally on topics such as precast post-tensioned slabs, two-way waffle slabs, and precast slabs that make use of LWC. However, none of these research studies focused on precast slabs for residential foundations that also carry the first floor structure. The aim of this research is to close this knowledge gap and provide a solution for precast residential foundation-related challenges by utilizing the knowledge and data gathered from previous research efforts.

Chapter 3: Research Methods

In order to ensure the successful completion of this research project, it was essential to follow a comprehensive approach that involved 4 different phases that built on each other. The first phase involved identifying the previous research conducted on precast post-tensioned slabs made with lightweight concrete (LWC). The second phase focused on developing a mix design that could be used for the precast post-tensioned slabs cast in this project. The third phase was concerned with designing the slab using various methods and software. The fourth and last phase of this research project involved carrying out tests on medium and large specimens of the slab design developed in Phase 3, using the mix developed in Phase 2.

3.1 Phase 1 - Literature review and study

The literature review was an essential component of this research as it provided a comprehensive understanding of precast post-tensioned slabs and their use in construction. This included gathering information on design, construction, and performance of these slabs. Furthermore, the literature review covered studies that have explored the quality and cost-effectiveness of precast post-tensioned slabs, including a comparative analysis with traditional cast-in-place methods. This review served as the basis for subsequent phases of this research and is included in detail in Chapter 2. In addition, the literature review provided an understanding of how LWC performs compared to normal weight concrete (NWC). Additionally, publicly available information

from companies using post-tensioned slab technology was reviewed to research practical applications, however that information was not included in this thesis.

3.2 Phase 2 – Mix Design

3.2.1 General

For this phase, a LWC mix was designed according to ACI 211.2-98: *Standard Practice for Selecting Proportions for Structural Lightweight Concrete.* These proportions were selected to achieve a mix meeting the requirements specified in Table 2 and also recommendations identified in the literature review. The specifications were considered achievable and comparable to NWC.

Table 2 – Target Properties of LWC mix

Mix Property	Target
Compressive Strength at 7 days (f'_{ci}) - (psi)	3,000
Compressive strength at 28 days (f'_c) - (psi)	4,000
Slump - (in.)	6-8
Fresh Unit Weight - (lb/ft^3)	Max 120
Equilibrium Unit Weight - (lb/ft^3)	Max 115

First, a target compressive strength of 3,000 psi at 7 days and 4,000 psi at 28 days was chosen based on what some companies had been using in their slabs on site in recent years. Second, the target slump was set to a range of 6 and 8 in. because this would provide sufficient workability to pour the precast slab forms and obtain adequate consolidation. Third, the target unit weight for LWC is important to reduce the weight of the precast slab by at least 20%.

However, the main objective of the mix design phase was to find a straightforward mix design using cement, lightweight coarse aggregate, normal weight fine aggregate, and water.

All trial batches were produced in accordance with ASTM C192 “Standard Practice for Making and Curing Concrete Test Specimens in the Laboratory”. Variables such as water content, cement content, and fine to coarse aggregate ratio were modified between trial batches to achieve the target properties listed in Table 2.

3.2.2 Lightweight Aggregate (LWA)

The lightweight coarse aggregate (LWA) used for the concrete mix design was provided by the company Arcosa©. Two Arcosa© lightweight aggregates were selected for evaluation through the more than 20 trial batches made. The products Brooks and Livingston, shown in Figure 7, were chosen due to the availability of these two options near the University of Oklahoma. Brooks and Livingston LWA are made of expanded shale and clay respectively, and their nominal maximum size is 3/4 in. However, most of the aggregate particles for each material are in the 3/8 in. range.

Figure 7 - LWA from Arcosa - Brooks (left) & Livingston (right)

As described in previous research summarized in the literature review, methods used for prewetting the LWA have significant impacts on the results of the mix. For this reason, the aggregates used for each mix were presoaked for more than 24 hours and drained for 24 hours as specified by the supplier. To achieve this presoaking, two barrels with draining systems were fabricated to ensure that the aggregate could be consistently subjected to the same conditions and therefore the moisture content of each mix would be consistent and have limited impact in the development of the mix. A hole was drilled at the bottom of each barrel and a 4-5 in. long, ½ in. diameter pipe was inserted into this hole. A hose of the same diameter was attached to the pipe to allow draining of the barrels. This mechanism is shown in Figure 8.

Figure 8 - Draining barrel mechanism for presoak of LWA.

The moisture content of the LWA used in the mixes is critical consideration because the mix designs were based on a saturated surface dry (SSD) condition. This helps to prevent the mixing water from being absorbed by the aggregate and not being fully available for the cement hydration process. Additionally, research described in the literature review suggests that pre-wetting the LWA would improve the cement hydration process during internal curing.

Specific gravity and absorption tests were performed according to ACI 211.2-98: *Standard Practice for Selecting Proportions for Structural Lightweight Concrete*, on each of the aggregates to obtain these crucial characteristics. Performance of these tests is shown in Figure 9. Several moisture content tests were performed on the LWA according to ASTM C566 – 19 "Standard Test Method for Total Evaporable Moisture Content of Aggregate by Drying" throughout the trial batching process. The aim of these tests was to

evaluate the actual moisture content of the aggregate at the time of mixing and achieve consistency in the results obtained from utilizing the barrels.

Figure 9 - Specific gravity test (left) and absorption test (right)

The specific gravity, absorption, and ranges of measured moisture content are shown in Table 3. It must be noted that these properties were compared to the information provided by the supplier, Arcosa©. However, the comparison showed a slight difference between the values calculated for specific gravity and it was decided to average both values for use in the mix design process. The moisture content is a range where the values were consistently found during trial batching and was used for adjusting the water content of the batches.

Table 3 - Characteristics of the LWA

Aggregate	Specific Gravity	Absorption (%)	Moisture Content (%)
Livingston	1.3	36.8	36.5 – 40.5
Brooks	1.8	14.3	24.5 – 28.5

Finally, the Arcosa© Livingston LWA was selected for use in the final mix design. This was also due to the fact the Arcosa© Livingston LWA is available at the port of Catoosa in Tulsa, which was the closest LWA source to the city of Oklahoma City and the University of Oklahoma. Furthermore, after several test batches modifying the parameters such as water-cement ratio and aggregate ratio, to achieve the objectives in Table 2, the mix design shown in Table 4 was selected for use in further testing. The values shown in Table 4 are based on an SSD condition.

Table 4 – Final LWC Mix Design

Material	Quantity	Volume (ft^3)
Cement (lb/yd^3)	609	3.10
LWA (Livingston) (lb/yd^3)	718	8.85
Sand (lb/yd^3)	1478	9.00
Water (lb/yd^3)	335	5.37
Air (%)	2.5	0.68

3.2.3 Concrete Properties

3.2.3.1 Mixing Procedure

All of the following tests, both fresh and hardened, were performed on concrete mixed at Fears Lab. The following mixing procedure was used for all batches.

1. Dampen the mixer and remove any excess water along with residual old concrete.
2. Introduce the aggregates, sand, and pre-wetted LWA, into the mixer.
3. Pour half of the required water into the mixer.
4. Allow the aggregates and water to mix thoroughly for a minimum of 2 minutes.

5. Incorporate the cement into the mixer.
6. Pour the majority of the remaining water into the mixture.
7. Continuously monitor the concrete's consistency while adding water.
8. Regularly assess the slump until the desired consistency is achieved.
9. Optionally, adjust the water content in the mixer as needed, either by omitting water or adding more to achieve the desired result.

3.2.3.2 Fresh Concrete Testing

The procedure described in ASTM C143 “Standard Test Method for Slump of Hydraulic-Cement Concrete”, was followed to measure slump for every trial batch, as shown in Figure 10. As described in the mixing steps above, water was added in a manner controlling the consistency of the concrete and various slump tests were conducted until the desired target slump of 6-8 in. was achieved. Sometimes, the concrete mix would not contain enough water or would have too much water. One of the reasons for this was that while the prewetting of the LWA was carefully controlled, environmental factors such as temperature and humidity could still affect it and cause variations in the aggregate moisture content for the different trial batches. The slump test was performed to ensure that the right amount of water was added to the mix. The water content was then recalculated after each trial batch by considering the actual moisture content of the aggregate and the added water in the mix. This was done to compare it with the target mix design and make necessary adjustments for the next trial batch.

Figure 10 - Slump test performed at Fears Lab showing slump cone with an approximate slump of 7 in.

The other fresh concrete property measured for each batch during the mixing process was the fresh unit weight. For this property, the procedure described in ASTM C138 “Standard Test Method for Density (Unit Weight), Yield, and Air Content (Gravimetric) of Concrete” was followed carefully. It was important to ensure that the concrete mix used in the precast post-tensioned slabs achieved the planned 20% weight reduction.

3.2.3.2 Hardened Concrete Testing

All the trial mix designs, as well as the final mix design shown in Table 4 were evaluated using a series of different hardened concrete tests. Compressive strength modulus of elasticity and flexural strength specimens cast for each batch were air cured in an environmentally controlled room at Fears Lab, maintained at 73°F with limited humidity control.

The mix designs were tested for compressive strength at 3, 7 and 28 days following the procedures of ASTM C39 "Standard Test Method for Compressive Strength of Cylindrical Concrete Specimens" using three 4 in. x 8 in. cylinders per testing age, as shown in Figure 11. A Forney compression machine was utilized for these tests with a preload of 5,000 lb and a loading rate of 35 psi/sec.

Figure 11 - Compressive strength testing

Modulus of elasticity was measured once the trial mix was considered “final”, and for this reason this test was only conducted on mix L12 and L14 (the mix used in the scaled prototype). The modulus of elasticity was measured following the testing procedures of ASTM C469 “Standard Test Method for Static Modulus of Elasticity and Poisson's Ratio of Concrete in Compression”. This test was done at the same testing ages for compressive strength using three 4 in. x 8 in. cylinders per testing age as well. This test, as shown in Figure 12, was run using a Forney compression machine along with a compressometer frame with a linear variable differential transformer (LVDT) attached to it to measure deformation of the specimen. Modulus of elasticity was then determined from the output of load and deflection as described in ASTM C469.

Figure 12 - Modulus of elasticity testing set-up.

Flexural strength was tested at 28 days following ASTM C78 “Flexural Strength of Concrete (Using Simple Beam with Third-Point Loading). Two 6 in. x 6 in. x 20 in. prism specimens with an 18 in. span and loads spaced at 6 in. were tested for the last five trial mixes (L9, L10, L11, L12, L13, and L14). These beams had no reinforcement and exhibited collapse immediately after first cracking, as shown in Figure 13. The maximum load recorded from each test was used along with the measured dimensions of the specimen to determine the flexural stress at failure.

Figure 13 - Modulus of rupture test after failure of specimen.

The density or unit weight of the LWC mix is a very important property, so this characteristic was measured in the fresh/wet state (as mentioned above) and hardened (dry) states. Hardened unit weight was measured using two different methods: dry unit weight (or “cylinder volume method (CVM)”), and equilibrium unit weight. The “volume

unit weight" was conducted by weighing a 6 in. by 12 in. cylinder and then diving the weight by the volume. The volume was calculated using an average of three dimensions taken for the diameter and length of the cylinder. The equilibrium unit weight was measured in accordance with ASTM C567 “Standard Test Method for Determining Density of Structural Lightweight Concrete”. For this test, three 4 in. x 8 in. cylinders wet cured for 7 days after casting were used. The specimens were immersed in water tanks within the Fears Lab’s environmentally controlled room for curing. This wet curing process was selected to ensure that the cylinders were fully saturated 7 days after demolding. After the 7 days of wet curing the cylinders were weighed submerged in water using the mechanism shown in Figure 14 (Weight C from ASTM C567). Then the cylinders were dried with a towel to achieve an SSD condition and they were weighed again, but this time in air (Weight B from ASTM C567). Finally, at different ages (1 week, 2 weeks, and 1 month) the cylinders were weighed again (Weight A from ASTM C567). The equilibrium unit weight was then calculated using the three weights in accordance with Equation 1 given by the ASTM C567.

$$Em\ \left(Density, \left[\frac{lb}{ft^3}\right]\right) = (A\ \times\ 62.3)/(B - C) \qquad (1)$$

where:

Em = measured equilibrium density, kg/m^3 [lb/ft^3].

A = mass of cylinder as dried, kg [lb].

B = mass of saturated surface-dry cylinder, kg [lb].

C = apparent mass of suspended-immersed cylinder, kg [lb].

Figure 14 - Mechanism at Fears Lab to weight apparent mass of suspended-immersed cylinder.

Finally, it is important to consider shrinkage in prestressed concrete structures, especially those using LWC, so three 3 in. x 3 in. x 12 in. specimens were tested for trial batch L12 following the ASTM C157 "Standard Test Method for Length Change of Hardened Cement Mortar and Concrete". These specimens were demolded three days after casting and measurements were taken every day for a period of seven days. After the first seven days measurements were taken every seven days, and after 100 days measurements were taken once a month. All these measurements were taken using the comparator shown in Figure 15. Between measurements the specimens were kept in the

environmental chamber at Fears Lab, where the conditions were maintained at approximately 73 °F with approximately 50% relative humidity.

Figure 15 - Comparator testing set-up for shrinkage specimens.

3.3 Phase 3 – Slab Design

3.3.1 Equivalent Frame Method

The Equivalent Frame Method was initially utilized in the design of the post-tensioned two-way slab to obtain the positive and negative moments affecting the structural element. This method involves modeling an equivalent frame that represents the contribution of the slab, beams, and supports under loading to determine the

magnitude and distribution of positive and negative moments. This initial method was used to provide some baseline design for dimensions, moment magnitudes and necessary amount of prestress provided by the post-tensioning tendons. The slab was designed to meet the requirements of the ACI 318-19 code, including the required strength, minimum thickness, minimum reinforcement ratio, maximum spacing of the tendons, and other detailing requirements. Loads acting on the slab used in the analysis were determined based on the ASCE 7-16 “Minimum Design Loads and Associated Criteria for Buildings and Other Structures”. The design was optimized based on the different support conditions that are anticipated including lifting, transport, and service loading in the structure required for the specific application. The design also took into consideration the use of LWC to reduce the weight and better facilitate transportation and installation.

3.3.2 RAM Concept

A computational model made using RAM Concept (Post-Tensioning) software was made to optimize the preliminary slab design obtained using the equivalent frame analysis and test different loading conditions. This software can be used to view, analyze, and audit sections in the slab to obtain a complete report. This includes service level stresses, moment demands, shear demands, calculated capacities and deflections. Furthermore, RAM Concept can optimize the number of tendons and layout. The mild steel reinforcement required in the slab can be calculated automatically by the software and modified later or it can be done manually. The slab dimensions used for optimization were 16 ft x 31 ft with a waffle pattern including exterior and interior beams, as shown in

Figure 16. Table 5 shows a summary of weights and volume for the final slab dimensions. Furthermore, post-tensioning tendons were included in both directions.

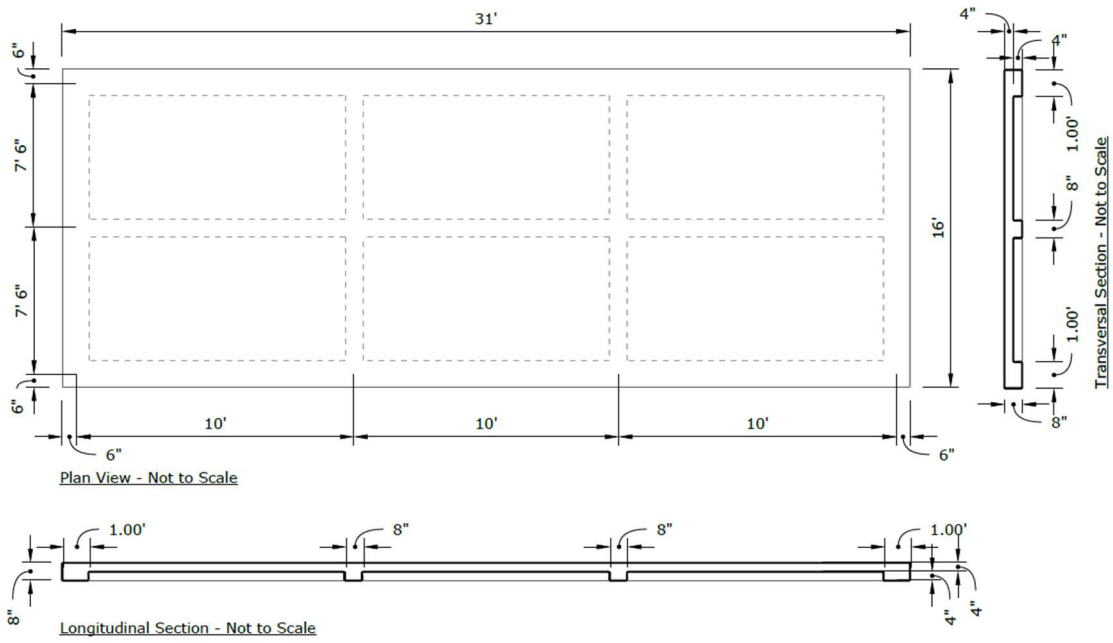

Figure 16 - Slab Proposed Dimensions

Table 5 - Volume and Weight Summary for Slab Design

Item	Quantity	Unit
Volume of Slab	7.71	yd^3
Weight of Slab using LWC	25,000	lb
Weight of Slab using NWC	31,250	lb

Three different loading conditions were examined in the slab analysis using RAM Concept. The first loading case is the service loads, which include all the dead loads (self-weight, second floor, roof, and walls) and live loads from all three levels. A 3D transparent perspective of slab model for this loading case is shown in Figure 17.

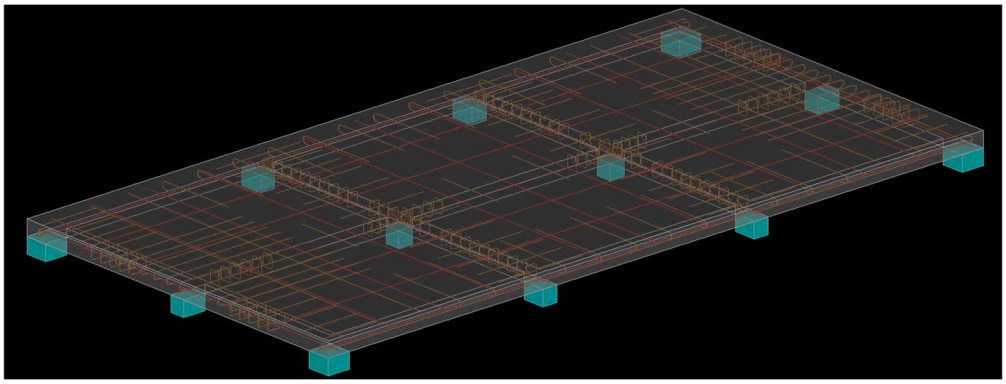

Figure 17 - First loading case (slab in service)

The second loading case was the pick-up of the slab alone to remove it from the formwork and place it on two steel wide flange (W)-section beams for construction of the first story structure and transportation to the project site. For this reason, the 3D transparent perspective in Figure 18 shows only 10 “blue” supports. These supports represent where the hooks for lifting the slab alone will be located.

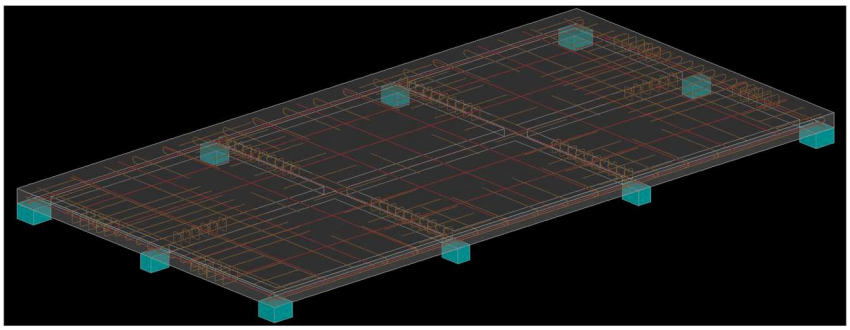

Figure 18 - Second loading case (pick up of slab alone).

The last loading case evaluated was the one where the slab would be placed on two steel W-section beams intended to support the slab during transport and placement at the job site. These steel beams will be carrying the self-weight of the slab plus the dead load of the first floor. The perspective shown in Figure 19, shows blue supports located

close to the exterior beams (specifically offset 12 in. from the center of the exterior beams), which is where the slab would be supported on each steel W-section beam.

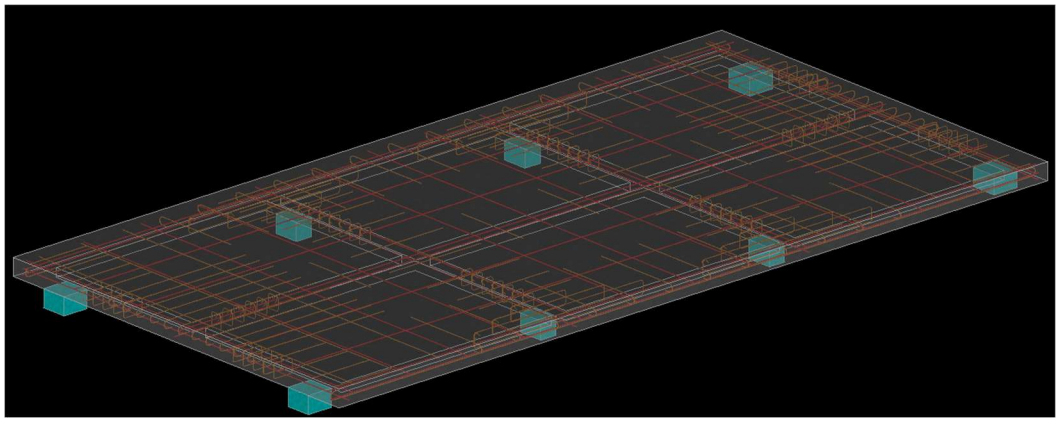

Figure 19 - Third loading case (W Beams for transport)

After evaluating all the load cases it was possible to use superposition to arrive at a final reinforcement plan where post-tensioning, mild steel flexural and shear reinforcement was sufficient to cover the demands from all load cases. Post-tensioning was done in both directions, placing 15 tendons in the short (16 ft) direction and 8 tendons in the long (31 ft) direction. Also, 1 additional tendon was placed at a different height within each interior beam. This additional tendon is located 6 in. from the top of the slab within each interior beam while all the other tendons are located 3 in. from the top of the slab, as shown in Figure 20. The required post-tensioning was determined and optimized using Ram Concept software. Final reinforcement plan, reinforcement schedule and plans for both the scaled prototype and the full-size slab can be found in Appendix A, B, D, and E.

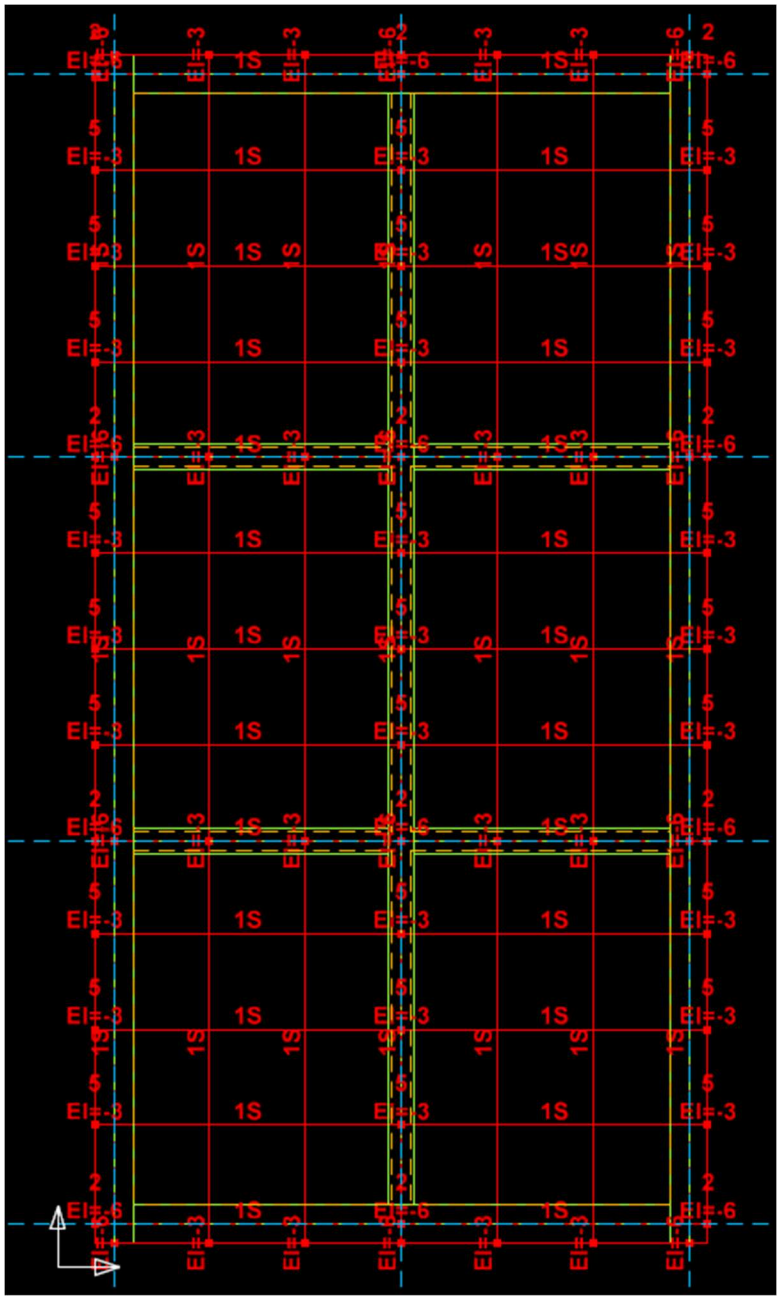

Figure 20 – Tendons locations.

In addition to load demands, Ram Concept can analyze the deflections for the structure over time providing a standard deflection plan for maximum short-term load, sustained load, and final instantaneous load as shown in Figure 21. Figure 21 shows the deflection under the steel beam supported loading condition because it resulted in the

maximum calculated value of 0.243 in. However, this maximum deflection value is lower than the 0.4 in. limit value calculated according to ACI Table 24.2.2 – maximum permissible calculated deflections where the deflection equation is L/480. Since the slab is supported on two steel beams placed along the long direction for this case, L is taken as the short span and is equal to 16 ft.

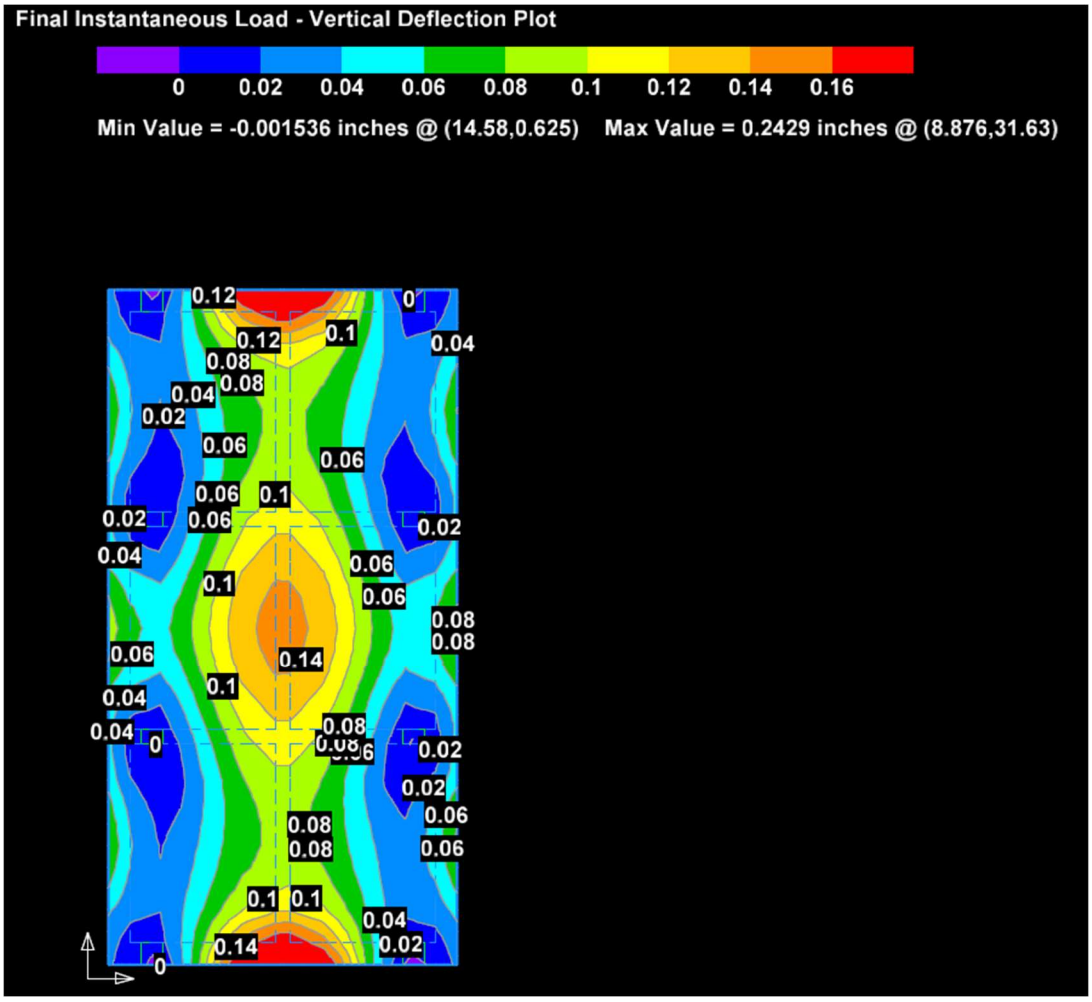

Figure 21 - Example deflection plan for the third loading condition.

3.3.3 Support Design

Furthermore, during this phase of slab design several different available methods for placement of supports into the two-way slab system for attachment to the pier foundation were evaluated. This pier foundation is being considered to be either helical piles or concrete piles with a shear cap at ground level. Consideration was made for realistic construction tolerances and required leveling adjustments. The final concept chosen for the trial slabs was an embedded steel plate with a threaded rod that would allow for leveling the slab, “Support A”, as shown in Figure 22.

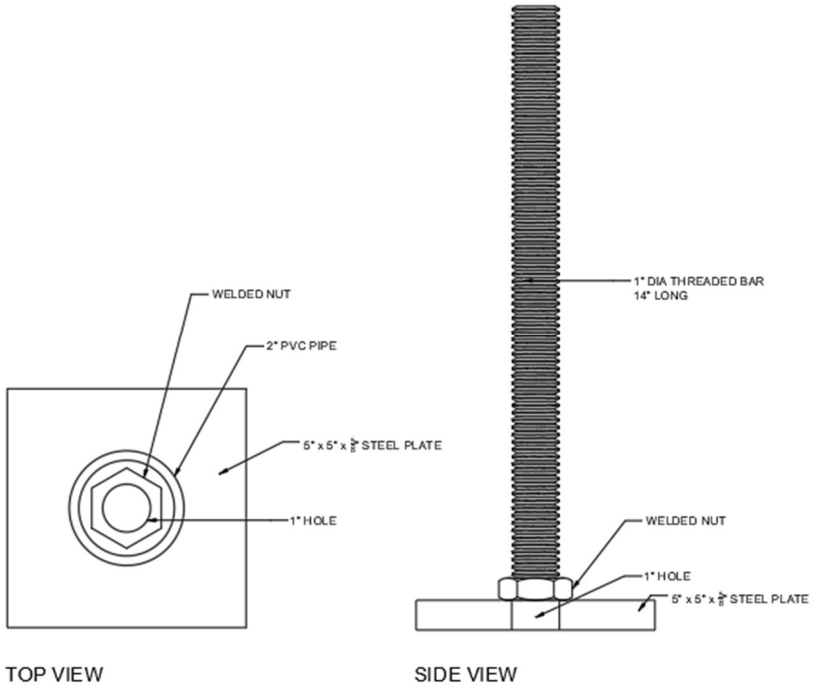

Figure 22 - Top view (left) and side view (right) of Support A (plate-nut support)

A gravity analysis was conducted to determine the required embedded plate and bolt sizes for use as a connection to the pier foundation. This gravity analysis took into

account the gravity loads as well as lateral loads (wind). Wind forces were calculated according to Table 28.2-1 “Steps to Determine Wind Loads on Main Wind Force Resisting System (MWFRS) Low-Rise Buildings” in chapter 28 of ASCE 7-16. The gravity loads in addition to the wind load were added together following the required load combinations to determine the required dimensions of the embedded plate. Final dimensions use for the trial slab specimens are 5 in. x 5 in. x 5/8 in., combined with a bolt of at least 1 in. diameter.

An additional concept, “Support B” consisting of a large nut with shear studs welded to the nut was examined and a trial specimen was cast for later testing, as shown in Figure 23. Both supports plans can be found in Appendix F.

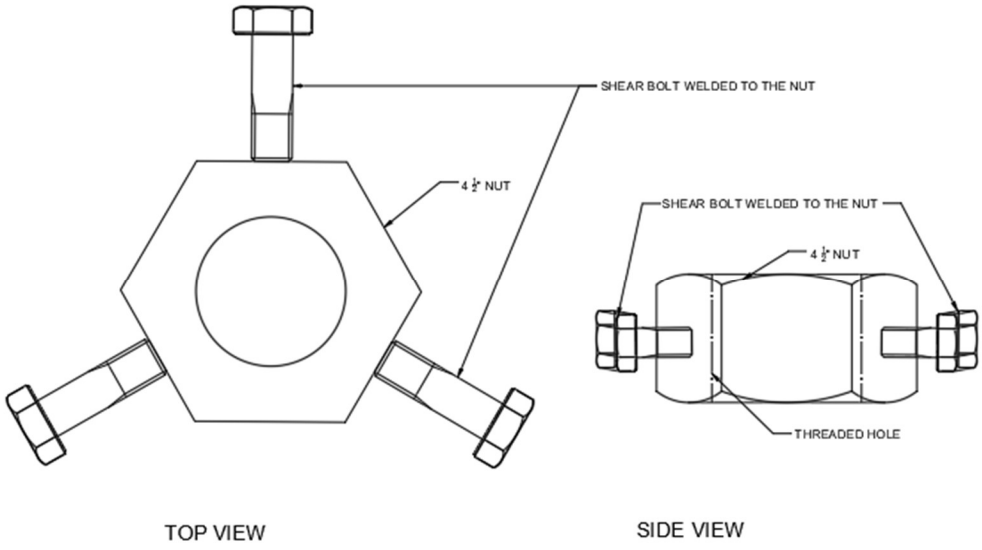

Figure 23 - Top view (left) and side view (right) of Support B (nut with welded shear studs support)

3.4 Phase 4 – Large Scale Testing and Monitoring

The next step in the research was to fabricate one scaled prototype of the designed slab at Fears Lab using LWC as well as conduct on-site large-scale testing in the House Factory facility using NWC. This test included the evaluation of performance for the loading conditions of lifting and setting on top of W beams. This evaluation involved the use of vibrating wire strain gauges (VWSGs) located inside the slab at the points of maximum deflection identified in the Ram Concept analysis to monitor slab deformation under the different loading conditions. This large-scale testing was to evaluate the performance of the slabs relative to the model results and the necessary safety and structural requirements. Additionally, the results of these tests provided valuable data for further analysis and optimization of the precast post-tensioned slab design and manufacturing process.

3.4.1 Scaled Prototype

The first of these two specimens created to evaluate the performance of this research was built at Fears Lab. It was decided to create a scaled prototype of 16 ft x 6 ft. The width of the slab was maintained while shortening the longer span. This was done to closely recreate the deflections and maximum moments generated in the width of the slab. It was also necessary to downsize the slab to ensure that it remained under the weight limit of the crane that was available in the facility. Before casting the trial slab two different types of formwork inserts were fabricated and tested in smaller prototypes to see which one would be more easily removable from the waffle slab.

3.4.1.1 Formwork Inserts

As identified in the literature review, formwork inserts used to create the waffle system are an important construction consideration when designing the formwork. Slabs on site usually utilize plastic forms that are easily removable from below the waffle slab, other times non-reusable formwork is utilized and left in the slab. However, in this phase a wood formwork insert was studied to be both easily removable and reusable.

The first insert, shown in Figure 24, consisted of a wood frame with insulation foam placed around the edges working as a joint to allow the concrete to expand or shrink without affecting the wood frame. Plastic sleeves were placed through the top of the slab to provide access to tap out the insert from above. A 3 ft x 3 ft slab with a 1 ft x 1 ft insert was cast using this design to test whether the insert could be easily removed.

Figure 24 – Insert formwork before casting (left) and insert removed from bottom of slab (right)

The second wood frame insert, following the same principle of being easily removable and reusable, was designed with a trapezoidal shape to allow for easier

removability. Plastic sleeves were again added to provide access to tap out the insert from above. Again, a 3 ft x 3 ft slab with a 1 ft x 1 ft insert was cast to test this insert design as shown in Figure 25.

Figure 25 - Second insert formwork prototype.

3.4.1.2 Slab Prototype

After conducting tests on the inserts and observing the various benefits they provided, a scaled prototype of the slab was constructed. For this prototype, the large-scale reinforcement and post-tensioning tendons were adjusted to fit the scaled specimen's dimensions. The dimensions, reinforcement plan, and tendon plan for this prototype can be found in Appendix A and D. The formwork was made of wood and was sealed with caulk around the joints to prevent concrete from seeping through.

Since both inserts were effective in the small-scale tests it was decided to use both designs for the slab prototype as shown in Figure 26. This provided a better picture of how large-scale inserts would work for the full-size slabs. The bottom of the slab's formwork was covered in plastic to break the bond between the concrete and the forms, while the sides were covered with form-release agent.

Figure 26 - Formwork for scaled prototype showing both types of inserts.

Both bent and straight steel reinforcing bars were used in the slab. The construction process involved placing the bottom and shear reinforcement first, then the tendons were laid down in their respective positions, followed by placing the top reinforcement.

To ensure adequate cover and meet the design requirements, steel chairs of 0.75 in., 1 in., and 1.5 in. were used throughout. Once the reinforcement and tendons were in

place within the formwork, the steel support plates were added as well as the sleeves used to provide access to tap out the inserts in the demolding stage. A picture of the entire formwork with the reinforcement, tendons, supports, and sleeves in place is shown in Figure 27. It must be mentioned that the software RAM Concept provided a height for the top reinforcement but without considering that bars would be laying on top of other bars, for this reason it was decided to place the interface between the two layers of steel reinforcing bars at the height used in the RAM Concept model.

Figure 27 - Formwork, reinforcement, tendons, and sleeves in ready for scaled-prototype's cast.

The tendons were inserted into the formwork with a dead end and a live end. Anchor plates were nailed to the wooden formwork at both ends. To create space for

introducing the wedges used for post-tensioning the tendons, reusable pocket formers were utilized. Post-Tension Services of Oklahoma, a local company, provided the anchor plates, wedges, and reusable plastic pocket formers, as a donation for the project. Reusable pocket formers were used to create space for the installation of two wedges into the steel anchorage, as depicted in Figure 28. These wedges were then tightened to the anchor plates once the tendon was released from the post-tensioning jack.

Figure 28 - Space left by pocket formers once removed from the slab.

As previously mentioned, ½ in. PVC pipe was used to create sleeves that were placed in the slab at each of the four corners of the formwork inserts that were then used for access to tap out the inserts from above. Additionally, in all four corners of the slab formwork, a 2 in. diameter PVC pipe with a 1 in. threaded bar in the middle were used to

recreate the supports used for the connection to the pier foundations. These PVC pipes were securely fixed to the embedded 5 in. x 5 in. x 5/8 in. base plates using silicone, as depicted in Figure 29. Moreover, a 1 in. nut was welded on top of each plate to provide a threaded hole for the 1 in. threaded bar that acted as an adjustable support for leveling the slab.

Figure 29 - Supports with steel base plate, bolt and nut and PVC fixed with silicone to the base plate.

Finally, six Geokon© Vibrating Wire Strain Gauges (VWSGs) were carefully placed inside the slab, at the points of maximum deflection identified in the RAM Concept analysis. These points were the center of the slab, and middle span in both directions, as shown in Figure 30. The following plan is included in Appendix G as well.

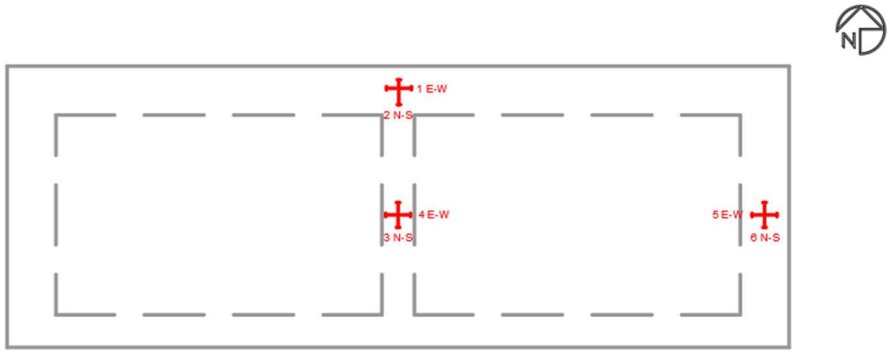

Figure 30 - VWSGs location in scaled prototype.

The VWSGs were installed in the formwork per the instructions provided by Geokon©, which included securing them firmly in place. They were arranged in three pairs with two gauges each, set at right angles to each other in both the East-West and North-South directions. The gauges in the North-South direction were raised 1 in. above the bottom of the slab and secured to 0.75 in. steel chairs using zip ties. The gauges in the East-West direction were tied to post-tensioning tendons, as shown in Figure 31. It is important to note that all VWSGs were offset from the tendons and chairs using foam blocks as interface at their tie-down points.

Figure 31 - Installation of VWSGs in scaled prototype.

The slab was cast with LWC provided by Dolese© Brothers Company following the final LWC mix design described in Table 4 and vibrated to ensure proper consolidation throughout and then was screeded to the final elevation and finished, as shown in Figure 32.

Figure 32 - Screeding and finishing the concrete to the approximate scaled slab elevation of 8 in.

This prototype was demolded three days later, and post-tensioned and tested a week after the cast. Furthermore, cylinders and beams were also cast to test the concrete for compressive strength, modulus of elasticity, unit weight, and modulus of rupture following the procedure described in Section 3.2.3.2 of this thesis. The concrete slab as well as the specimens cast for hardened property testing are shown in Figure 33 and Figure 34.

Figure 33 – Scaled slab immediately after demolding at seven days.

Figure 34 - Specimens for hardened concrete property testing.

The slab was post-tensioned 7 days after casting to allow the concrete to gain sufficient strength to withhold the precompression stresses. After testing the three compressive strength cylinders and corroborating the desired strength of at least 3,000 psi, the slab was post-tensioned using the jack shown in Figure 35.

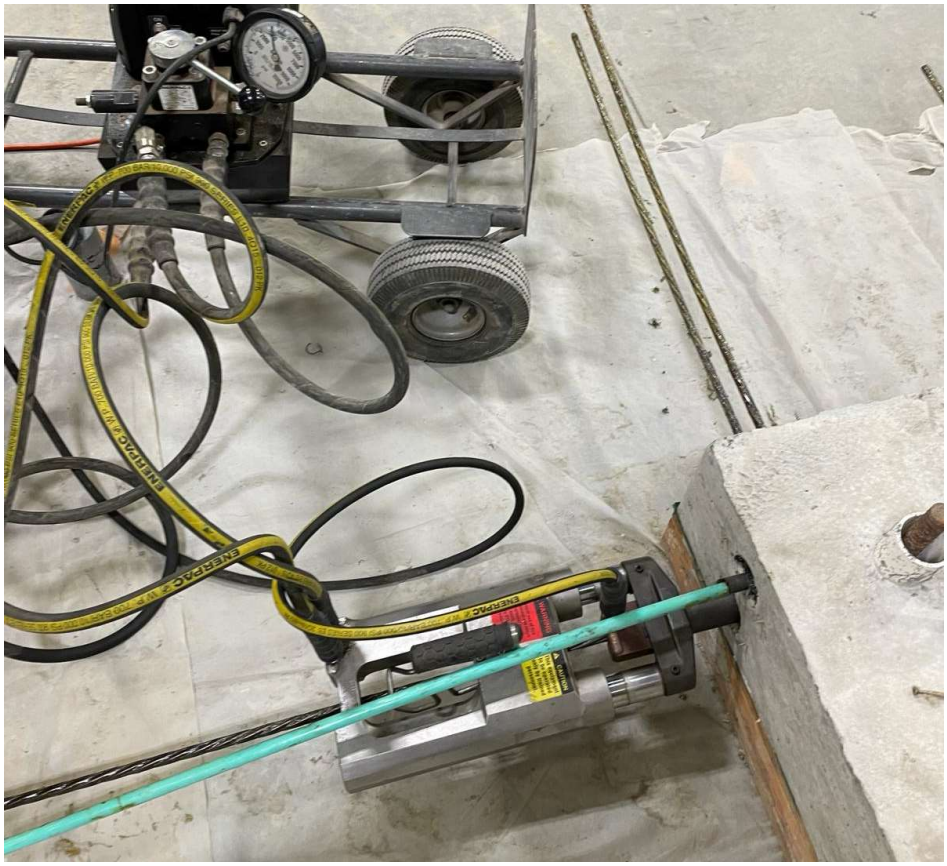

Figure 35 - Post-tensioning of tendons using hydraulic jack on scaled prototype.

The post-tensioning process was carried out according to the sequence illustrated in Figure 36 to prevent potential cracking caused by stressing strands located in the same area of the slab. Each tendon was tensioned to 26,800 lb (162.5 ksi), which was the tension used in the slab design calculations and approximately translates to 4,500 psi in the jack gauge. However, it was also decided to first tensioned each tendon to two-thirds

of the expected pretension and then follow the sequence one more time to achieve the required stress for each tendon. The post-tensioning sequence plan can be found in Figure 36 as well as in Appendix H.

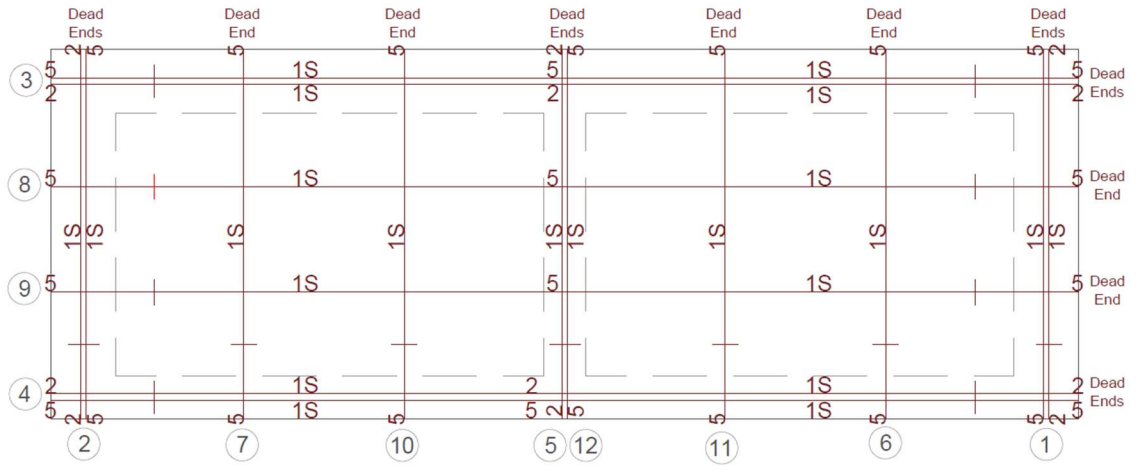

Figure 36 - Post-tensioning sequence of tendons for scaled prototype.

Additionally, during the post-tensioning process, the VWSGs were closely monitored, and a thorough examination of the slab was conducted to check for possible cracks between the tensioning of each cable. Both inspections were conducted to ensure that the slab was effectively holding the precompression produced by tensioning the tendons.

After post-tensioning all tendons to the specified stress level, the computer was disconnected from the data logger. The slab was then lifted by the overhead crane at Fears Lab, as shown in Figure 37. After elevating the slab over the floor level by more than 2 ft the slab was checked for cracks.

Figure 37 - Slab being pick up from four lifting hooks using overhead crane at Fears Lab.

After testing the slab's self-weight loading condition, it was placed on steel W beams to simulate preparation for transport as shown in Figure 38.

Figure 38 - Slab supported by steel W beams.

3.4.1.3 Support Prototype

The original plan was to use a plate support to connect the slab to the pier foundation. However, it was decided to also test a support design B described in Section 3.3.3. Instead of using a plate and a threaded bolt, a larger bolt was chosen with a large nut having three steel shear studs welded to it that would be encapsulated in the concrete and replace the steel plate, as shown in Figure 39.

Figure 39 - Support B before being casted.

Moreover, the already threaded nut eliminates the necessity to weld a nut to the plate. The second option specimen was cast to evaluate the feasibility of a different support mechanism.

3.4.2 Large-Scale Prototype

The full-size slab, measuring 16 ft x 31 ft, was built on the floor of the House Factory facility with wooden formwork and included wood frame inserts. Furthermore, plastic was also used to break the bond between the concrete slab and the floor of the facility, as shown in Figure 40.

Figure 40 - Formwork of full-scale slab.

The reinforcement, post-tensioning tendons, supports, and sleeves were placed into the formwork following the same procedure used for the prototype at Fears Lab, as shown in Figure 41. The reinforcement plan as well as the tendon plan for this prototype can be found in Appendix B and C.

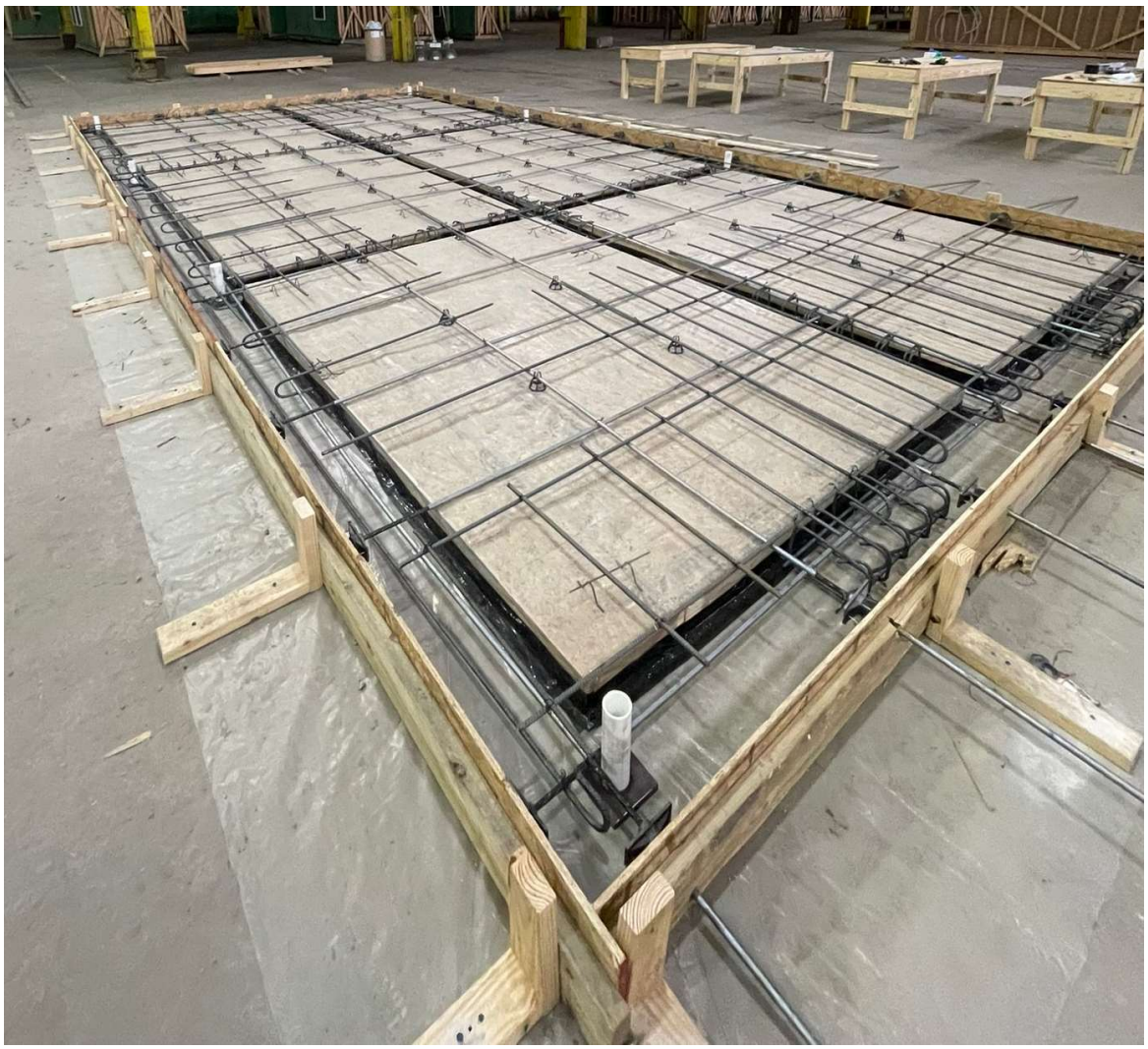

Figure 41 - Formwork, reinforcement, tendons, and sleeves in place for full-scale prototype's casting.

Furthermore, 6 VWSGs were installed in this formwork to monitor the deformations during the different loading cases used in the analysis phase. These gages were also placed at the points of maximum deflection found using the RAM Concept analysis, as shown in Figure 42. Once again, they were carefully zip-tied and installed in the formwork per the instructions provided by Geokon©, as shown in Figure 43 and Appendix G.

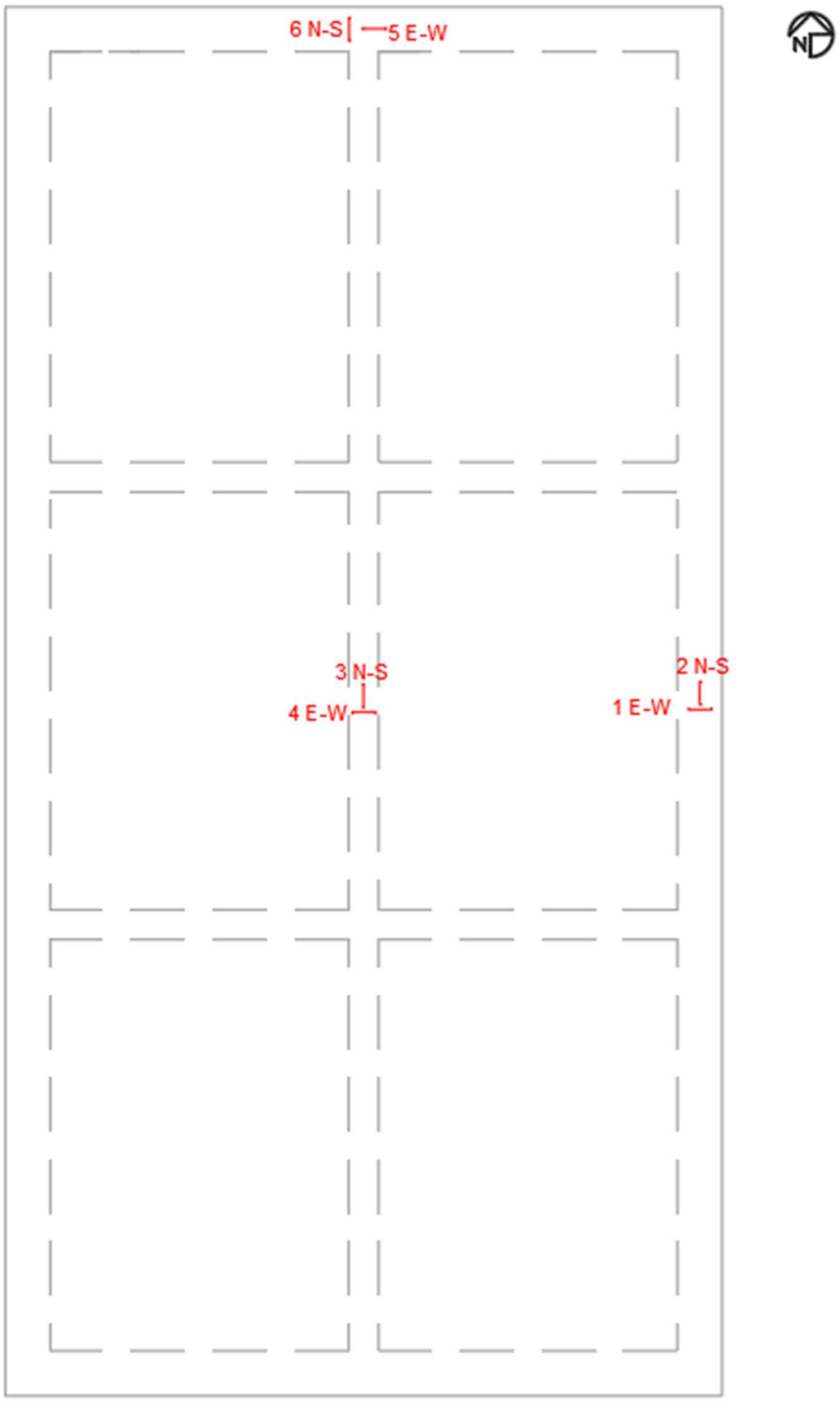

Figure 42 - VWSGs location in full-scale prototype.

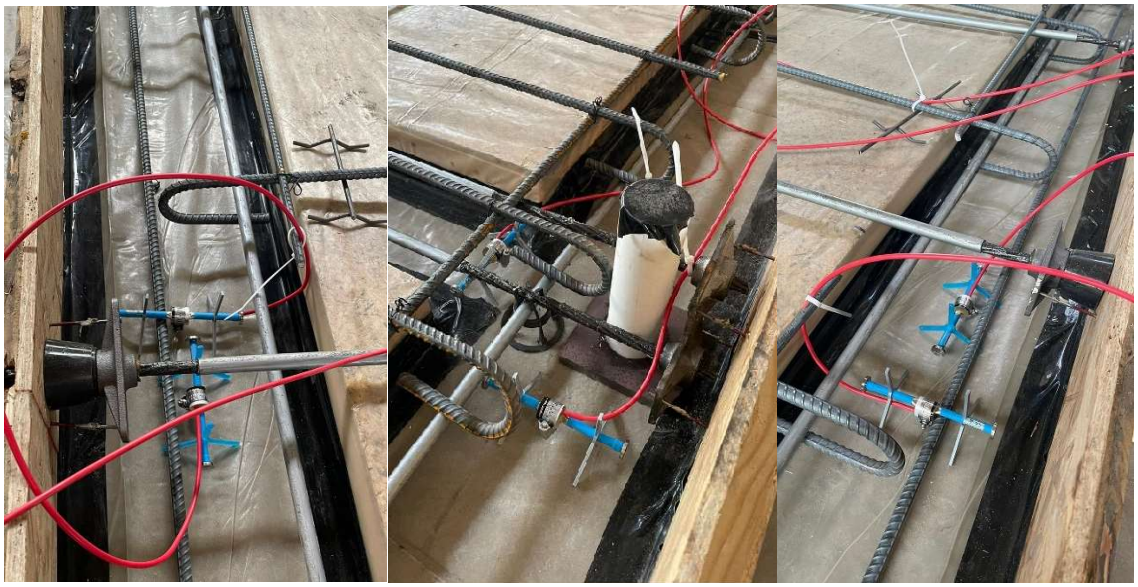

Figure 43 - Installation of VWSGs in full-scale prototype.

To obtain precise data from the strain gauges, these were connected to a data logger that would record the strain of the vibrating wire in different intervals. For example, 5 minutes when casting, 15 minutes in the first 7 days, 1 minute during the post-tensioning procedure, and 30 seconds when the slab underwent the different loading conditions. Figure 44 shows a picture of the slab being cast, screeded, and finished, and Figure 45 shows a picture of the slab after casting with NWC where the data logger can be seen as well. The NWC was ordered from Dolese with a requirement of 4,000 psi compressive strength at 28 days as well as 6 in. slump.

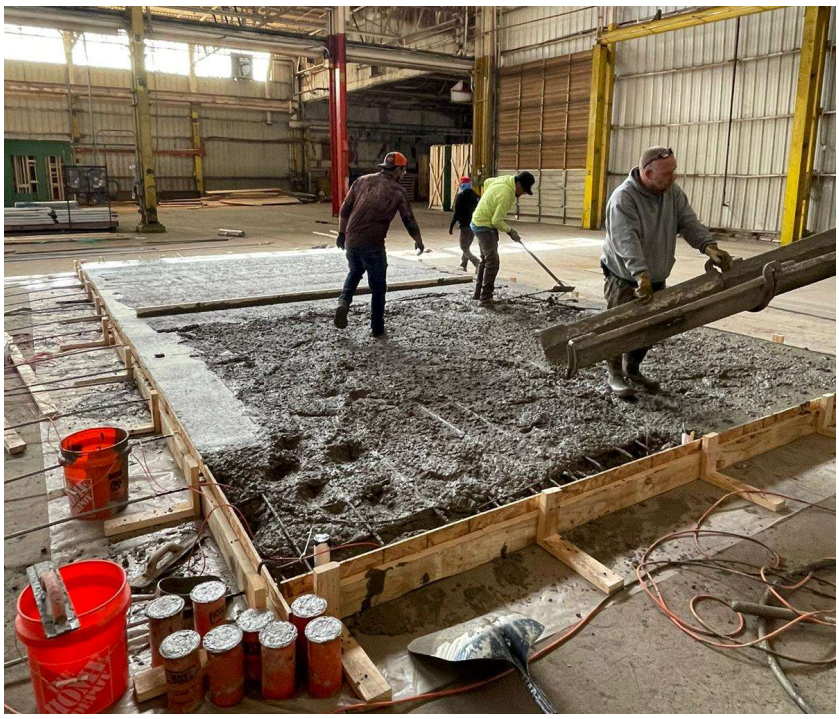

Figure 44 – Placement, screeding and finishing the concrete to the approximate full-scale slab elevation of 8 in.

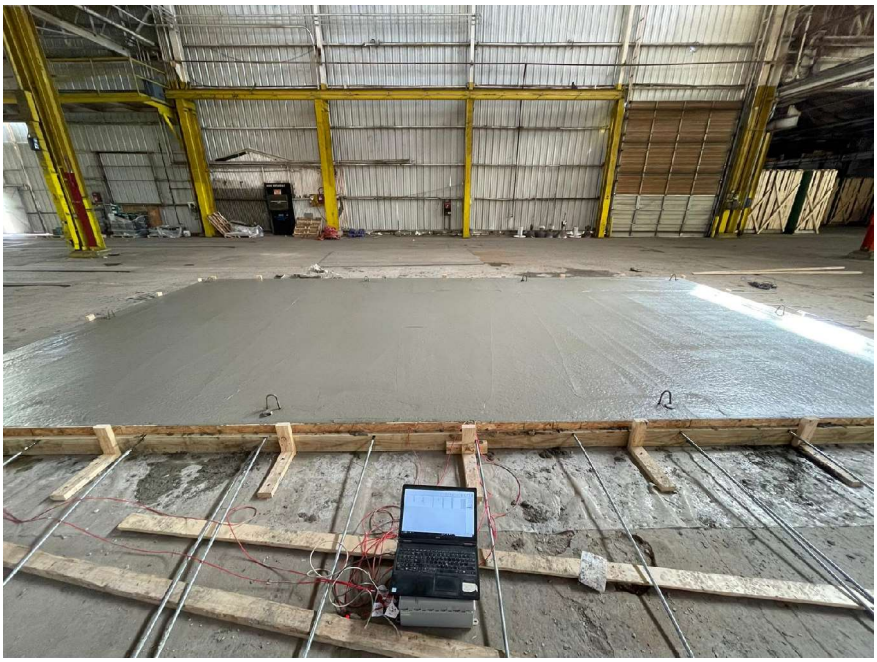

Figure 45 - Finished full-scale slab after casting with VWSGs connected to data logger in the bottom of the image.

The slab was post-tensioned 7 days after casting to allow the concrete to gain sufficient strength to withhold the precompression stresses. After testing the three cylinders and corroborating the desired strength of at least 3,000 psi, the slab was post-tensioned using a jack, as shown in Figure 46.

Figure 46 - Post-tensioning of tendons using hydraulic jack on full-scale prototype.

The post-tensioning process was carried out according to the sequence illustrated in Figure 47 to prevent potential cracking caused by stressing strands located in the same area of the slab. As in the scaled prototype, each tendon was tensioned to 26,800 lb (162.5 ksi), which translates to 4,500 psi in the jack gauge. However, it was also decided to first tension each tendon to two-thirds of the expected pretension and then follow the sequence one more time to achieve the required stress for each tendon. This post-tensioning sequence can be found in Appendix I.

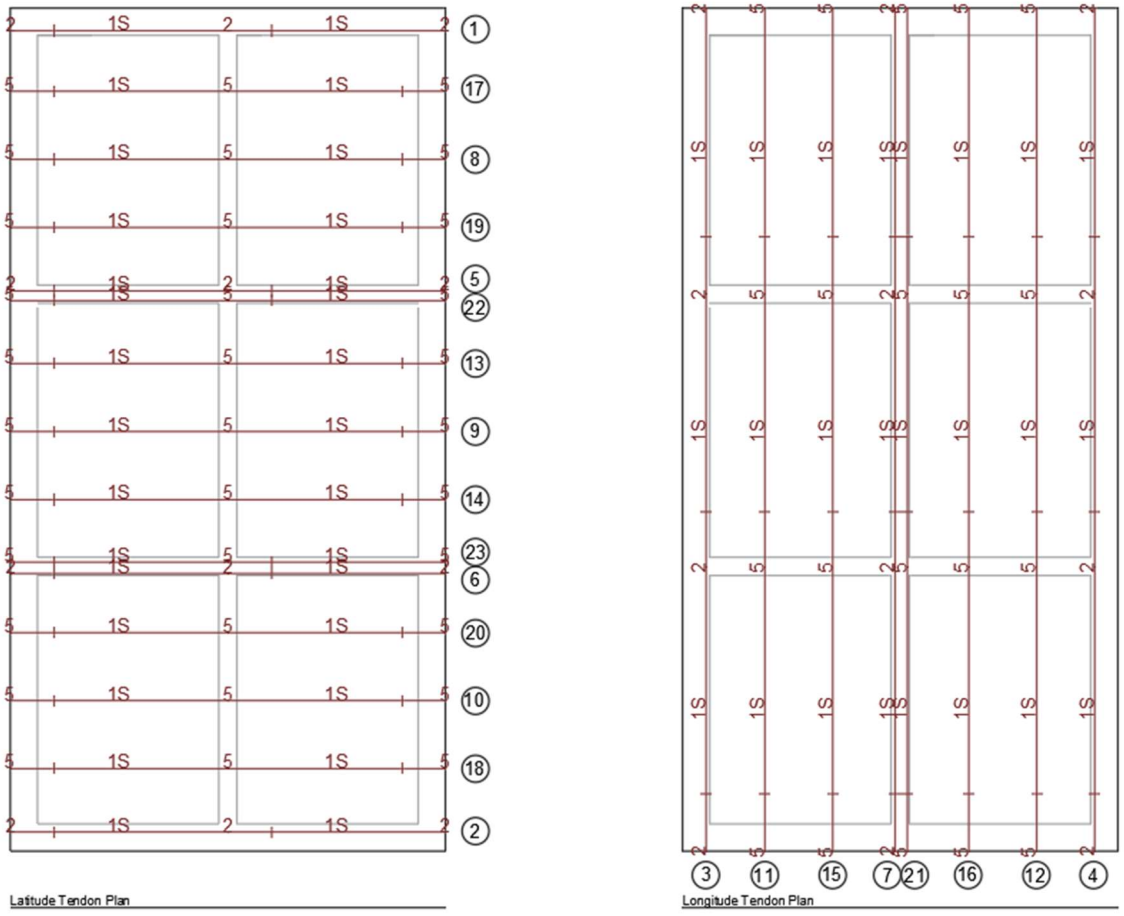

Figure 47 – Tendon post-tensioning sequence for full-scale prototype.

The VWSGs were closely monitored during the post-tensioning process, and a thorough examination of the slab was conducted between the tension of each cable to check for possible cracks. Both inspections were conducted to ensure that the slab was effectively holding the precompression produced by tensioning the tendons.

After post-tensioning the tendons the slab was picked up. It was originally designed to be picked up from 8 hooks but due to unexpected conditions in the factory it was decided at the moment to pick up the slab from the four middle hooks, as shown in Figure 48. The following figure shows a picture of the slab elevated at 1 ft from the factory

floor. However, this picked up was the only load case tested and the full-scale was not placed on steel W-section beams.

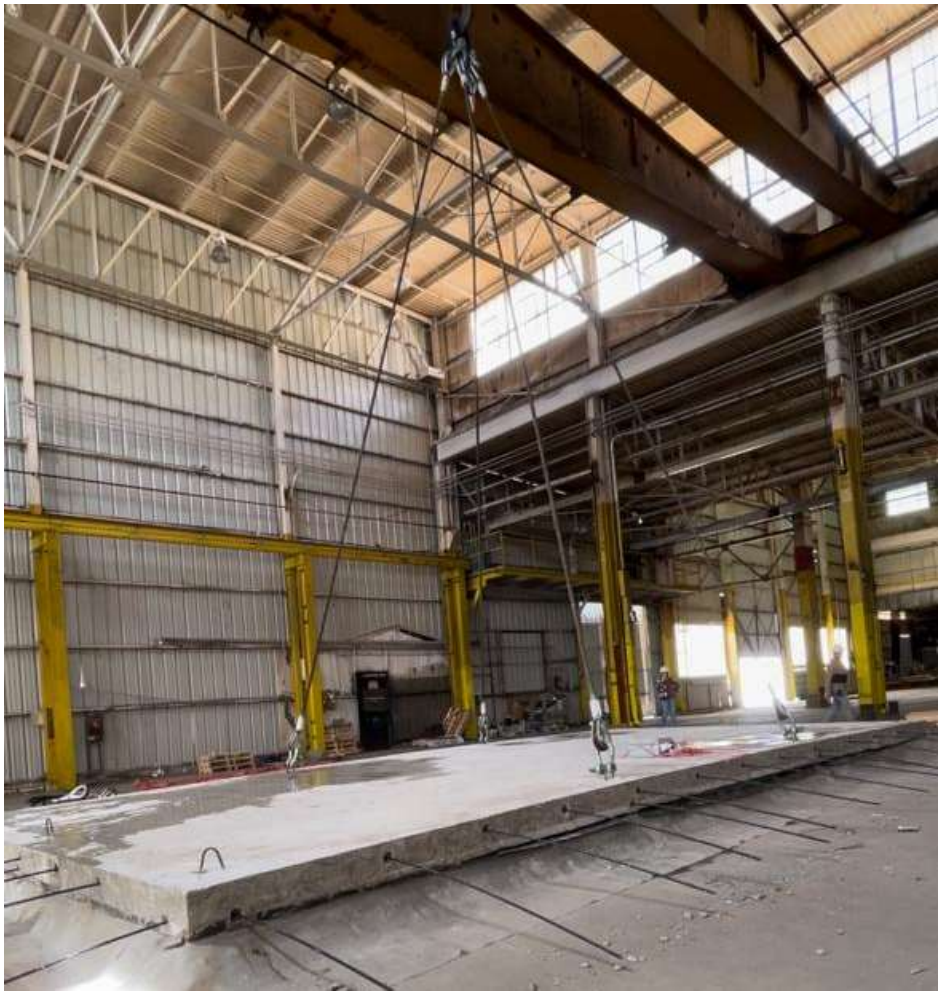

Figure 48 – Full-scale slab being pick up from four middle lifting hooks using overhead crane at the factory.

Chapter 4: Results and Analysis

This research project aims to develop a practical design for precast post-tensioned slabs that use lightweight concrete, as discussed in Chapter 2. The project's findings are presented in three parts. First, the results of the mix design phase will be discussed. Second, the outcomes from the first slab prototype, including various insert prototypes and the support prototype, are presented. Finally, the findings from the large-scale prototype are discussed.

4.1 Mix Design Results

The final mix design mentioned in Section 3.2.2.1 “LWCA Properties” was tested as previously stated for compressive strength, modulus of elasticity, flexural strength, unit weight and shrinkage. The results shown in the following figures contain the results obtained from the last 6 mixes using Livingston (L9, L10, L11, L12, L13, and L14). The last one, L14, was provided by Dolese for the first slab prototype following the mix design proportion provided to them. All these mixes can be found in Appendix J.

4.1.1 Fresh Concrete

The concrete was tested for different fresh properties including slump and unit weight, and notes on ambient temperature and humidity were taken during each trial mix cast. Table 6 shows these data for the 6 mixes mentioned previously.

Table 6 - Characteristic of the last 6 trial mixes in fresh state.

Mix	Date	Time	Slump (in.)	Unit Weight (lbs/ft^3)	Air Temp. (°F)	Humidity (%)	Notes
L9	9/15/2023	9:30 AM	7.5 - 8	111.1	75.0	55	4.95 lb of water added
L10	9/22/2023	10:00 AM	7.25	112.0	86.4	56	5.5 lb of water left
L11	10/13/2023	11:15 AM	6.0	114.0	70.0	55	-
L12	11/3/2023	12:45 PM	7.0	115.0	75.0	60	2.73 lb of water left
L13	2/2/2024	12:30 PM	7.0	114.5	65.0	58	3.5 lb of water added
L14	3/5/2024	10:20 AM	7.5	118.9	54.0	70	-

Table 6 shows that the unit weight of all these mixes ranged between the target objective of 110 to 120 lb/ft^3. Also, this unit weight is wet unit weight which means the actual unit weight or density of the concrete was considerably lower when dry. The unit weight values are also shown in Figure 49. Furthermore, it is also possible to appreciate that the slump of all these trial mixes were in the range of 6 – 8 in. as previously required. Finally, in the "notes" column the amount of water added or left outside the mix is noted; this shows how variable the water content in the mix can be when dealing when LWA.

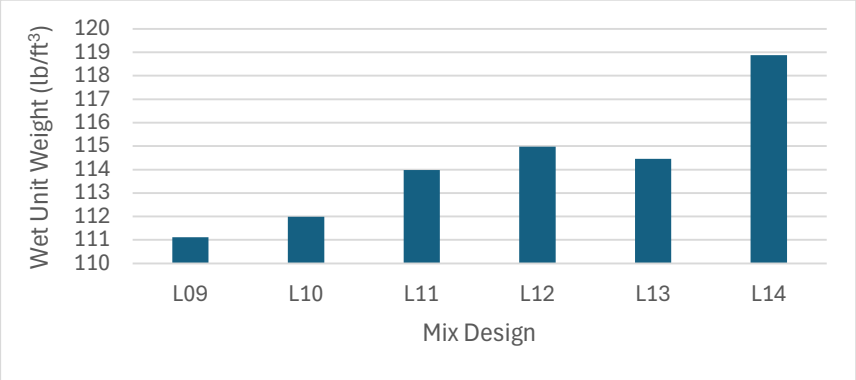

Figure 49 - Wet unit weight of LWC mixes.

4.1.2 Compressive Strength

Figure 50 presents the compressive strength results for the final 6 trial batches. All compressive strength cylinders attained close to 3,000 psi compressive strength at 3 days, similar to conventional concrete. However, the crucial data point of this test is the strength of the concrete at 7 days, when post-tensioning will be done. For mixes L9, L10, L11, and L12, the strength at this age ranged between 3,300 psi to 3,800 psi. Whereas, the last two mixes (L13 and L14), which had modified parameters, had a strength of approximately 4,000 psi at 7 days and compressive strength between 4,000 and 5,000 psi at 28 days which is important to service loading. These modified parameters can be seen in Appendix J where all the mixes done with Livingston are listed. Moreover, in Figure 50 is possible to see that the compressive strength for L14 was around 500 psi higher than L13 or L12. It is also possible to see a correlation between higher density and higher compressive strength.

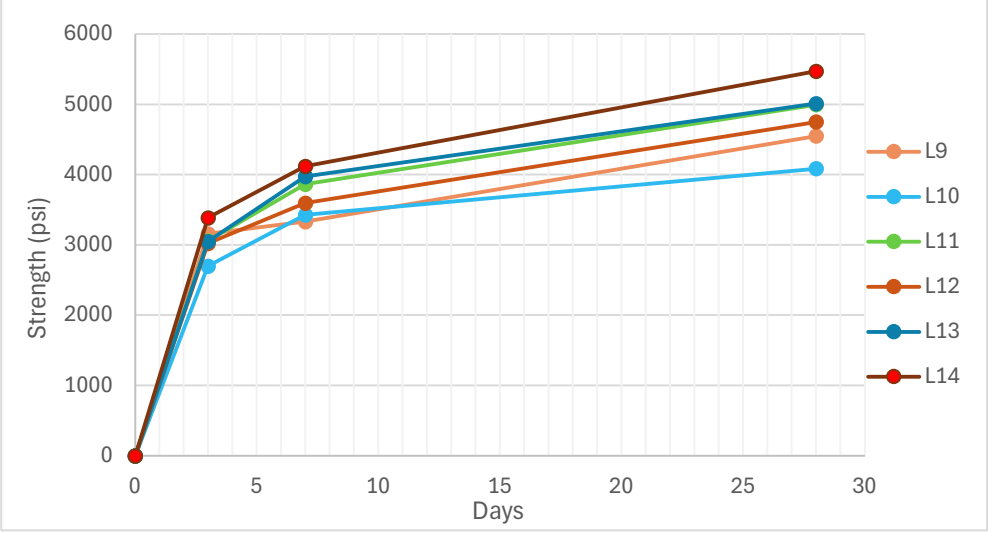

Figure 50 - Compressive strength of LWC trial mixes.

4.1.3 Modulus of Elasticity

The modulus of elasticity was only evaluated for mixes L12 and L14 as they were close to the final LWC mix design to be used for the trial slabs. It should be noted that two L12 specimens were discarded due to uncertain data at three days, leaving only one specimen for this mix at that age.

According to ACI 318-19 section 19.2.2.1 (a), for values of unit weight between 90 and 160 lb/ft^3 the modulus of elasticity (E_c) should be calculated according to Equation 2.

$$E_c = {w_c}^{1.5} * 33 * \sqrt{f'_c} \qquad (2)$$

By using this equation, it is possible to compare the theoretical values from ACI 318-19 with the experimental measured values, as shown in Table 7. ACI 318-19 specifies that the testing age for MOE shall be 28 days, however in this research, it was decided to measure this property at the three different testing ages to be able to obtain more data points.

Table 7 - Modulus of Elasticity comparison between measured values and calculated values using ACI 318-19.

Age (days)	L12				L14			
	w_c (lb/ft^3)	f'c (psi)	ACI - Ec (psi)	Measured Ec (psi)	w_c (lb/ft^3)	f'c (psi)	ACI - Ec (psi)	Measured Ec (psi)
3	104	3,020	1,920,000	2,670,000	110	3,390	2,215,000	2,080,000
7		3,600	2,100,000	2,130,000		4,120	2,440,000	2,040,000
28		4,750	2,410,000	2,330,000		5,470	2,820,000	2,720,000

Table 7 displays the comparison between the theoretical values obtained from the ACI formula and the measured values, indicating that both values lie in the same range. This suggests that the ACI formula provides a good estimation for this mix design, which is needed for prestressing because a high or low modulus can result in inaccurate calculations. This is also shown in the bar graph in Figure 51.

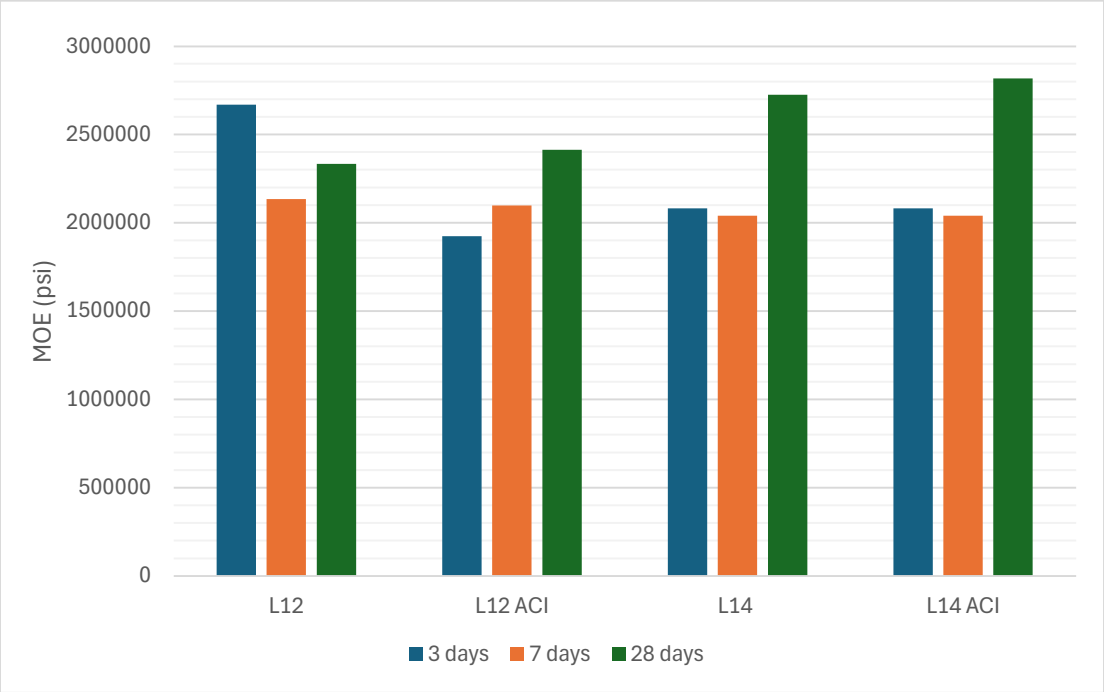

Figure 51 - Modulus of Elasticity comparison between measured values and calculated values using ACI 318-19.

4.1.4 Modulus of Rupture

The results from the two prism test at 28 days for mixes L9, L10, L11, L12, L13, and L14 were lower than expected, and lower in comparison to the value obtained following Equation 3 provided by ACI 318-19 section 19.2.3.1.

$$f_r = 7.5 * \lambda * \sqrt{f'_c} \qquad (3)$$

where the value of λ was conservatively taken equal to 0.75 according to 19.2.4.2 since the value of equilibrium density, w_c, changed between mixes. The results are presented in Figure 52.

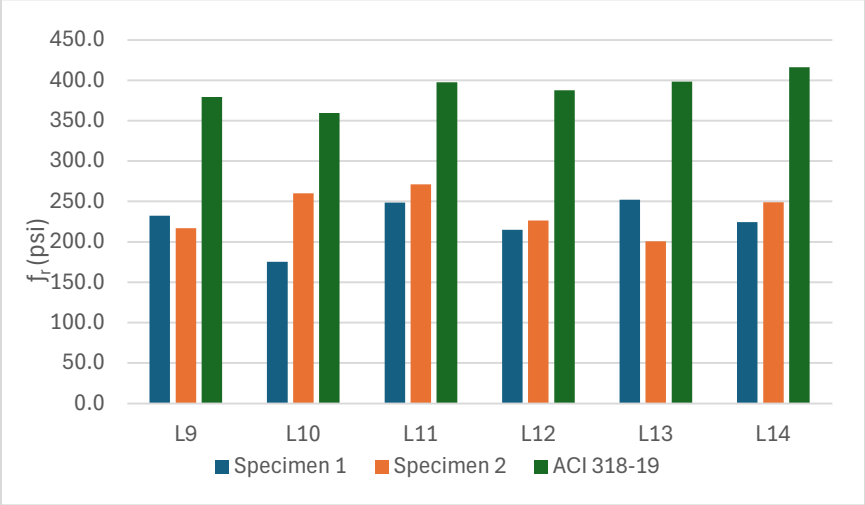

Figure 52 - Modulus of Rupture comparison between value measured from mixes and calculated value provided by ACI 318-19.

Figure 52 shows that the values obtained from the mixes were between 30 to 40% less than the values calculated according to ACI 318-19. Mix L11 had the highest flexural strength and mix L12 had the most consistent test results of the two specimens tested for that mix. Although both mixes have the same water cement ratio as well as the same amount of cement. Mix L11 had higher compressive strength at 28 days.

4.1.5 Shrinkage

Shrinkage was measured in order to ensure that the final mix design would not suffer from excessive shrinkage, and subsequently prestress loss, over time. Three

specimens from Mix L12, because this was considered to be the final LWC mix design, were measured at intervals described in Section 3.2.3.2 starting 3 days after casting. The values obtained from these measurements were used to create a shrinkage curve where the y-axis indicated the strain change in microstrain relative to time measured in days, shown in Figure 53.

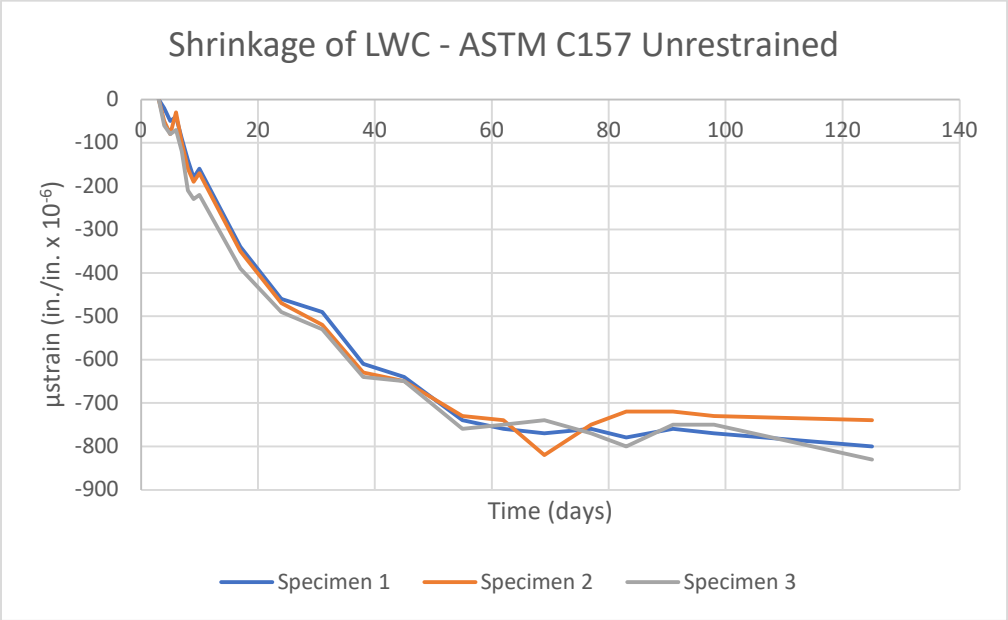

Figure 53 - Shrinkage of LWC mix measured according to ASTM C157.

Figure 53 shows that the shrinkage curve started to plateau after approximately 60 days. Before this point, a substantial almost linear increment in shrinkage was observed up to the range between 700 to 800 microstrain. According to research in the literature review, the near exponential trend could be a result of the internal curing of the concrete due to the presence of water inside the LWA days after casting.

Furthermore, it is useful to compare these shrinkage results to specimens of NWC and LWC tested for shrinkage in previous research done by Wendling et al. (2018), the

results obtained in that study are shown in Figure 54. It is possible to see how the mix developed in this research had shrinkage faster and plateaued sooner than the mix in the research done by Wendling et al. (2018).

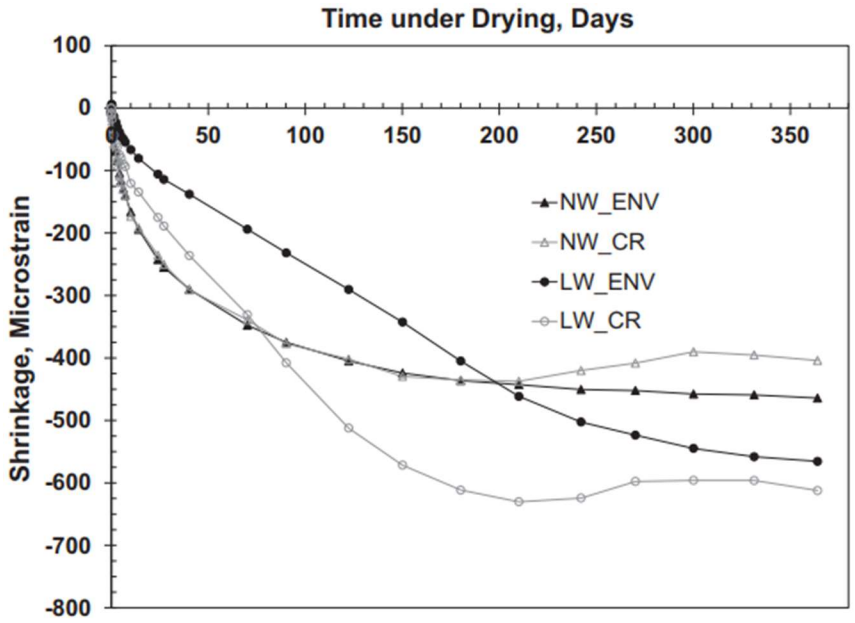

Figure 54 - Shrinkage strain of cylindrical specimen with measurements beginning at one day by Wendling et al. (2018).

However, in the graph from Wendling et al. (2018) the LWC mixes had a measured shrinkage of 225 microstrain for LW_ENV ("ENV" specimens were stored in air in the outside curing room at Fears lab) at 100 days and approximately 400 microstrain for LW_CR ("CR" specimens were stored in a tent built in the main high bay and maintained relatively constant temperature) at 100 days, while in the current study the shrinkage measured for the LWC mix was between 700 and 800 microstrain. This would mean that the shrinkage obtained for the mix developed in this research is at least twice as much as the one obtained by Wendling et al. (2018). This additional shrinkage could have a

significant impact on the prestress losses and cracking behavior of the slab. It seems that the ENV specimens from Wendling et al. (2018), and the specimens used in the current study were both stored in the same curing room in air, which may explain why they both show a near exponential trend followed by a plateau. This behavior could be attributed to the consistent storage and environmental conditions.

4.1.6 Unit Weight

As described in Section 3.2.3.2, unit weight was also measured for the hardened concrete. This property was measured following the two methods: the cylinder volume method (CVM) and the equilibrium unit weight done following ASTM C567 on the trial mixes L10, L11, L12, L13, and L14. The results of these measurements showed that the CVM results were close to the results from the equilibrium unit weight. Figure 55 shows the results from both methods at the testing age of 28 days and 56 days after casting.

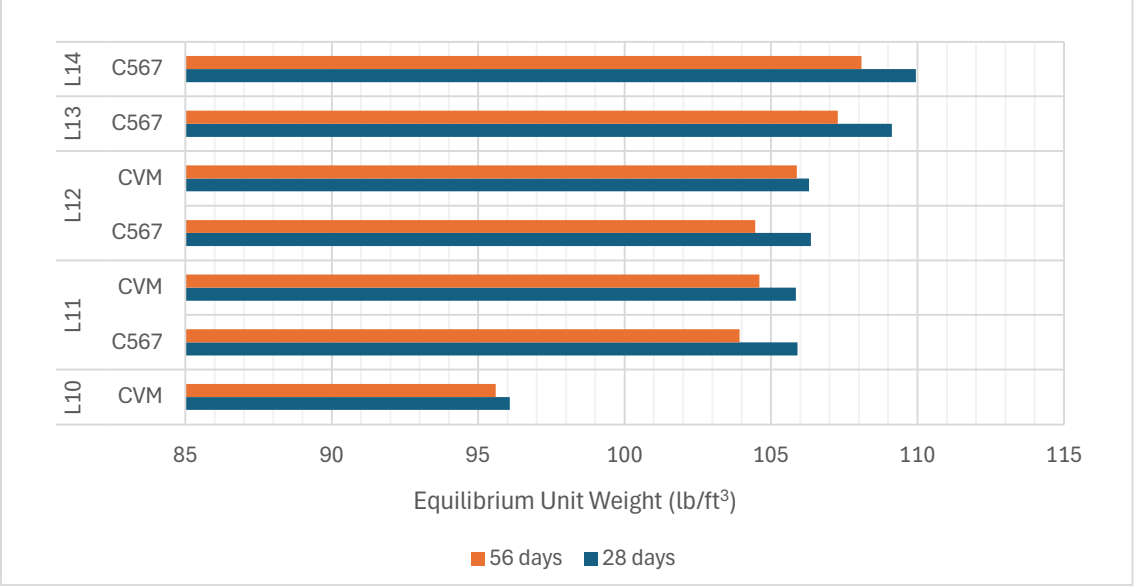

Figure 55 - Dry unit weight (CVM) and equilibrium unit weight (ASTM C567) of trial batches.

The dry unit weight of LWC mixes was 5-10% lower, compared to the wet unit weight. This indicates the water inside the LWA is evaporating through time making the LWC even lighter than first measured.

4.2 Slab Design Results

In Chapter 3, it was mentioned that the slab design was an iterative process that involved evaluating multiple models using various techniques, methods, and software. The two primary methods used were the equivalent frame method for analyzing two-way slabs and Ram Concept. Other design software, such as SAFE 21, developed by CSI, was also used in this stage but was later abandoned in favor of Ram Concept. The next section discusses the results from the different models and explains how the iterations were performed to achieve a final design that would respond appropriately to all loading conditions.

4.2.1 Equivalent Frame Method Spreadsheet

The results obtained from the equivalent frame method, which was performed only on the service load case using a spreadsheet developed as part of previous research at the University of Oklahoma, served as a good starting point with regard to the dimensions, prestressing amount, and number of tendons required for the slab. However, since the spreadsheet was originally designed for use on columns, it did not properly take into account the stiffness of the supports. As a result, the calculated rotation at both sides of the supports, as well as the rotation deflection (δ'' in.), were higher than expected, leading to excessive central long-term deflection, which in turn resulted in "NG" (Not

Good) short-term and long-term checks, as shown in Table 8. A sample of the equivalent frame method developed in previous research at the University of Oklahoma can be found in Appendix K.

Table 8 - Part of Equivalent Frame Method spreadsheet showing excessive deflections.

66	Basic Deflection, δ' (in.)	0.0039	0.0039	0.0039	0.0039
67	Column Strip, δ_c (in.)	0.0039	0.0039	0.0039	0.0039
68	Middle Strip, δ_s (in.)	0.0039	0.0039	0.0039	0.0039
69	Rotation at Left End, θ_A (rad)	0.0008	0.0147	0.0015	0.0272
70	Rotation at Right End, θ_B (rad)	0.0147	0.0047	0.0272	0.0088
71	Rotation Deflection, δ'' (in.)	0.174	0.218	0.324	0.405
72	Net column Strip, δ_{cx} (in.)	0.178	0.222	0.328	0.409
73	Net Middle Strip, δ_{sx} (in.)	0.178	0.222	0.328	0.409
74	Central Deflection, Δ (in.)	**0.347**	**0.398**	**0.497**	**0.585**
75	Long Term Deflection, Δ_{lt} (in.)	0.929	1.065	1.330	1.566
76	Deflection Limit, L/480 (in.)	0.1875	0.1875	0.1875	0.1875
77	Short-Term Check	**NG**	**NG**	**NG**	**NG**
78	Long-Term Check	**NG**	**NG**	**NG**	**NG**

The design for a precast post-tensioned two-way waffle slab underwent multiple iterations and changes in the slab dimensions and prestressing. The spreadsheet used to represent the design was modified several times as well. However, after careful consideration, it was determined that the deflection results obtained from the spreadsheet were not entirely reliable. It was decided to use the baseline design from the spreadsheet and verify slab deflections using design software for varying loading conditions.

As previously mentioned, the design software SAFE 21 was initially used for developing the slab design. However, it was decided to switch to RAM Concept, after a few iterations and changes, due to the unavailability of its license.

4.2.2 RAM Concept

The slab was designed to withstand three different loading cases, each with different support conditions. The first loading case represents the entire loading of the townhome unit, with all the supports under the slab. The second loading case is just the self-weight of the slab during removal from the forms, and the third loading case is the slab on top of steel W-section beams with the loads from the first-floor module in place for transport. Unfortunately, it was not possible to simulate all these loading conditions in the same file, so three different models were generated for each iteration, changing the supports and loads. This section displays some of the iterations and support condition results. It demonstrates how they were modified to achieve an overlapping slab design that would respond to all loading conditions. A summary of some of the different iterations can be found in Table 9. In total, approximately 30 iterations were done were parameters like interior and exterior beams sizes, thickness of slab, number of tendons, location of tendons and amount of total prestress, were changed.

Table 9 - Summary of slab design models using RAM Concept.

#	Slab Type	Supports # and max. spacing between them o.c.	Load Case Evaluated	Notes
3	Flat Plate	8 supports. 15 ft	2	Excessive deflection.
6	Waffle slab	8 supports. 15 ft	2	Small shear cores. Excessive deflection.
8	Waffle slab	8 supports. 15 ft	1 / 2	Failed in long spans. Small shear cores. Excessive deflection.
11	Waffle slab	12 supports. 9 ft	1	Small shear cores. Passed first loading condition only. Deflections under the limit.
13	Waffle slab	12 supports. 9 ft	2	Profile points outside slab. The space for reinforcement is too tight. Tendons sticking out of concrete section. Did not pass any loading condition.
17	Waffle slab	8 supports. 15 ft	2	Small shear cores. Did not pass second loading condition. The space for reinforcement is too tight. Excessive deflection
24	Waffle slab	12 supports. 9 ft	1	Passed first loading condition. Deflections under the limit.
25	Waffle slab	10 supports. 9 ft	2	Passed second loading condition. Deflections under the limit.
26	Waffle slab	2 beams. 12 ft	3	Passed third loading condition. Deflections under the limit.

RAM Concept defines the shear core as the parts of the “trimmed” cross section that include any vertical slices that extend from the top of the cross section to the bottom of it, as shown in Figure 56 provided by the software.

Figure 56 - Shear cored (shaded) for cross section by Bentley (RAM Concept Help).

In iteration 3 a model of a flat plate slab of the dimensions needed was modelled in RAM Concept. However, as depicted in Figure 57, its final instantaneous load deflection for load case 2 was over the deflection limit.

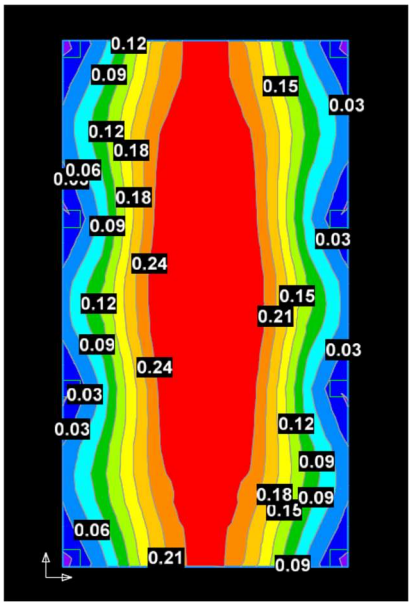

Figure 57 - Instantaneous load deflection results for iteration 3.

Iteration 6, and 8 had small shear cores due to the fact that it was modelled trying to reduce the weight of the slab more by reducing the cross section of the inner beams to 6 in. x 6 in., which resulted in not have enough concrete section to withstand the demands. Figure 58 shows excessive deflections for iterations 6 and 8 of approximately

4.05 in. and 1.03 in. and Figure 59 shows design check failures in the long span for iteration 8.

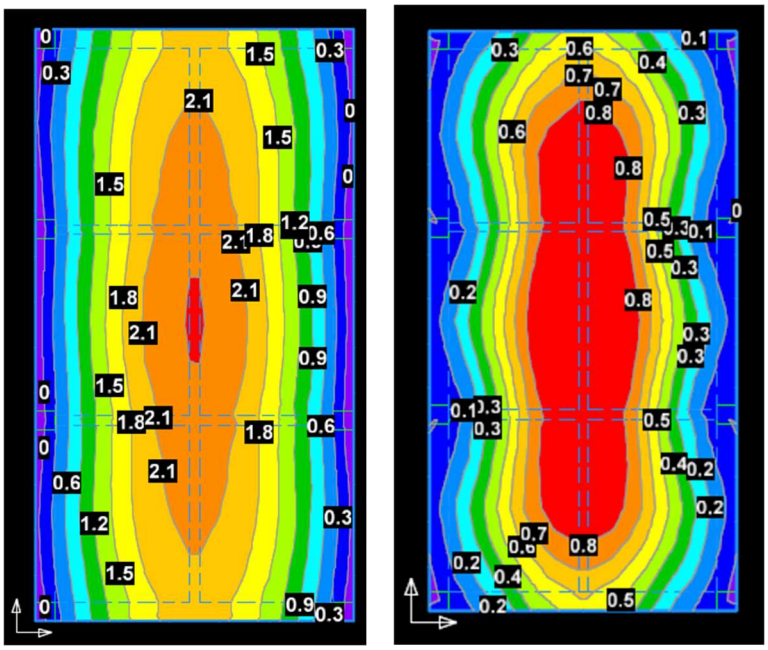

Figure 58 - Instantaneous load deflection results for iteration 6 (left) and iteration 8 (right) in load case 2.

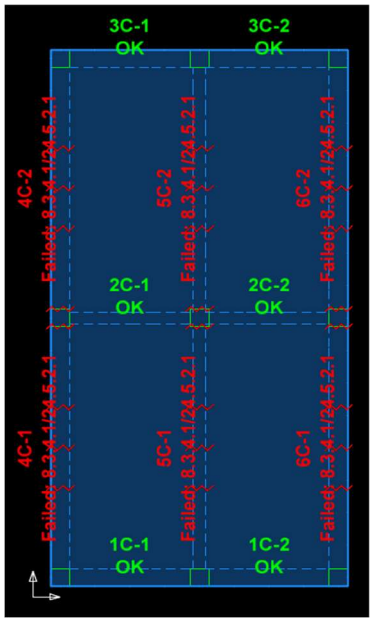

Figure 59 - Design status plan for iteration 8 in load case 1.

Iteration 11 passed the design checks, and the deflection checks, however this slab design iteration also had small shear cores for the same reason as iterations 6 and 8. Figure 60 shows slab passing design checks and deflection checks.

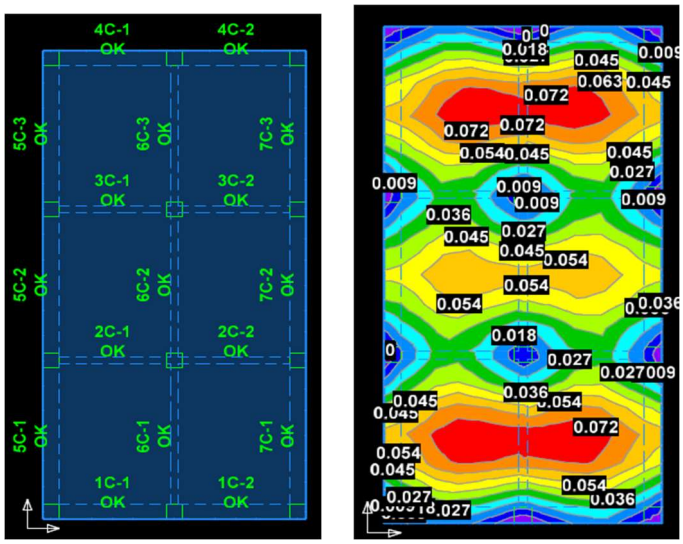

Figure 60 - Design status plan (left) and instantaneous load deflection (right) results for iteration 11 under load case 1.

Iterations 13 and 17 had very tight reinforcement spacing because RAM Concept would provide more reinforcement than that provided for the user if needed. This meant that the slab dimensions, support conditions or tendon layout were not adequately designed. Figure 61 and Figure 62 show 3D transparent perspectives of the slab reinforcement congestion for iterations 13 and 17 under the second loading condition.

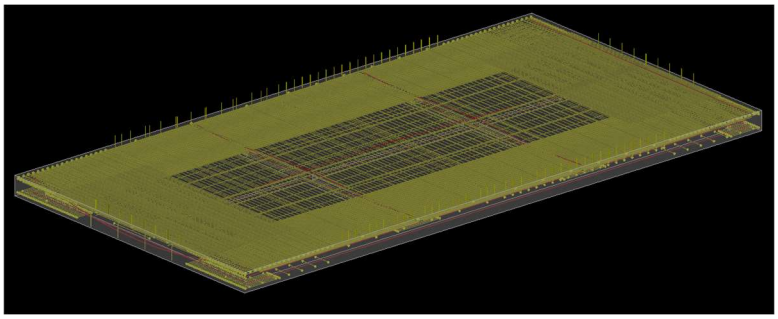

Figure 61 - Reinforcement perspective for iteration 13.

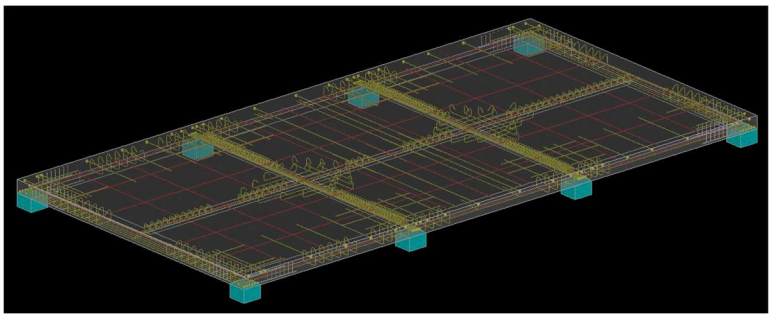

Figure 62 - Reinforcement perspective for iteration 17.

Between iterations 13 and 17 it is possible to see an improvement in the amount of reinforcement, however a close-up of the area between inner beam and support shows the reinforcement congestion (Figure 63).

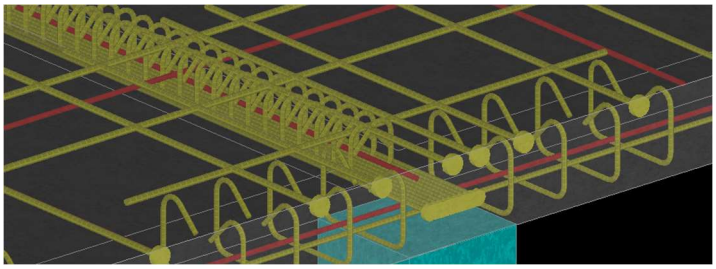

Figure 63 - Reinforcement perspective close-up between inner beam and support on iteration 17.

The last three iterations (24, 25, and 26) were the ones utilized for the final design, they also have the same dimensions and tendon layout but were done for the different loading

cases respectively. After these three models passed the design, deflection and service checks it was necessary to interpolate the required reinforcement determined for each of these models to obtain a reinforcement design adequate and equal for all three loading conditions. Once this was achieved the checks were run again on a model with this reinforcement configuration and the slab design was found to be adequate for the different load cases. Figure 64 shows the design checks for all three loading conditions.

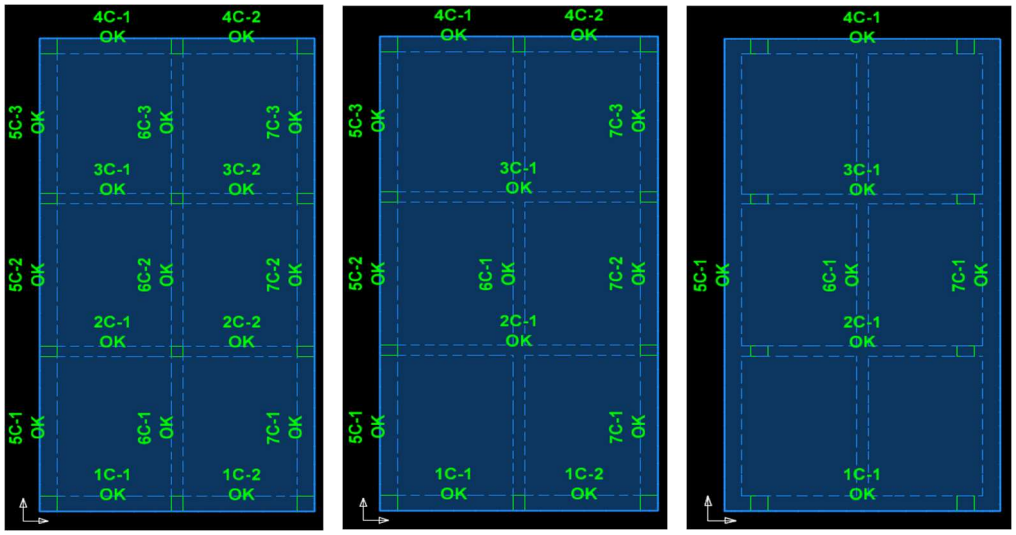

Figure 64 - Design status plan for iterations 24 (left), 25 (middle), and 26 (right).

Furthermore, Figure 65 shows the different deflection modes and values caused by the loading conditions in the three models.

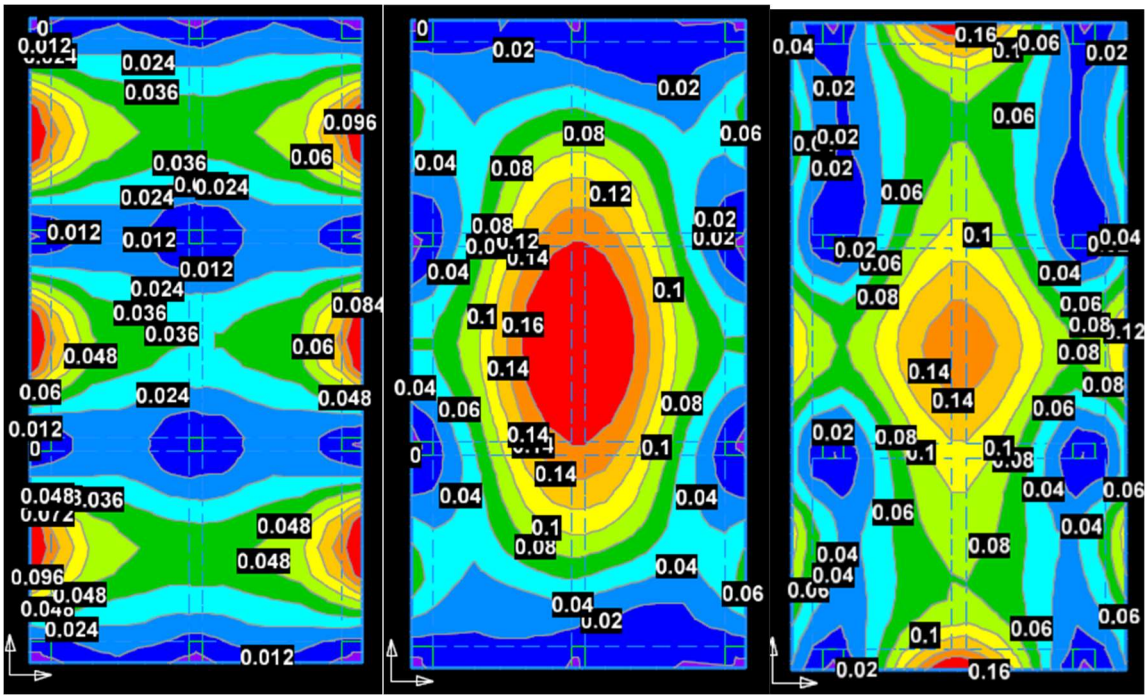

Figure 65 - Instantaneous load deflection plan for iteration 24 (left), 25 (middle), and 26 (right).

In Figure 65, the maximum deflections, represented in red in the slab, are:

- 0.12 in. for the first loading condition,
- 0.20 in. for the second loading condition, and
- 0.20 in. for the third loading condition.

These values are well under the limit previously presented in Chapter 3 of 0.4 in. calculated according to ACI Table 24.2.2 where the deflection equation is L/480. The value of L is taken as 16 ft which would be the maximum span without supports (second loading condition in the middle of the slab).

4.3 Scaled Prototype Results

The scaled prototype underwent testing at Fears Lab and the results obtained from this prototype are divided into three sections. First, the casting conditions and comments during the seven-day period prior testing are presented. Second, the results of the lifting testing are presented. Finally, the results of the steel W-section beam loading conditions are presented.

4.3.1 Casting

The scaled prototype was cast with LWC provided by Dolese. The mix was ordered according to the final mix design proportions specified in Table 4. It is important to presoak the LWA aggregate, but since the exact method used by Dolese was unknown, 20 gallons, or 3%, of water was excluded from the mix when batching the concrete. This was done to ensure that the concrete would arrive at Fears Lab neither too wet nor too dry, and the remaining water could be added carefully to achieve the desired 6-8 in. slump. Once the desired workability was achieved the slab was cast and vibrated. The vibration process was carried out on the entire slab specimen, which provided valuable insights. It was observed that in areas where there was a higher density of reinforcement, tendons, and supports, it was difficult to ensure proper consolidation of the concrete.

Furthermore, the data logger connected to the six VWSGs placed in the slab recorded data every 5 minutes. The measured values presented in Figure 66 show changes in strain during the casting process and throughout the rest of the casting day.

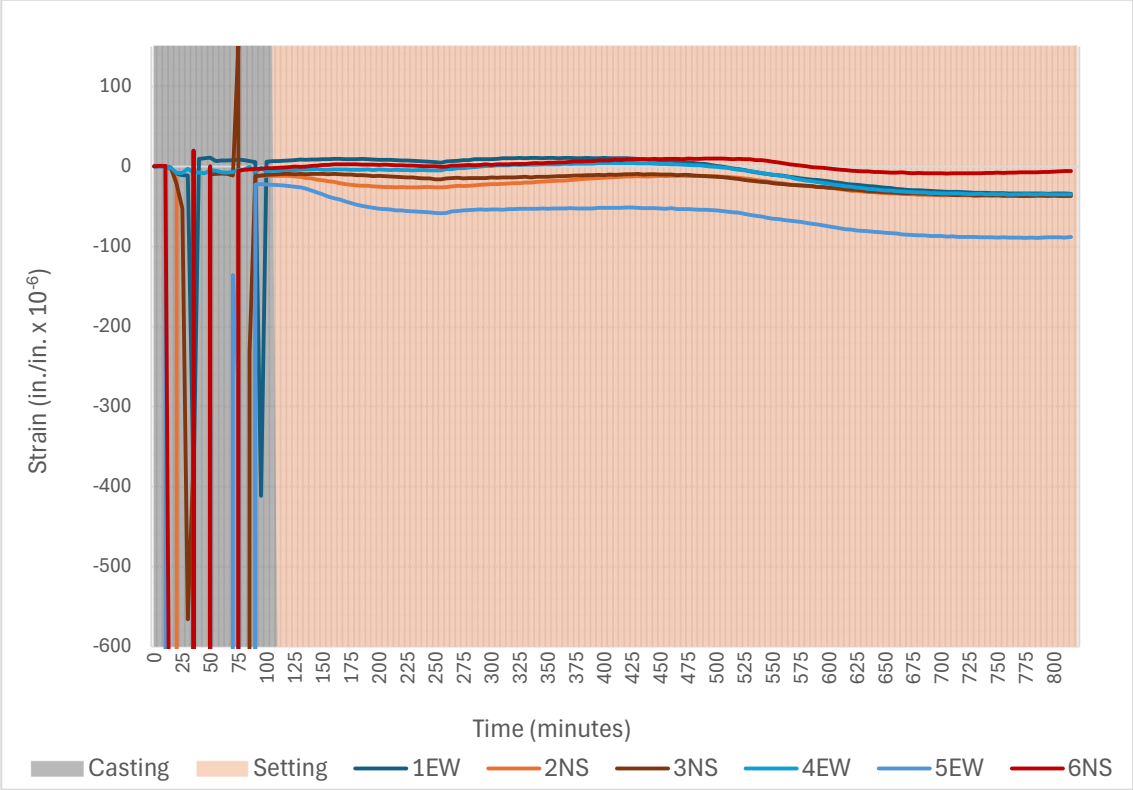

Figure 66 - VWSG measured strains over time with zero time as start of casting for scaled slab.

From Figure 66, it is evident that certain VWSGs did not record data accurately while the casting process was underway. The reason behind this anomaly is believed to be the extremely high frequency of vibrations produced by the concrete being poured into the forms. These intense vibrations caused the gauges to malfunction and not register accurate data. However, later the same day when the concrete started to set the gauges started to work properly again, that is why it is possible to see how the gauges curve stabilize during the rest of the day. Approximately 8 to 10 hours after casting, some shrinkage occurred in the concrete slab. Specifically, 5EW located at the mid-span on one of the ends of the long span of the slab experienced more shrinkage (close to 100 microstrain) than the other VWSGs.

Figure 67 shows the six VWSGs curves for the six days prior to post-tensioning and testing. Over the six days of curing the gauges reading showed an expansion of about 100 microstrain.

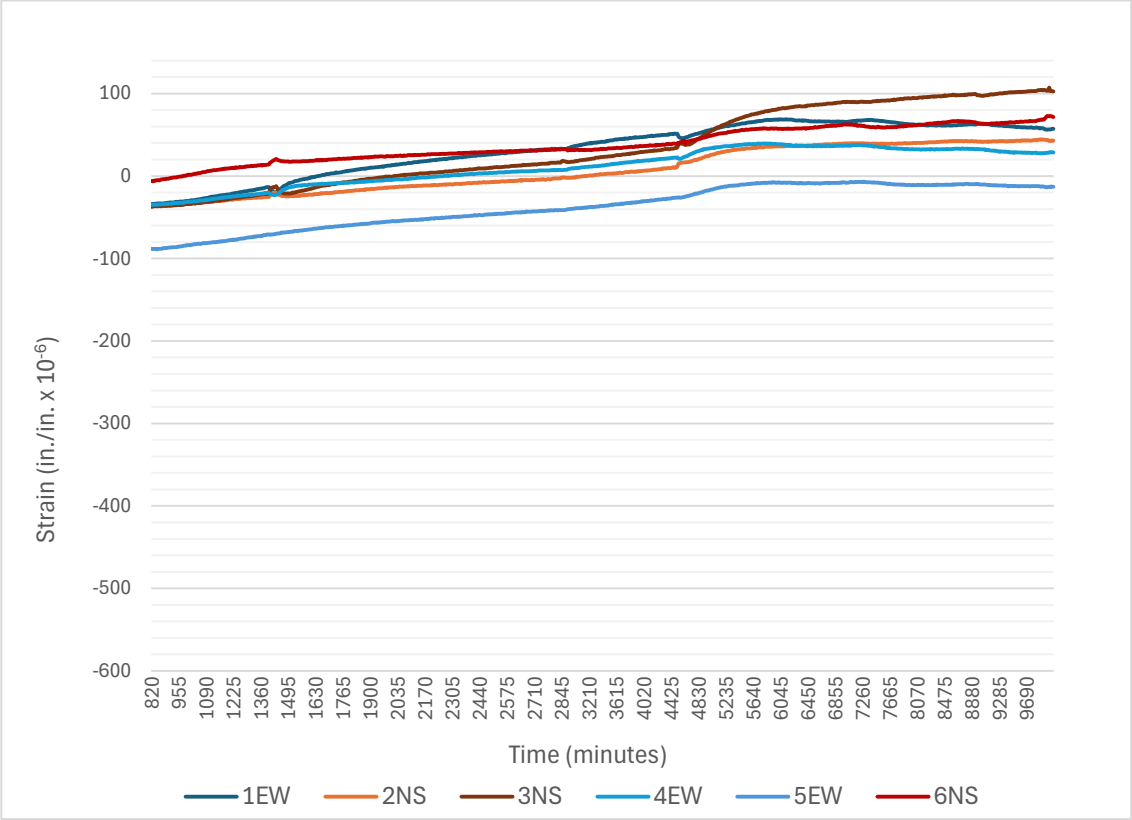

Figure 67 - VWSG measured strains during curing phase.

Throughout the entire process of curing, there was a complete absence of any discernible crazing or bleeding on the surface of the concrete and no cracking was observed.

4.3.2 Lifting Loading conditions

Two of the three loading conditions used in the RAM Concept models were evaluated for the scaled prototype at Fears Lab: the second load case (lifting from the

forms) and the third load case (placement on steel W-section beams for transport). To evaluate the second load case, the slab was lifted from four rebar lifting hooks placed in each corner. As the slab was being lifted, it was carefully checked for any cracks or deflections, and no cracks or excessive deflection were apparent to the naked eye. Figure 68 shows how the inserts were trying to be removed while the slab was being lifted representing the second load case.

Figure 68 - Attempt to remove removable inserts.

The first insert design (a wood frame with insulation foam placed around the edges) was easier to remove but was still more difficult than the prototype cast earlier. Meanwhile, the second insert design (a trapezoidal-shaped wood frame) did not come out at all, even though it was the easier of the two to remove in the previously cast smaller prototype. This is believed to be because of their size and the pre-compression applied to

the slab through post-tensioning, which was not present in the insert prototypes specimens.

For the third loading condition (transport on steel beams), a detailed visual observation was conducted after the slab was placed on top of the W beams. The purpose of the observation was to identify if cracks or deflections appeared.

Figure 69 shows the measured strain over time, during the post-tensioning, lifting, and placing on top of the W beams process, with zero time as the start of the post-tensioning process. It should be noted that the gauges were zeroed out using the values at the start of the post-tensioning process and therefore show zero strain before the post-tensioning process even though the VWSGs measured an expansion in the range of 100 microstrain during the curing phase.

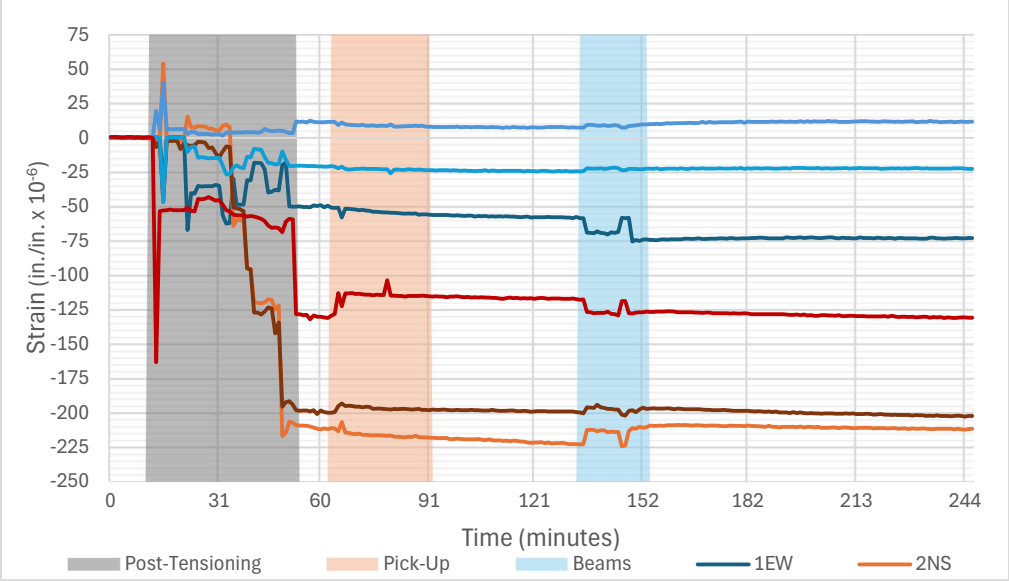

Figure 69 - VWSG measured strains during post-tensioning and loading with zero time as start of post-tensioning of the scaled prototype.

Figure 69 shows some interesting things. First, in the post-tensioning process (shadowed gray) primarily compression was observed for all of gauges except for VWSG 5 EW which showed less than 20 microstrain of increase in the reading, which would make sense because the post-tensioning sequence began in the North-South direction in the tendon located above this gauge that was in the East-West. Also, since the post-tensioning was done in two phases to avoid applying the full stress at once, it is possible to see two sudden changes in the readings. The maximum compression was measured by the gauges located in the North-South direction which makes sense since that direction that had more total post-tensioning. These three gauges measured a decrease between 125 and 225 microstrain. The maximum compression measured by gauge 2 NS in the middle of the long span was almost 225 microstrain, which was closely followed by gauge 3 NS, in the very center of the scaled slab, measuring 220 microstrain. Gauge 6 NS measured 125 microstrain which makes sense to be less than the previous two because the post-tensioning was not uniform having two tendons in the middle of the long span and only one in the direction of 6 NS.

Furthermore, the North-South gauges showed increases in the reading, i.e. tension, during the lifting phase (shadowed orange in Figure 69). However, these changes were only approximately 10 microstrain, while the East-West gauges did not record any significant changes. This is believed to be due to the lightweight of the slab (around 6,000 lb) and the short span. Once the slab was set on top of the W beams not much change was recorded either, again due to the lightweight of the slab. However, 10 to 15

microstrain changes were observed for almost all of the gauges except 4 EW and 5 EW. These small changes are both compression and tension in the slab. Finally, gauges 3NS and 6 NS measured creep in the following 4 hours when the scaled prototype was sitting on the support bolts. Table 10 shows the total post-tensioning and net eccentricity in each direction.

Table 10 - Total post-tensioning and net eccentricity in each direction for the scaled prototype.

Span	# of tendons	Cross section of concrete (in^2)	Total Post-tensioning force (lb)	Total Post-tensioning stress (psi)	Net Eccentricity (in) From the bottom
Long Span	8	896	211,200	236	3.875
Short Span	4	384	105,600	275	3.5

After placing the slab on the W beams, it was lifted again and set on the support bolts (end of shadowed blue). The support bolts responded as expected with no cracking or damage observed. As shown in Figure 69, no excessive compression or tension in the slab was measured after the bolts were in place (shown in Figure 69 after 152 minutes). In fact, it is noticeable that their curves are rather steady and do not present any jumps.

4.4 Full-Scale Prototype Results

In Chapter 3, it was mentioned that the full-scale prototype was produced at the House Factory facility using NWC. This prototype was distinct from the scaled prototype and was only tested for the pick-up loading condition (load case 2). The results will be presented in two sections: casting results and loading results.

4.4.1 Casting

The slab was cast slowly using the ready-mix truck chute to fill the slab forms and the concrete was distributed across the forms while the mixer truck moved parallel to the long direction. At the same time, the concrete was being poured into the forms, it was vibrated to ensure proper consolidation. The measured data from the six VWSGs during the casting phase and the following seven days of curing is presented in Figure 70.

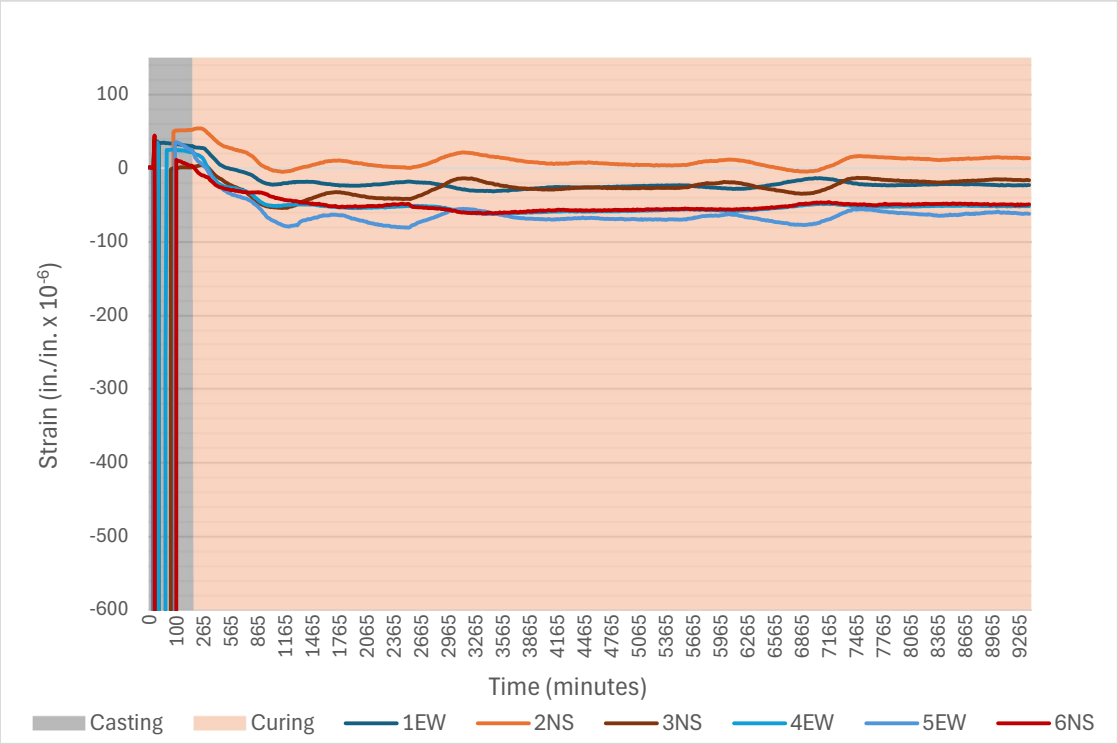

Figure 70 - VWSG measured strains over time with zero time as start of the full-scale prototype.

It is evident that certain VWSGs did not record data accurately while the casting process was underway. However, later that day and for the following 6 days the strain gauges functioned correctly, and the shrinkage strain measured by all of them was in a range of 100 microstrain. It should be noted that the internal temperature of the NWC

was between 8 and 18°C less, than the internal temperature measured in the scaled prototype. Once again, throughout the entire process of curing, there was a complete absence of any discernible crazing or bleeding on the surface of the concrete and no cracking was observed.

4.4.2 Loading conditions

After the 7 days of curing, the slab was post-tensioned following the procedure explained in Section 3.4.2. Figure 71 shows the measured strains during the post-tensioning period.

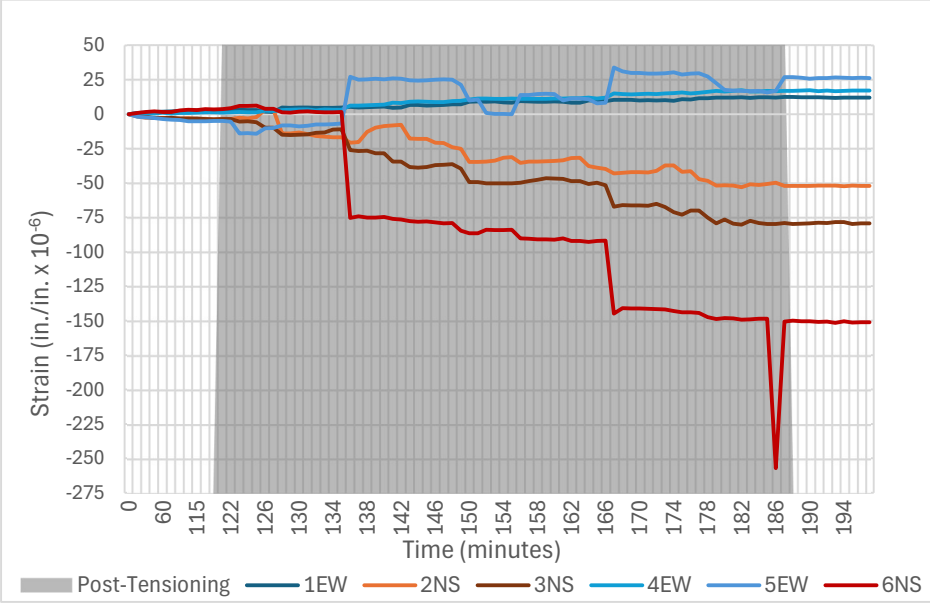

Figure 71 - VWSG measured strains with zero time set some minutes before start post-tensioning.

It is evident from Figure 71 that the gauges in the North-South direction experienced more compression compared to the gauges in the East-West direction, which measured hardly any change. This indicates that the longer span experienced greater precompression than the shorter span even though the net applied prestress was similar

in both directions. Table 11 displays the total post-tensioning forces and stresses, and the net eccentricity in both directions.

Table 11 - Total post-tensioning and net eccentricity in each direction for the full-scale prototype

Span	# of tendons	Cross section of concrete (in^2)	Total Post-tensioning force (lb)	Total Post-tensioning stress (psi)	Net Eccentricity (in)
Long Span	16	1,648	422,400	256	4.2
Short Span	8	896	211,200	236	3.875

The amount of post-tensioning stress (psi) applied to the long span of the full-scale slab is almost equivalent to the amount applied in the scaled prototype, indicating an accurate representation in the scaled prototype. However, the short span has a significantly lower total post-tensioning of 236 psi compared to the scaled prototype's 275 psi, which was not intended.

The smaller prestress, combined with the fact that the picking mechanism that was utilized in the factory was not the one taken into account during the design, had an impact on the results of the slab pick-up loading condition. The full-scale slab was meant to be lifted from at least 8 points, but ideally 10 points, and these lifting hooks were included in the slab during casting. However, only 4 equal length wire ropes with shackles were available and were used instead of the anticipated spreader beam or 8 adjustable chains. These 4 wire ropes were used to first lift the slab from the 4 picking hooks located at 1/3 and 2/3 of the long span. Although the slab was lifted from the ground, there was significant deflection observed towards the ends of it, as shown in Figure 72.

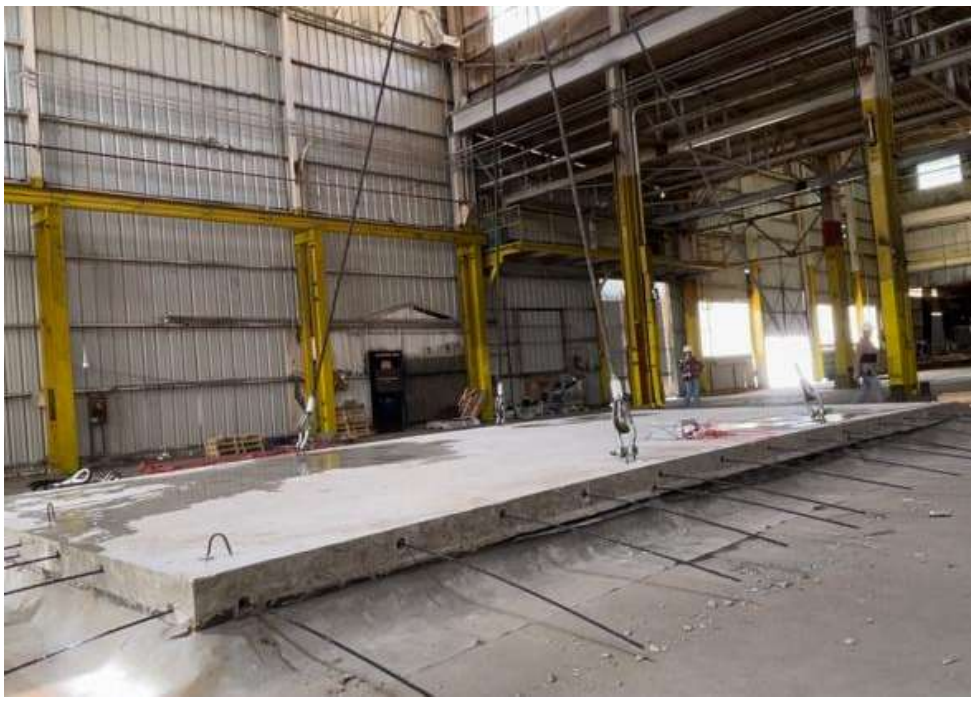

Figure 72 - Full-scale slab being picked up by the four middle hooks.

After that the slab was lifted at these four internal points, the slab was placed back on the ground and an attempt was made to lift it from the 4 lifting hooks at the corners. This second loading resulted in a large deflection in the middle of the slab (more than 8 in.). Both lifting methods used for the full-scale slab are shown in Figure 73.

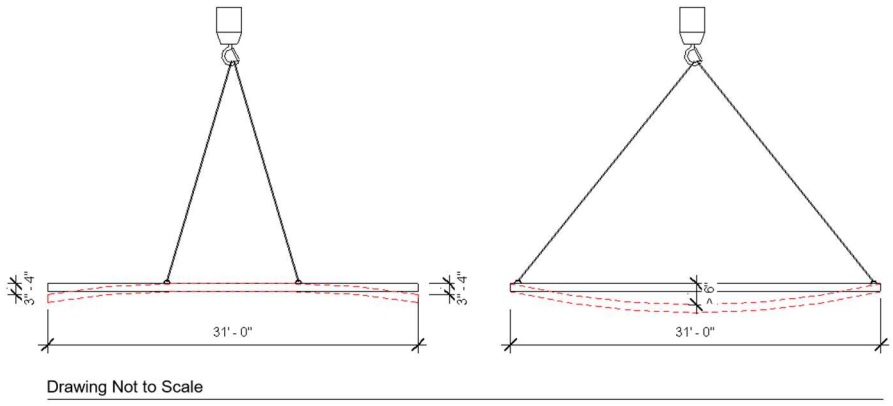

Figure 73 – Lifting methods used for the full-scale slab including Middle lift (left) and end lift (right).

When the slab was lifted from the middle sets of lifting hooks, no cracks were observed. However, when the slab was lifted from the ends, some minor cracks were observed despite the large deflection in the middle. Fortunately, no large cracks or concrete crushing were detected anywhere.

The strain measured by the VWSGs during the two pick-up options utilized are shown in Figure 74. Time zero is taken as the time when post-tensioning started for this reason the following graph initial reading was at 197 minutes.

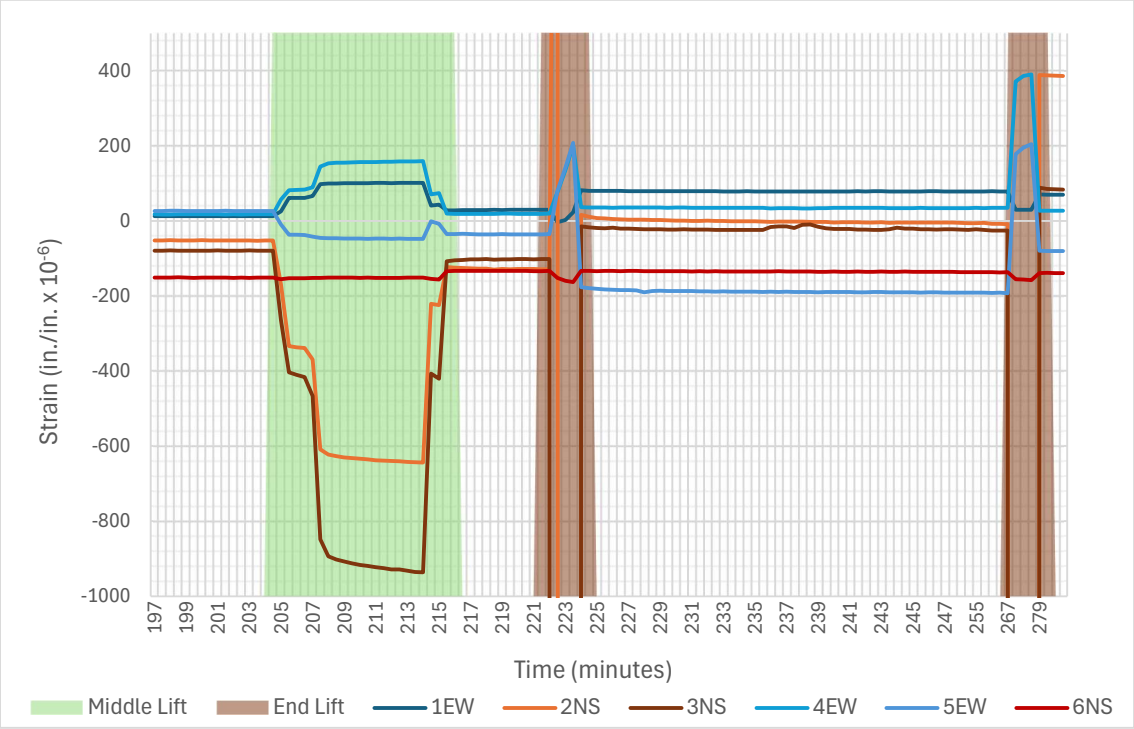

Figure 74 - VWSG measured strains during the different lifting conditions.

Due to the large deflections mentioned previously it is possible to see large changes in compression and tension measured by the different gauges. Figure 74 shows how the 4 gauges located in the middle of the long span measured the largest change during the middle lift. Gauges 2 NS and 3 NS underwent a change of approximately 550 and 750 microstrain in compression respectively, while gauges 1 EW and 4 EW both changed around 100 microstrain in tension. When it comes to the end lift the changes measured by the gauges were considerably larger due to the large deflection the slab suffered, and for gauges 2 NS and 3 NS the measurements were beyond their range. Furthermore, the slab was cast directly on top of the concrete floor of the House Factory facility with only plastic as a bond breaker, this created certain vacuum force between the two concrete which made it harder for the overhead crane to lift initially.

Since the slab was not picked up the way it was originally modelled and did not perform well under these conditions, it was decided to model the conditions under which it was actually picked up using RAM Concept and compare the results.

The results from RAM Concept confirmed the observations done in the field. Furthermore, the slab did not pass the design checks under this condition and showed even larger deflections than observed for both cases (this was also a result that these observed deflections were estimated since it was unsafe to get close for a measurement). Figure 75 shows the design status of the slab and the deflection produced by picking it up from the middle 4 lifting hooks. Figure 76 shows the design status of the slab and the deflection produced by picking it up from the lifting hooks located at the four corners of the slab.

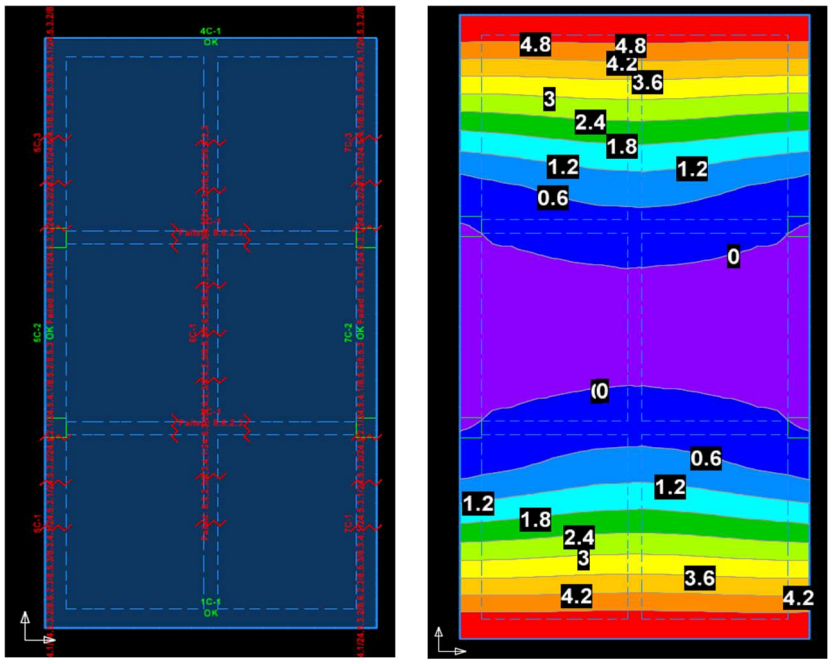

Figure 75 - Design status plan (left) and instantaneous load deflection (right) plans for model created to represent the full-scale slab middle lift.

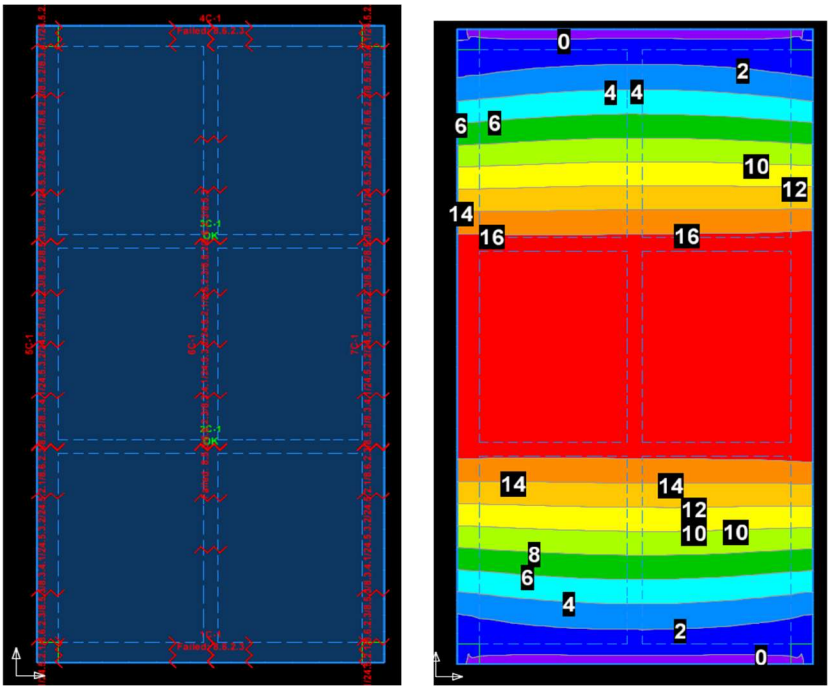

Figure 76 - Design status plan (left) and instantaneous load deflection (right) plans for model created to represent the full-scale slab end lift.

4.5 Support Results

The scaled prototype as well as the full-scale prototype were built using support option A as mentioned earlier. Figure 77 shows the support option A fabricated for the full-scale prototype, while Figure 78 shows the formwork with support option B in place before casting the concrete.

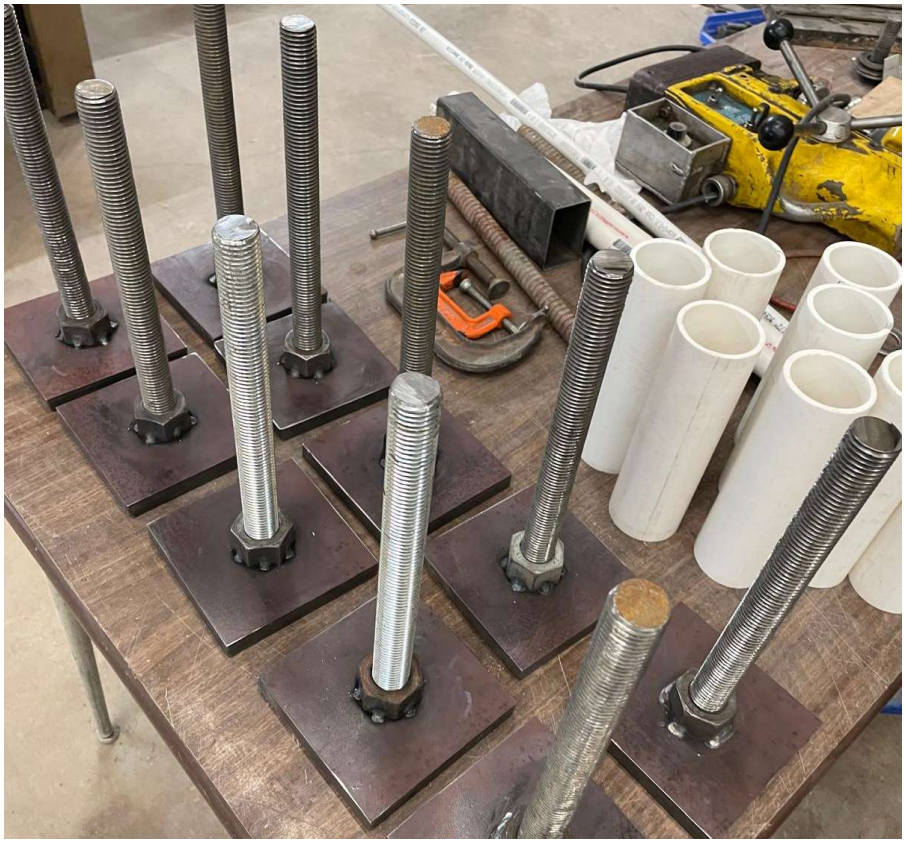

Figure 77 - Support option A fabrication.

Figure 78 - Support option B inside formwork before concrete was cast.

Support A performed as expected in the scaled prototype, but challenges were encountered during full-scale testing. The issue was due to some bolts not making contact with the ground, and a faulty nut that was tack welded on the plate's top. These tack welds ultimately failed, likely because the weight of the slab was supported by a few tack welds instead of the plate itself, as originally intended.

As for support B, it was only cast in a 2 ft x 2 ft x 8 in. LWC test specimen that was tested for punching shear at Fears Lab, as shown in Figure 80.

Figure 79 - Punching shear testing set-up for support B.

This specimen failed as expected and the test was considered successful. The shape of the shear failure as well as the type of failure corresponded to what was expected. Figure 81 shows the specimen punching shear failure after the maximum capacity was achieved.

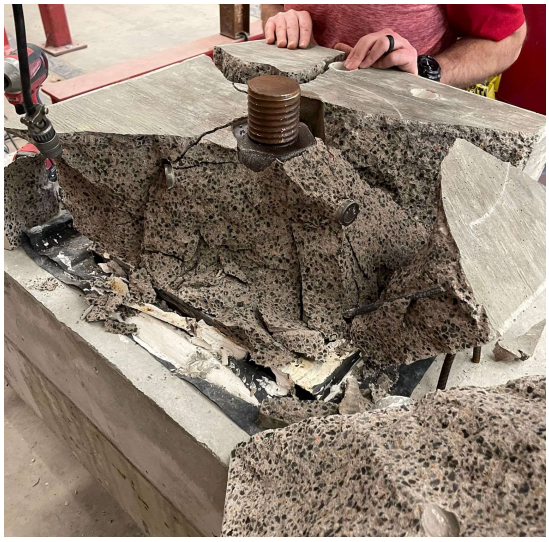

Figure 80 - Punching shear failure for support B test specimen.

Furthermore, the only data recorded during this test was the load applied to the specimen, as shown in Figure 82, the maximum load that Support B reached before the failure appeared was approximately 45,000 lb.

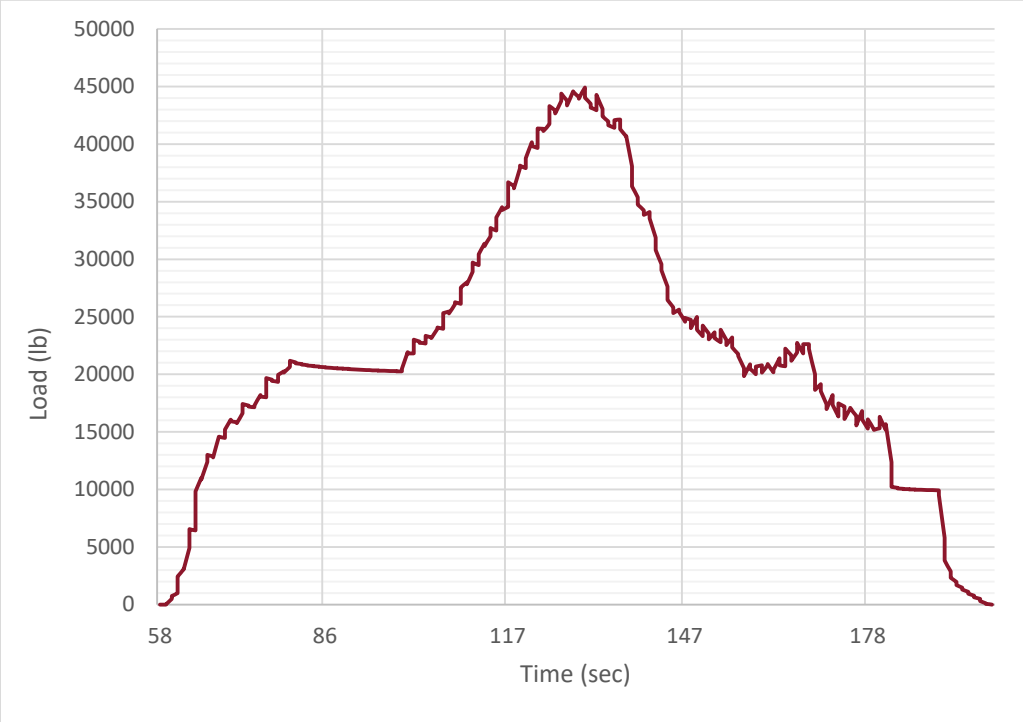

Figure 81 - Load applied to support B over time.

Chapter 5: Summary, Conclusions and Recommendations

5.1 Summary

This research aimed to find a feasible design for a precast post-tensioned slab foundation for a two-story townhome using LWC, which could be manufactured off-site and transported to the job site with the first floor already in place. The research was conducted in four phases.

First, a thorough study was conducted on existing publicly available research, which highlighted the existing gap in research related to precast LWC slabs. This phase also provided valuable insight into the behavior of LWA as well as the utilization of LWC in structures. Second, a mix design phase was undertaken, which involved designing a straightforward mix that would only utilize the basic components of concrete. One component was exchanged to make it LWC, but no additives were included that would require more skilled labor. Third, the slab design phase focused on designing a slab optimized for weight, post-tensioning, and reinforcement but would still behave correctly under the required loading conditions. Finally, the prototype testing phase was conducted to evaluate the actual stresses the slab would undergo if production started.

5.2 Conclusions

5.2.1 Mix Design Conclusions

In terms of the mix design phase in this research, it is possible to affirm that a feasible final mix design was developed, it performed as planned, and the results were positive.

- The mix's strength is similar to NWC, with similar cement content, at the final testing age of 28 days.
- Development of strength is somewhat slower due to the internal curing; however the different batches achieve almost 75% of strength 7 days after casting.
- Testing cylinders usually broke through the aggregate instead of breaking in the interface between the cement paste and the aggregate as researched identified in the literature review. This indicates that the LWA has a lower and more comparable strength and modulus of elasticity to the cement paste than the aggregate used in NWC.
- No excessive bleed water was observed on top of prototypes or specimens cast for testing.
- The final LWC mix was at least 20% lighter than the comparable NWC with a maximum fresh unit weight of 120 lb/ft^3.
- The measured flexural strength of the final LWC mix was approximately 33.3% lower than the estimated value calculated following ACI 318-19 section 19.2.3.1. This is thought to be because of the low specific gravity of the LWA utilized in this

study. Furthermore, the lower flexural strength of the concrete should be considered in the design of reinforcement and post-tensioning.

- Modulus of elasticity of the final LWC mix was in the same range as that predicted by ACI 318-19, but lower when compared to NWC.
- The shrinkage of the mix is within the same range as previous studies conducted in LWC.

5.2.2 Slab Design Conclusions

- RAM Concept was found to be an effective method for modeling post-tensioned slabs when comparing the model results with the results obtained from the scaled slab prototype and the revised model results from the full-scale prototype.
- It should be noted that RAM Concept does not account for reinforcement and tendon congestion, which means that it is necessary to be aware of these factors for the sake of constructability.
- The optimized tendon layout from RAM Concept resulted in a design that performed effectively in this research.
- Based on the results of this study it is concluded that if the model is correct and built following the supports and loading conditions, then close results can be expected in terms of deflection.

5.2.3 Scaled Slab Prototype Conclusions

- The scaled prototype worked efficiently with the LWC mix design.

- Results from the scaled prototype indicated that top tendons in the exterior beams were not necessary.
- There was a high degree of congestion in the corners of the slab, which could possibly be resolved by modifying the support design.
- It was necessary to include a minimum of one No.4 reinforcing bar longitudinally in the influence zone (6 in.) behind each anchor plate for post-tensioning. The RAM Concept design did not provide for this code requirement.
- The first insert designed (wood frame with insulation foam at the edges) came out and the other did not (trapezoidal wood frame). This may be due to the larger dimensions relative to the initial testing and the prestress applied to the slab.
- There was almost no deflection observed during either tested loading condition, which matched with the Ram Concept models.
- No cracks were observed throughout the slab.
- The leveling bolt supports (support A) functioned well as long as the slab was placed on them evenly.
- The design of support B can be improved for a better and more efficient design.

5.2.4 Full Scale Prototype Conclusions

- The proper tying of reinforcement in the full-scale prototype is critical to prevent the rebar cage from shifting during casting.
- The post-tensioning sequence can be improved so the post-tensioning can be completed more quickly.

- Not picking the slab up in the same way it was modeled in RAM Concept led to failure of the slab test.
- The lifting hooks utilized in this test were able to support over 7,500 lb each based on weight of the slab and the number of lifting hooks utilized.
- The NWC mix had a compressive strength of around 500 psi less than the LWC mix after 7 days. To ensure that this difference in strength does not affect the slab, it may be necessary to revise the NWC mix to achieve a strength closer to that of the LWC mix.
- It may be necessary to revise the leveling bolt design by welding the nuts to the bottom of the plate instead of the top due to the supports breaking in the weld between the nuts and plates.
- Excessive deflection was observed in both lifting cases examined for the full-scale prototype.
- Cracks were observed at midspan of the full-scale slab when it was picked up from the ends.
- The vacuum between the slab and concrete floor caused a downforce that made it harder for the overhead crane to lift initially.

5.3 Recommendations

The study revealed some noteworthy advancements in the development of a precast post-tensioned slab using LWC for residential foundations. However, further research and prototypes are required to establish the feasibility of this construction technology. If proven successful, it could replace the traditional on-site pouring of slabs and lead to additional prefabrication of residential buildings. The following recommendations should be taken into consideration in future research.

- There are several possibilities worth considering for optimization of the structural design. First, replacing the traditional steel reinforcing bar with fiber reinforced polymer would be a great idea to reduce the overall weight of the structure, without compromising its strength. Additionally, using headed reinforcing bars instead of 180° hooks at the ends of the top reinforcement and straight reinforcing bars at the bottom of the beams would ease the reinforcement congestion and simplify the construction process.
- Other support design options should be considered to avoid excessive congestion of reinforcement and sleeves inside the formwork.
- For inserts, other designs should be considered. An example would be to use inserts made out of insulation foam that would stay inside the concrete, thus reducing labor and providing more thermal insulation to the slab.
- It is recommendable to properly consider the prewetting of the LWA to achieve a consistency in the moisture content of it.

- Lifting the slab with the same configuration it was designed is recommended to avoid inaccurate data.
- To avoid excessive vacuum force, it is recommended to use a stronger bond breaker between the slab and the casting floor. This can be achieved by laying a thin layer of sand or allowing for more voids in the slab to allow air to flow underneath it.

Chapter 6: References

"ACI 318-19, Building Code Requirements for Structural Concrete," American Concrete Institute, Farmington Hills, MI.

"ACI 318-19, Commentary on Building Code Requirements for Structural Concrete," American Concrete Institute, Farmington Hills, MI.

"ACI 211.2-98, Standard Practice for Selecting Proportions for Structural Lightweight Concrete," American Concrete Institute, Farmington Hills, MI.

"ACI 421.3R-15, Guide to Design of Reinforced Two-Way Slab Systems," American Concrete Institute, Farmington Hills, MI.

"ASCE 7-16, Minimum Design Loads and Associated Criteria for Buildings and Other Structures," American Society of Civil Engineers, Reston, VA

Ahmad, M. S., Tuan Abdullah, J. Y., & Mannan, M. A. (2008). Effect of Aggregate Type on the Properties of Lightweight Concrete. In Proceedings of the 2008 International Symposium on Advances in Concrete Technology (pp. 627-634).

Darwin, D. (2020). Design of Concrete Structures (16th ed.). McGraw-Hill Higher Education.

EPA. (1993). AP-42, CH 11: Mineral Products Industry. US EPA. https://www.epa.gov/sites/default/files/2020-10/documents/c11s20.pdf

Gannon, J. R., & O'Brien, D. J. (2000). Design and Construction of Post-Tensioned Slabs-on-Ground. Concrete International, 22(7), 53-59.

Gao, X., Lo, Y., & Tam, C. (2002). Investigation of micro-cracks and microstructure of high performance lightweight aggregate concrete. Building and Environment, 37(5), 485-489.

Gomes, L., de Brito, J., & Alves, R. (2017). Precast Concrete Construction: A Review. Engineering Structures, 132, 259-267.

Graybeal, R. T. (2006). Precast Concrete Systems in Architectural Engineering. Journal of Architectural Engineering, 12(1), 1-8.

Moldovan, I., & Mathe, A. (2016). A Study on a Two-Way Post-Tensioned Concrete Waffle Slab. Procedia Technology, 22, 227-234.

Naaman, A. E. (2002). Engineered Lightweight Concrete. ACI Materials Journal, 99(5), 417-424.

Phang, W. W., & Phang, K. S. (2014). Analysis and Design of Post-Tensioned Concrete Slabs. International Journal of Structural Stability and Dynamics, 14(4).

Skupien, P. (2019). Composite Slab Made from Precast, Pre-Tensioned Concrete Planks and Lightweight Concrete. IOP Conference Series. Materials Science and Engineering, 471(5), Article 052055.

Szydłowski, R., & Mieszcak, M. (2017). Study of Application of Lightweight Aggregate Concrete to Construct Post-tensioned Long-span Slabs. Procedia Engineering, 172, 1077-1085.

Szydłowski, R., & Łabuzek, B. (2021). Experimental Evaluation of Shrinkage, Creep and Prestress Losses in Lightweight Aggregate Concrete with Sintered Fly Ash. Materials, 14(14), Article 3895.

Thienel, K., Haller, T., & Beuntner, N. (2020). Lightweight Concrete-From Basics to Innovations. Materials, 13(5), 1120.

Turner-Fairbank Highway Research Center issuing body. (2013). Lightweight Concrete: Mechanical Properties.

Wang, X., Fang, C., Kuang, W., Li, D., Han, N., & Xing, F. (2017). Experimental investigation on the compressive strength and shrinkage of concrete with pre-wetted lightweight aggregates. Construction & Building Materials, 155, 867-879.

Wendling, A., Sadhasivam, K., & Floyd, R. (2018). Creep and shrinkage of lightweight self-consolidating concrete for prestressed members. Construction & Building Materials, 167, 205-215.

Yang, K.-H., Mun, J.-H., & Kim, G.-H. (2013). Flexural Behavior of Post-tensioned Normal-strength Lightweight Concrete One-way Slabs. Engineering Structures, 56, 1295-1307.

Chapter 7: Appendix

Appendix A: Reinforcement Plan & Tendon Plan for scaled prototype.

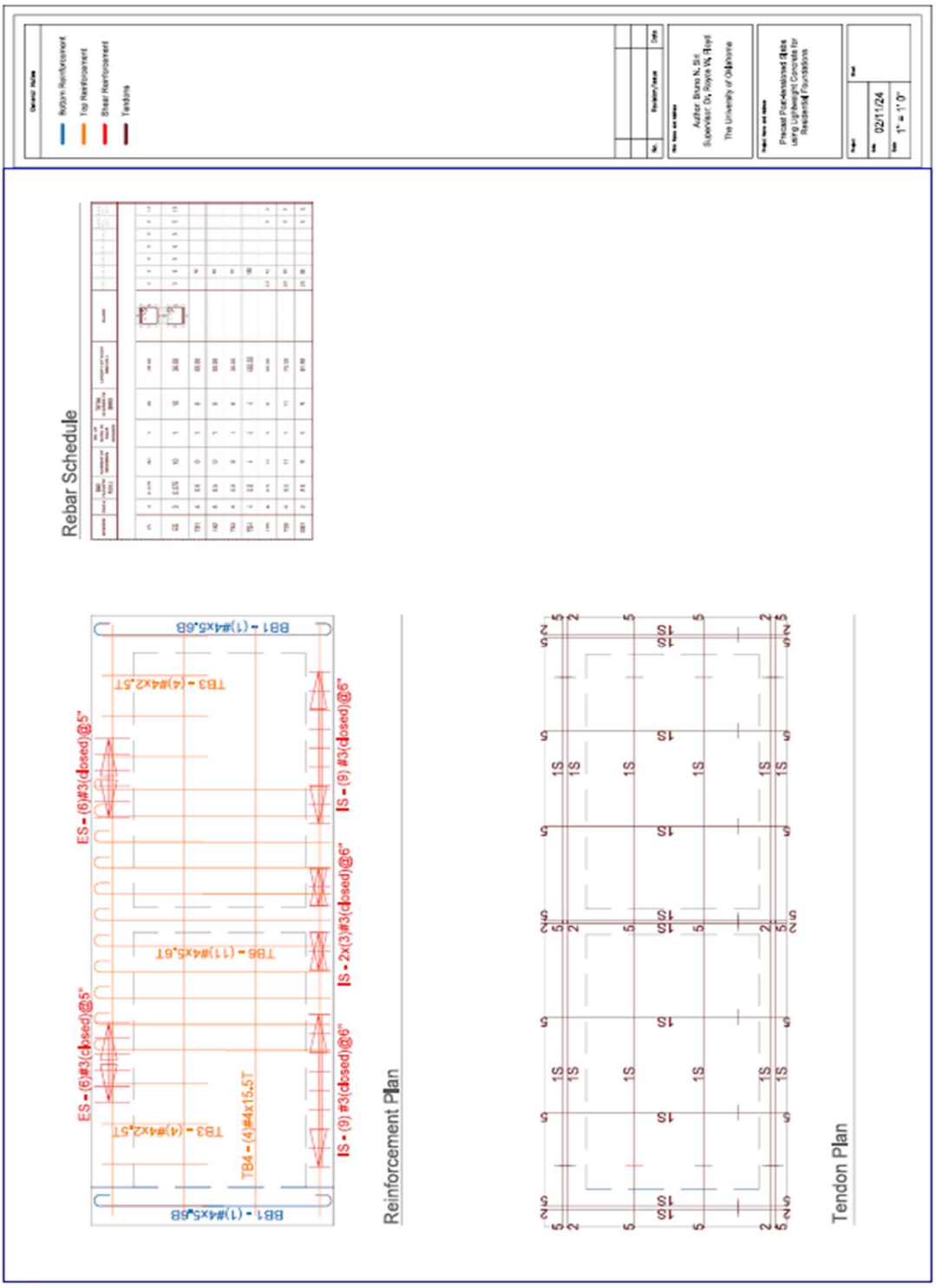

Appendix B: Reinforcement Plan for full-scale prototype

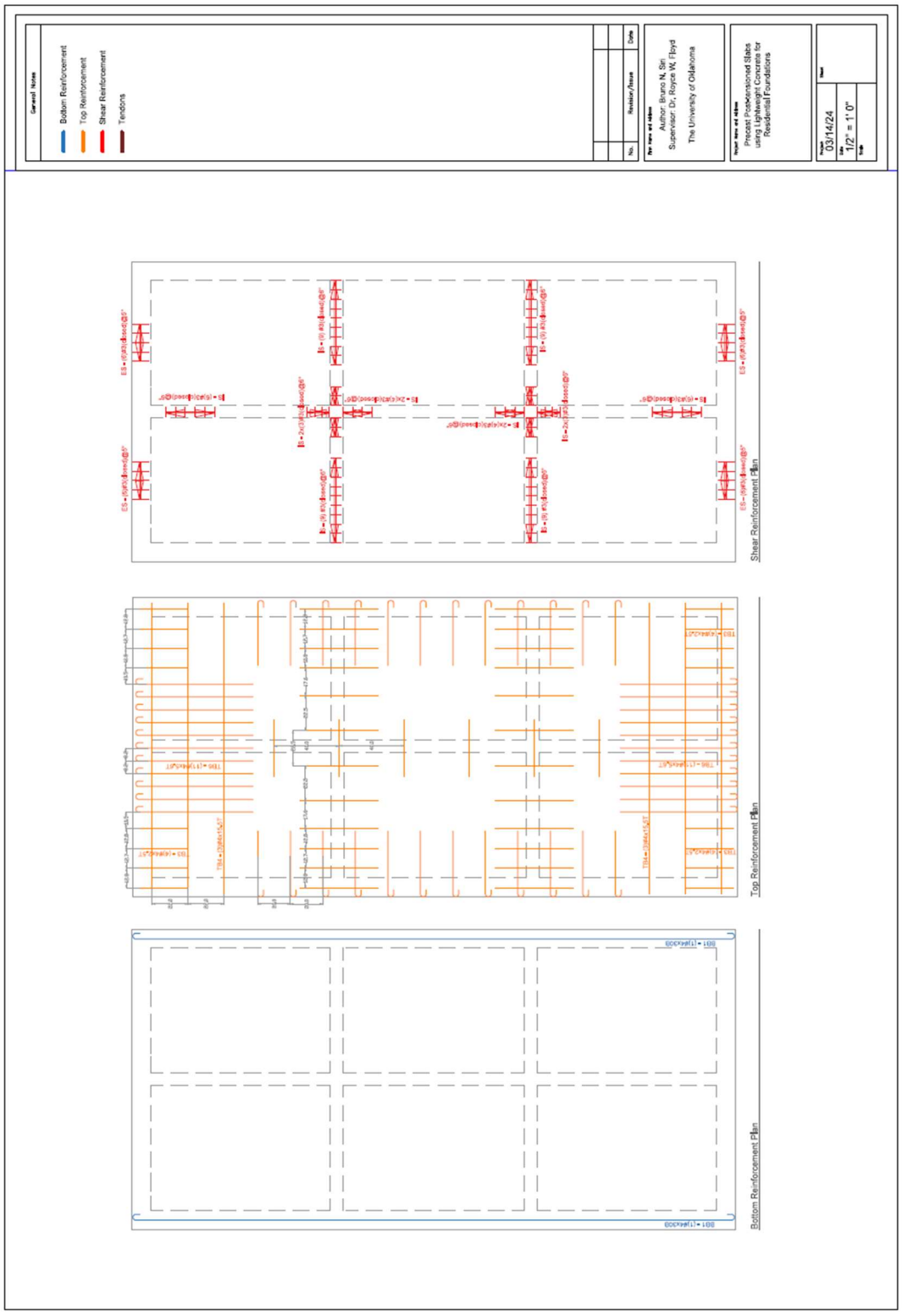

Appendix C: Tendon Plan for full-scale prototype

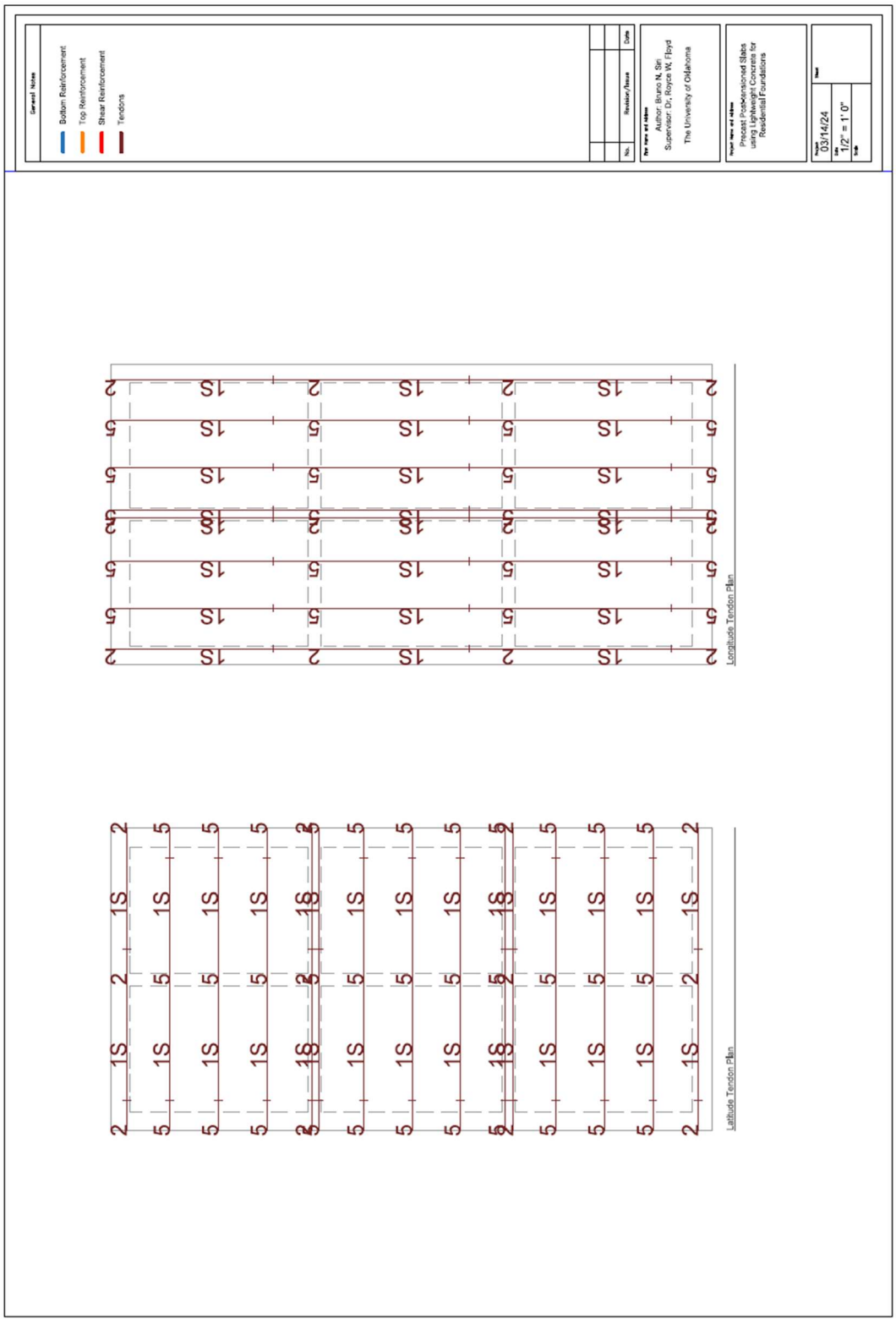

Appendix D: Reinforcement Bar schedule for scale prototype

SLAB PROTOTYPE 16 ft x 6 ft - Rebar Schedule														
MEMBER	BAR #	BAR DIAMETER (in.)	NUMBER OF MEMBERS	No. OF BARS IN EACH MEMBER	TOTAL NUMBER OF BARS	LENGTH OF EACH BAR (in.)	SHAPE	A (in.)	B (in.)	C (in.)	D (in.)	E (in.)	Curve Peri. (in.)	Bend Dia. (in.)
IS	3	0,375	30	1	30	28,00		3	5	5	5	5	5	1,5
ES	3	0,375	10	1	10	36,00		3	9	5	9	5	5	1,5
SBE	3	0.375	8	1	8	30.00			30					
SBI	3	0.375	4	1	4	168.00			168					
TB1	4	0,5	0	1	0	00,00			36					
TB2	4	0,5	0	1	0	00,00			48					
TB3	4	0.5	8	1	8	30.00			30					
TB4	4	0.5	4	1	4	186.00			186					
TB5	4	0,5	0	1	0	00,00		2,5	42				5	3
TB6	4	0,5	11	1	11	73,50	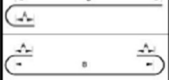	2,5	66				5	3
BB1	4	0.5	2	1	2	81.00		2,5	66				5	3

TOTAL LENGTH OF #3 BARS	2112	in
	176	ft
	8.8	20' bars

TOTAL LENGTH OF #4 BARS	1955	in
	162.9	ft
	8.14	20' bars

Appendix E: Reinforcement Bar schedule for full-scale prototype

SLAB PROTOTYPE 16 ft x 31 ft - Rebar Schedule

MEMBER	BAR #	BAR DIAMETER (in.)	NUMBER OF MEMBERS	No. OF BARS IN EACH MEMBER	TOTAL NUMBER OF BARS	LENGTH OF EACH BAR (in.)	SHAPE	A (in.)	B (in.)	C (in.)	D (in.)	E (in.)	Curve Peri. (in.)	Bend Dia. (in.)
IS	3	0.375	80	1	80	28.00		3	5	5	5	5	5	1.5
ES	3	0.375	20	1	20	36.00		3	9	5	9	5	5	1.5
SBX	3	0.375	16	1	16	180.00			180					
SBY	3	0.375	16	1	16	72.00			72					
TB1	4	0.5	6	1	6	36.00			36					
TB2	4	0.5	24	1	24	48.00			48					
TB3	4	0.5	16	1	16	30.00			30					
TB4	4	0.5	6	1	6	186.00			186					
TB5	4	0.5	24	1	24	49.50		2.5	42				5	3
TB6	4	0.5	11	1	11	79.50		2.5	72				5	3
BB1	4	0.5	2	2	4	381.00		2.5	366				5	3

TOTAL LENGTH OF #3 BARS	6992	in
	582.7	ft
	29.13	20' bars

TOTAL LENGTH OF #4 BARS	6551	in
	545.9	ft
	27	20' bars

Appendix F: Supports Plan

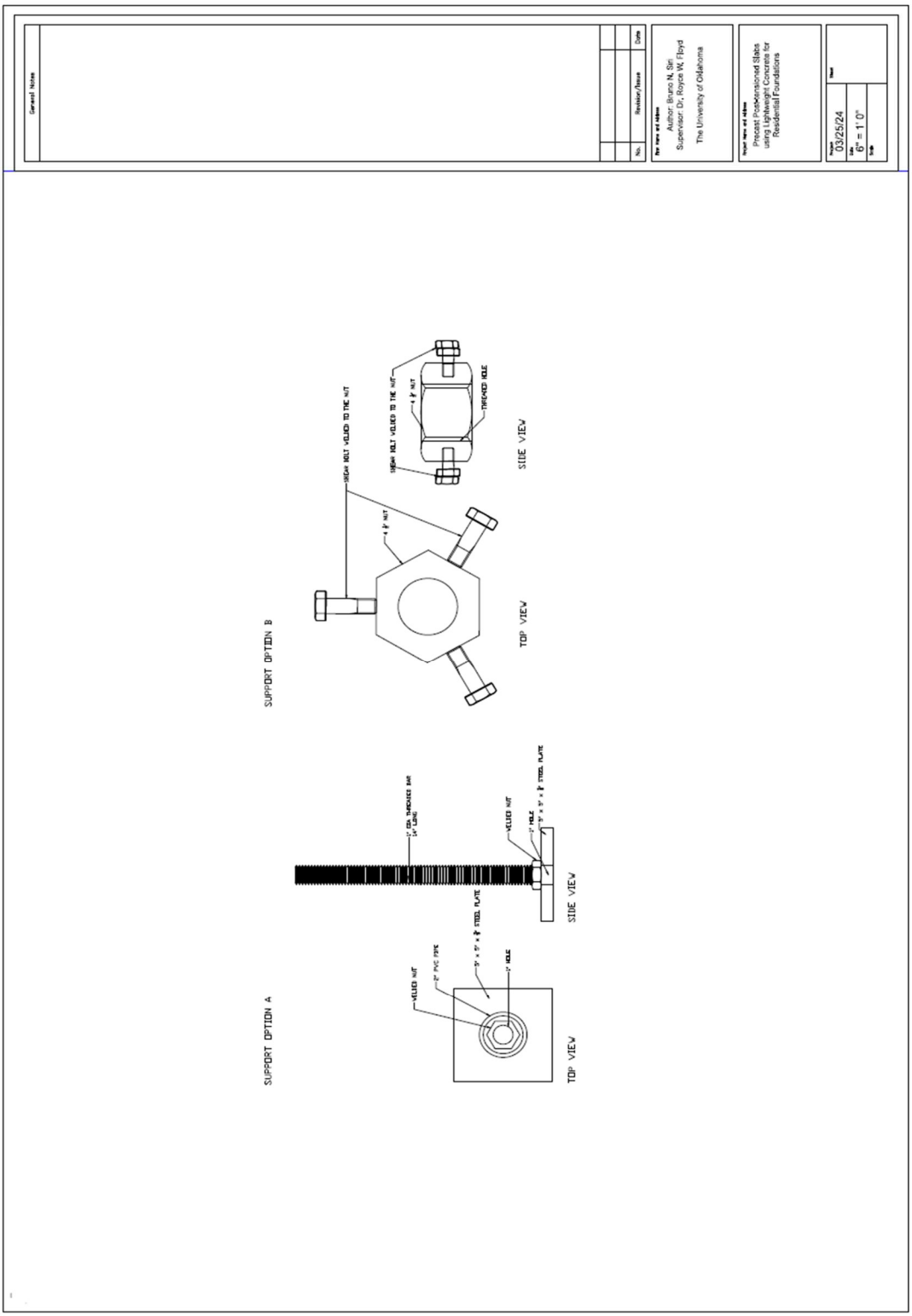

Appendix G: VWSGs Plan location for scaled and full-scale prototype

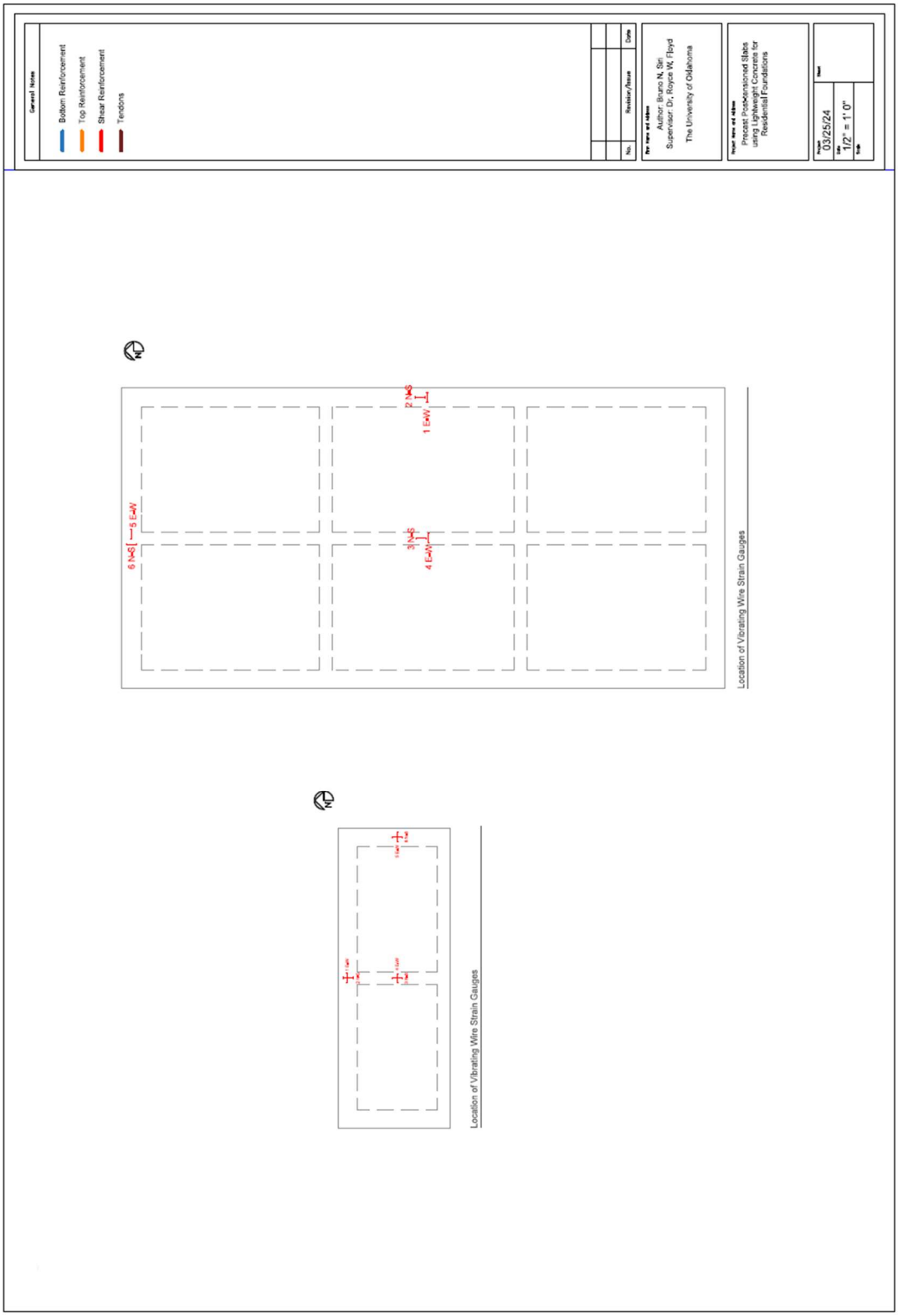

Appendix H: Sequence of post-tensioning for scale prototype

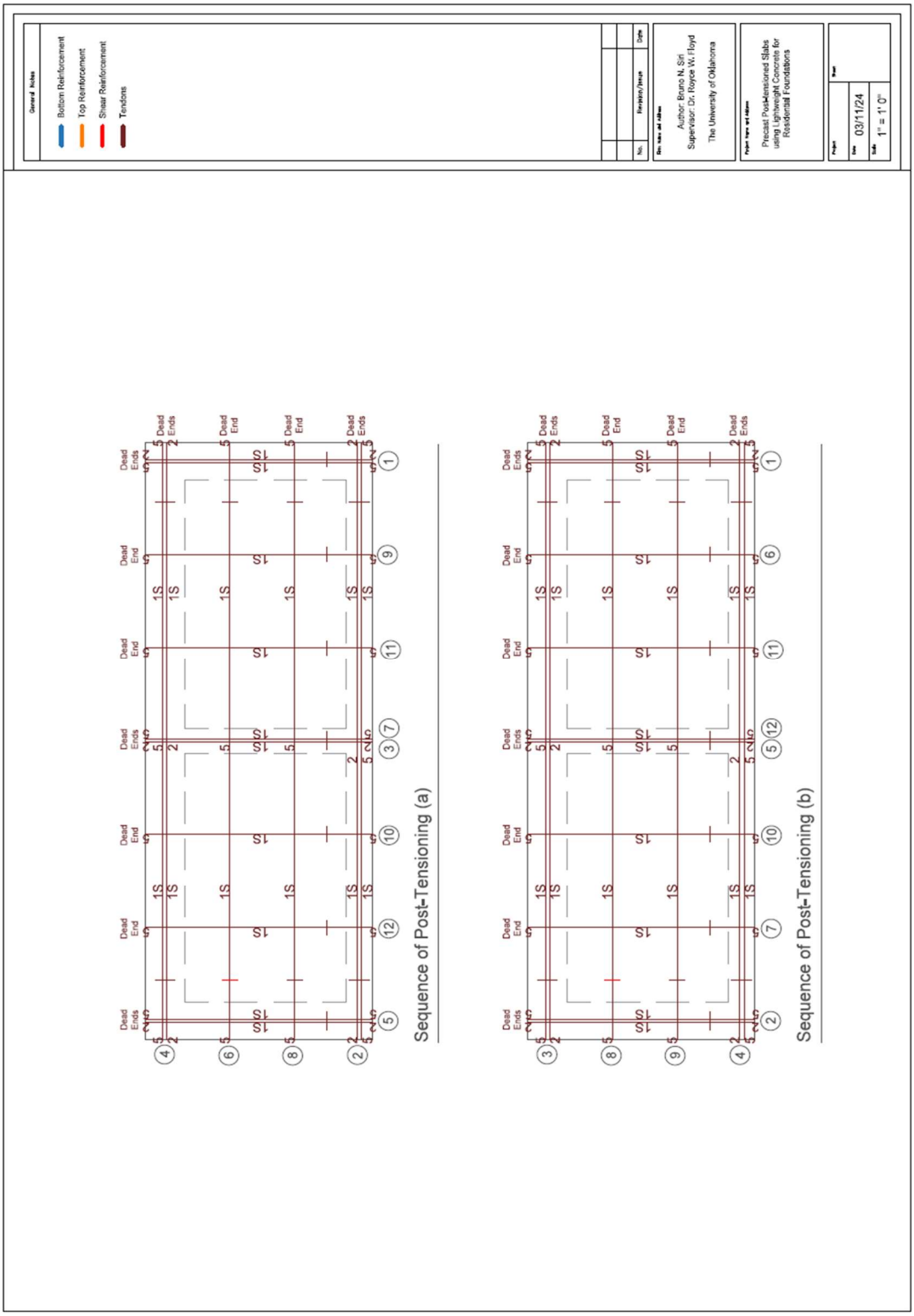

Appendix I: Sequence of post-tensioning for full-scale prototype

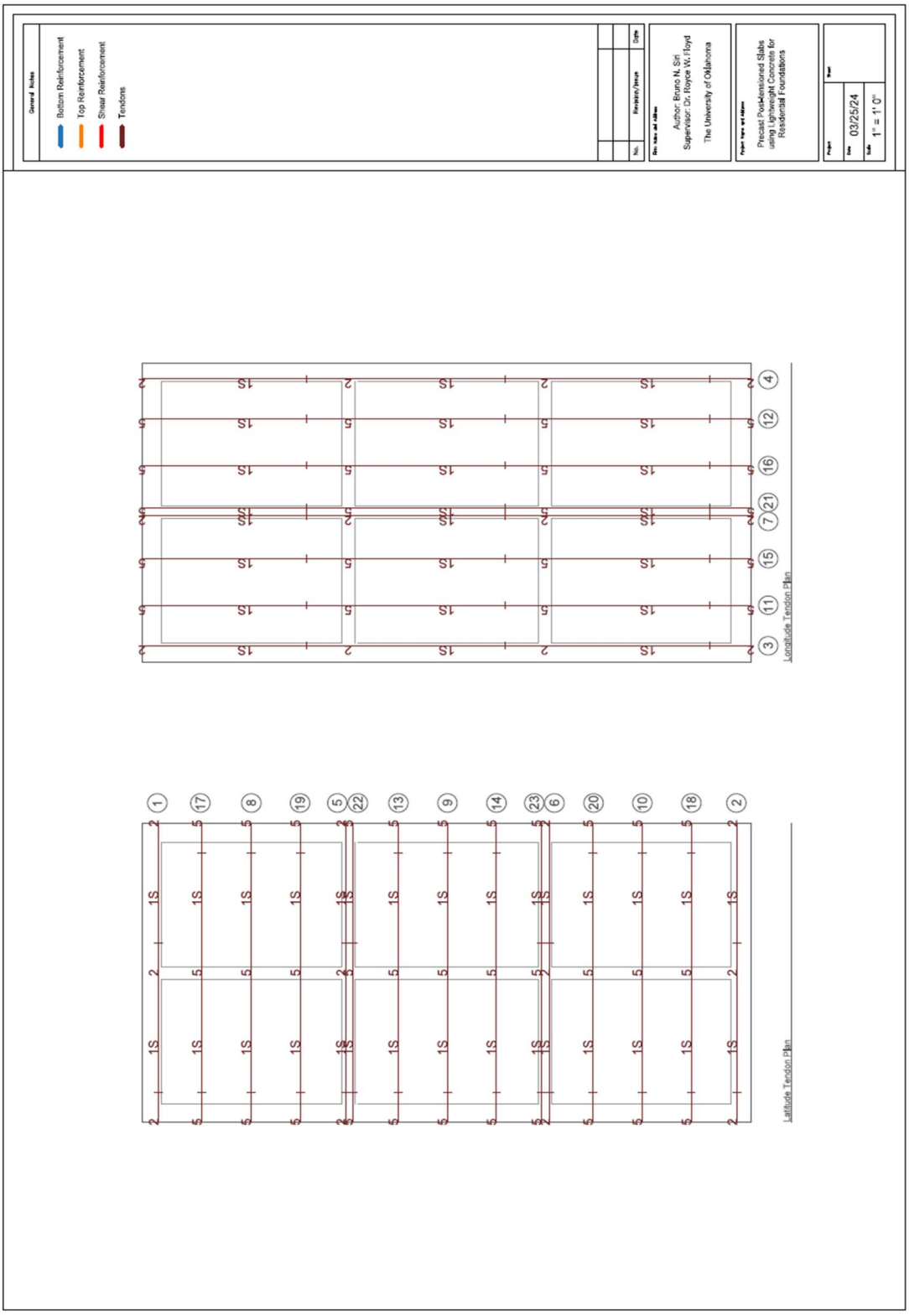

Appendix J: Mix Proportions of trial batches using Livingston LWA

Mix Proportion (SSD) of Livingston trial batches														
Mix Proportion (SSD)	**L1**	**L2**	**L3**	**L4**	**L5**	**L6**	**L7**	**L8**	**L9**	**L10**	**L11**	**L12**	**L13**	**L14**
w/c	0.48	0.48	0.52	0.55	0.55	0.55	0.55	0.55	0.55	0.55	0.55	0.55	0.55	0.55
Material	Weight (lb)													
Cement	760.4	760.4	653.8	609.0	609.0	727.0	636.0	609.0	609.1	600.0	609.0	609.0	609.0	609.0
LWA	832.0	832.0	832.0	832.0	832.0	802.0	832.0	832.0	756.0	725.8	718.0	718.0	718.0	718.0
Sand	1043.0	1043.0	1198.0	1248.0	1248.0	1255.0	1410.0	1248.0	1401.2	1483.1	1478.0	1478.0	1478.0	1478.0
Water	365.0	365.0	340.0	335.0	335.0	400.0	350.0	335.0	335.0	330.0	335.0	335.0	335.0	335.0
Air%	0.025	0.025	0.025	0.025	0.025	0.025	0.025	0.025	0.025	0.025	0.025	0.025	0.025	0.025
Total	3000.4	3000.4	3023.8	3024.0	3024.0	3184.0	3228.0	3024.0	3101.3	3138.9	3140.0	3140.0	3140.0	3140.0
Material	Volume (ft^3)													
Cement	3.87	3.87	3.33	3.10	3.10	3.70	3.24	3.10	3.10	3.05	3.10	3.10	3.10	3.10
LWA	10.25	10.25	10.25	10.25	10.25	8.57	8.88	10.25	9.32	8.95	8.85	8.85	8.85	8.85
Sand	6.36	6.36	7.30	7.61	7.61	7.65	8.59	7.61	8.54	9.04	9.00	9.00	9.00	9.00
Water	5.85	5.85	5.45	5.37	5.37	6.41	5.61	5.37	5.37	5.29	5.37	5.37	5.37	5.37
Air%	0.68	0.68	0.68	0.68	0.68	0.68	0.68	0.68	0.68	0.68	0.68	0.68	0.68	0.68
Total	27.0	27.0	27.0	27.0	27.0	27.0	27.0	27.0	27.0	27.0	27.0	27.0	27.0	27.0
Calculated Unit Weight	111.1	111.1	112.0	112.0	112.0	117.9	119.6	112.0	114.9	116.3	116.3	116.3	116.3	116.3

Appendix K: Equivalent Frame Method spreadsheet sample

Input	Value	Units
A-D Dimension	31	ft
1-3 Dimension	16	ft
A-D # Mech	5	
1-3 # Mech	3	
Edge Distance	0.5	ft
A-E Spacing, y	7.5	ft
1-6 Spacing, x	7.5	ft
Slab Thickness	6	in.
Lift	6	in.
Lift	0.500	ft
Capital Thickness	0	in.
Capital Dimension	0	in.
Capital Dimension	0.000	ft
Support Dimension	4.75	in.
Support Dimension	0.396	ft
Interior Beam Depth	6	in.
Interior Beam Width	6	in.
Interior Beam, A	36	in^2
Interior Beam, y'	1	in.
Interior Beam, I	252	in^4
Exterior Beam Depth	12	in.
Exterior Beam Width	6	in.
Exterior Beam, A	72	in^2
Exterior Beam, y'	3	in.
Exterior Beam, I	4320	in^4
Lifting Bolt Size	1.5	in.
f'_c	4000	psi
E_c	3605	ksi
E_s	29000	ksi
f_y rebar	60000	psi
f_{pc} targeted	125	psi
Strand Diameter, d_{ps}	0.5	in.
Strand Area, A_{ps}	0.153	in^2
Effective Prestress, f_{se}	175,000	psi
Slab top to cable cg (support)	4	in.
Slab bot. to cable cg (end)	2	in.
Slab bot. to cable cg (ms)	2	in.

# Stories	1	
Lettered Lines	Span 1-2	Span 2-3
Roof DL, psf	10	10
Ceiling DL, psf	5	5
1st Floor DL, psf	100	100
Roof LL, psf	20	20
Ceiling LL, psf	0	0
1st Floor LL, psf	40	40
2nd Floor LL, psf	40	40

Numbered Lines	Span A-B	Span B-C	Span C-D
Roof DL, psf	10	10	10
Ceiling DL, psf	5	5	5
1st Floor DL, psf	100	100	100
Roof LL, psf	20	20	20
Ceiling LL, psf	0	0	0
1st Floor LL, psf	40	40	40
2nd Floor LL, psf	40	40	40

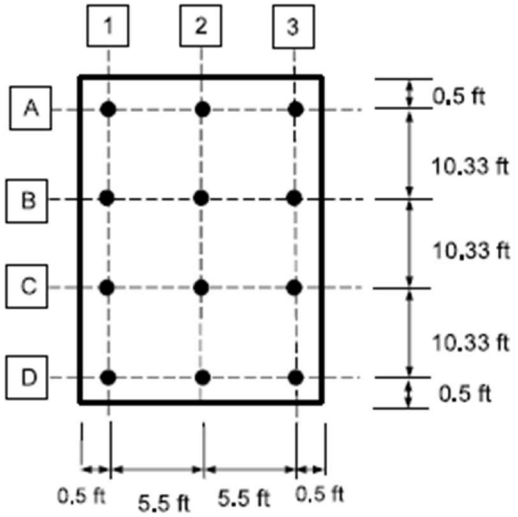

Lettered Column Lines

		Bay Location	A/1-2	A/2-3	B/1-2	B/2-3
		Int/end	end	end	end	end
		full/edge	edge	edge	full	full
	1	Slab Thickness, h (in.)	6	6	6	6
	2	Dead Load (psf)	115	115	115	115
	3	Live Load (psf)	100	100	100	100
	4	Capital Width, b (in.)	0	0	0	0
	5	Capital Depth, d (in.)	0	0	0	0
	6	C_1 (in.)	4.75	4.75	4.75	4.75
	7	C_2 (in.)	4.75	4.75	4.75	4.75
	8	Bolt diameter, D (in.)	1.5	1.5	1.5	1.5
	9	L_1 (ft)	7.5	7.5	7.5	7.5
	10	L_2 (ft)	4.25	4.25	7.5	7.5
	11	L_n (ft)	7.10	7.10	7.10	7.10
	12	story height, L_c (ft)	0.25	0.25	0.25	0.25
	13	Column Unbraced, L_u (ft)	0.50	0.50	0.50	0.50
	14	w_c slab (ksf)	0.298	0.298	0.298	0.298
	15	w slab (ksf)	0.215	0.215	0.215	0.215
	16	w_d slab (ksf)	0.115	0.115	0.115	0.115
	17	w_{sw} slab (psf)	215.0	215.0	215.0	215.0
	18	w_{sd} slab (psf)	0.0	0.0	0.0	0.0
	19	$M_{o/b} = w_{sd}l_2L_n^2/8$ (ft-k)	7.99	7.99	14.10	14.10
	20	$M_{o/s} = wL_n^2/8$ (ft-k)	5.76	5.76	10.17	10.17
	21	$M_{o/d} = w_dL_n^2/8$ (ft-k)	3.08	3.08	5.44	5.44
	22	$I_s = L_2h^3/12$ (in^4)	918.00	918.00	1620.00	1620.00
	23	I_b (in^4)	4320.00	4320.00	252.00	252.00
	24	A_{cs} (in^2)	342.00	342.00	540.00	540.00
	25	y'_{cb} (in.)	8.16	8.16	3.00	3.00
	26	I_{cs} (in^4)	2200.74	2200.74	1620.00	1620.00
	27	$I_c = \pi*(D/2)^4/4$ (in^4)	0.25	0.25	0.25	0.25
	28	$C = n(1-0.63x/y)(x^3y/3)$	107.44	107.44	107.44	107.44
	29	$K_{sb} = 4EI_s/L_1$	382921	382921	281875	281875
	30	$K_c = 4EI_c/L_c$	4804	4804	4804	4804
	31	$K_b = 4EI_b/L_1$	692159.33	692159.33	40375.96	40375.96
	32	$K_t = \Sigma(9*E_{cs}*C/(l_2*(1-C_2/L_2)^3))$	64297334	64297334	91147	91147
	33	$K_{ec} = 1/(1/\Sigma K_t + 1/K_c)$	4804	4804	4564	4564
	34	$\alpha_{ft} = E_{cs}/E_{cs}$	4.71	1.81	0.14	0.14
	35	L_c/L_1	0.57	0.57	1.00	1.00
	36	$\alpha_{ft}(L2/L1)$	2.67	1.02	0.14	0.14
	37	β_b = LL/DL	0.87	0.87	0.87	0.87
Max Factored M_{max}	38	M_{max}^- (left) (kip-ft)	1.17	8.14	2.10	14.54
	39	M_{max}^+ (kip-ft)	4.61	3.64	8.13	6.42
	40	M_{max}^- (right) (kip-ft)	8.15	2.74	14.36	4.84
Max Service M	41	M (left) (kip-ft)	0.98	5.87	1.75	10.35
	42	M^+ (kip-ft)	3.65	3.04	6.45	5.35
	43	M (right) (kip-ft)	5.88	2.28	10.36	4.03
Net Service M_{ser}	44	M_{ser}^- (left) (kip-ft)	0.31	5.87	0.58	10.35
	45	M_{ser}^+ (kip-ft)	3.33	2.54	5.87	4.49
	46	M_{ser}^- (right) (kip-ft)	5.88	1.89	10.36	3.35
Net Service Stress f	47	f_c (left) (psi)	-350	-350	-198	-198
	48	f_c (mid) (psi)	-350	-350	-198	-198
	49	f_c (right) (psi)	-350	-350	-198	-198
	50	support limit $6*sqrt(f'_c)$	379	379	379	379
	51	midspan limit $2*sqrt(f'_c)$	126	126	126	126
Balanced Service M_{bal}	52	M_{bal}^- (left) (kip-ft)	0.00	0.00	0.00	0.00
	53	M_{bal}^+ (kip-ft)	0.00	0.00	0.00	0.00
	54	M_{bal}^- (right) (kip-ft)	0.00	0.00	0.00	0.00
Primary Moment $M_1 = P_u e$	55	M_1^- (left) (kip-ft/ft)	-2.10	-2.10	-1.19	-1.19
	56	M_1^+ (kip-ft/ft)	2.10	2.10	1.19	1.19
	57	M_1^- (right) (kip-ft/ft)	-2.10	-2.10	-1.19	-1.19
Secondary Moment $M_1 = P_u e$	58	M_s^- (left) (kip-ft)	8.93	8.93	8.93	8.93
	59	M_s^+ (kip-ft)	-8.93	-8.93	-8.93	-8.93
	60	M_s^- (right) (kip-ft)	8.93	8.93	8.93	8.93
Design Moment M_u	61	**M_u^- (left) (kip-ft)**	**-7.75**	**-0.79**	**-6.82**	**5.42**
	62	**M_u^+ (kip-ft)**	**13.54**	**12.57**	**17.05**	**15.35**
	63	**M_u^- (right) (kip-ft)**	**-5.39**	**-9.83**	**-2.69**	**-10.51**
	64	n strands in column strip	2	2	2	2
	65	n strands in middle strip	2	2	2	2
	66	Basic Deflection, δ' (in.)	0.0039	0.0039	0.0039	0.0039
	67	Column Strip, δ_c (in.)	0.0039	0.0039	0.0039	0.0039
	68	Middle Strip, δ_s (in.)	0.0039	0.0039	0.0039	0.0039
	69	Rotation at Left End, θ_a (rad)	0.0008	0.0147	0.0015	0.0272
	70	Rotation at Right End, θ_b (rad)	0.0147	0.0047	0.0272	0.0088
	71	Rotation Deflection, δ'' (in.)	0.174	0.218	0.324	0.405
	72	Net column Strip, δ_{cp} (in.)	0.178	0.222	0.328	0.409
	73	Net Middle Strip, δ_{sp} (in.)	0.178	0.222	0.328	0.409
	74	Central Deflection, Δ (in.)	**0.347**	**0.398**	**0.497**	**0.585**
	75	Long Term Deflection, Δ_{lt} (in.)	0.929	1.065	1.330	1.566
	76	Deflection Limit, L/480 (in.)	0.1875	0.1875	0.1875	0.1875
	77	Short-Term Check	NG	NG	NG	NG
	78	Long-Term Check	NG	NG	NG	NG

Numbered Column Lines

		Bay Location	1/A-B	1/B-C	1/C-D	2/A-B	2/B-C	2/C-D
		Int/end	end	int	end	end	int	end
		full/edge	edge	edge	edge	full	full	full
	1	Slab Thickness, h (in.)	6	6	6	6	6	6
	2	Dead Load (psf)	115	115	115	115	115	115
	3	Live Load (psf)	100	100	100	100	100	100
	4	Capital Width, b (in.)	0	0	0	0	0	0
	5	Capital Depth, d (in.)	0	0	0	0	0	0
	6	C_1 (in.)	4.75	4.75	4.75	4.75	4.75	4.75
	7	C_2 (in.)	4.75	4.75	4.75	4.75	4.75	4.75
	8	Bolt diameter, D (in.)	1.5	1.5	1.5	1.5	1.5	1.5
	9	L_1 (ft)	7.5	7.5	7.5	7.5	7.5	7.5
	10	L_2 (ft)	4.25	4.25	4.25	7.5	7.5	7.5
	11	L_n (ft)	7.10	7.10	7.10	7.10	7.10	7.10
	12	story height, L_c (ft)	0.25	0.25	0.25	0.25	0.25	0.25
	13	Column Unbraced, L_u (ft)	0.50	0.50	0.50	0.50	0.50	0.50
	14	w_c slab (ksf)	0.298	0.298	0.298	0.298	0.298	0.298
	15	w slab (ksf)	0.215	0.215	0.215	0.215	0.215	0.215
	16	w_d slab (ksf)	0.115	0.115	0.115	0.115	0.115	0.115
	17	w_{sw} slab (ksf)	215.0	215.0	215.0	215.0	215.0	215.0
	18	w_{sd} slab (psf)	0.0	0.0	0.0	0.0	0.0	0.0
	19	$M_{o/b} = w_{sd}l_2L_n^2/8$ (ft-k)	7.99	7.99	7.99	14.10	14.10	14.10
	20	$M_{o/s} = wL_n^2/8$ (ft-k)	5.76	5.76	5.76	10.17	10.17	10.17
	21	$M_{o/d} = w_dL_n^2/8$ (ft-k)	3.08	3.08	3.08	5.44	5.44	5.44
	22	$I_s = L_2h^3/12$ (in^4)	918.00	918.00	918.00	1620.00	1620.00	1620.00
	23	I_b (in^4)	4320.00	4320.00	4320.00	252.00	252.00	252.00
	24	A_{cs} (in^2)	342.00	342.00	342.00	540.00	540.00	540.00
	25	y'_{cb} (in.)	8.16	8.16	8.16	3.00	3.00	3.00
	26	I_{cs} (in^4)	2200.74	2200.74	2200.74	1620.00	1620.00	1620.00
	27	$I_c = \pi*(D/2)^4/4$ (in^4)	0.25	0.25	0.25	0.25	0.25	0.25
	28	$C = n(1-0.63x/y)(x^3y/3)$	107.44	107.44	107.44	107.44	107.44	107.44
	29	$K_{sb} = 4EI_s/L_1$	382921	382921	382921	281875	281875	281875
	30	$K_c = 4EI_c/L_c$	4804	4804	4804	4804	4804	4804
	31	$K_b = 4EI_b/L_1$	692159.33	692159.33	692159.33	40375.96	40375.96	40375.96
	32	$K_t = \Sigma(9*E_{cs}*C/(l_2*(1-C_2/L_2)^3))$	64297334	64297334	64297334	91147	91147	91147
	33	$K_{ec} = 1/(1/\Sigma K_t + 1/K_c)$	4804	4804	4804	4564	4564	4564
	34	$\alpha_{ft} = E_{cs}/E_{cs}$	4.71	4.71	4.71	0.16	0.16	0.16
	35	L_c/L_1	0.57	0.57	0.57	1.00	1.00	1.00
	36	$\alpha_{ft}(L2/L1)$	2.67	2.67	2.67	0.16	0.16	0.16
	37	β_b = DL/LL	0.87	0.87	0.87	0.87	0.87	0.87
Max Factored M_{max}	38	M_{max}^- (left) (kip-ft)	1.61	7.07	6.36	1.61	7.07	6.36
	39	M_{max}^+ (kip-ft)	4.87	3.05	4.07	4.87	3.05	4.07
	40	M_{max}^- (right) (kip-ft)	7.14	6.26	3.31	7.14	6.26	3.31
Max Service M	41	M (left) (kip-ft)	1.34	5.46	4.94	1.34	5.46	4.94
	42	M^+ (kip-ft)	3.80	2.54	3.37	3.84	2.54	3.37
	43	M (right) (kip-ft)	5.52	4.90	2.74	5.49	4.90	2.74
Net Service M_{ser}	44	M_{ser}^- (left) (kip-ft)	0.68	5.10	4.59	0.68	5.10	4.59
	45	M_{ser}^+ (kip-ft)	3.48	1.62	2.94	3.51	1.62	2.94
	46	M_{ser}^- (right) (kip-ft)	5.22	4.51	2.39	5.35	4.51	2.39
Net Service Stress f	47	f_c (left) (psi)	-350	-350	-350	-198	-198	-198
	48	f_c (mid) (psi)	-350	-350	-350	-198	-198	-198
	49	f_c (right) (psi)	-350	-350	-350	-198	-198	-198
	50	support limit $6*sqrt(f'_c)$	379	379	379	379	379	379
	51	midspan limit $2*sqrt(f'_c)$	126	126	126	126	126	126
Balanced Service M_{bal}	52	M_{bal}^- (left) (kip-ft)	0.00	0.00	0.00	0.00	0.00	0.00
	53	M_{bal}^+ (kip-ft)	0.00	0.00	0.00	0.00	0.00	0.00
	54	M_{bal}^- (right) (kip-ft)	0.00	0.00	0.00	0.00	0.00	0.00
Primary Moment $M_1 = P_u e$	55	M_1^- (left) (kip-ft)	-2.10	-2.10	-2.10	-1.19	-1.19	-1.19
	56	M_1^+ (kip-ft)	2.10	2.10	2.10	1.19	1.19	1.19
	57	M_1^- (right) (kip-ft)	-2.10	-2.10	-2.10	-1.19	-1.19	-1.19
Secondary Moment $M_1 = P_u e$	58	M_s^- (left) (kip-ft)	8.93	8.93	8.93	8.93	8.93	8.93
	59	M_s^+ (kip-ft)	-8.93	-8.93	-8.93	-8.93	-8.93	-8.93
	60	M_s^- (right) (kip-ft)	8.93	8.93	8.93	8.93	8.93	8.93
Design Moment M_u	61	**M_u^- (left) (kip-ft)**	**-7.32**	**-1.85**	**-2.56**	**-7.32**	**-1.85**	**-2.56**
	62	**M_u^+ (kip-ft)**	**13.79**	**11.97**	**13.00**	**13.79**	**11.97**	**13.00**
	63	**M_u^- (right) (kip-ft)**	**-6.65**	**-5.71**	**-9.69**	**-6.65**	**-5.71**	**-9.69**
	64	n strands in column strip	2	2	2	2	2	2
	65	n strands in middle strip	2	2	2	2	2	2
	66	Basic Deflection, δ' (in.)	0.0039	0.0039	0.0039	0.0039	0.0039	0.0039
	67	Column Strip, δ_c (in.)	0.0039	0.0039	0.0039	0.0039	0.0039	0.0039
	68	Middle Strip, δ_s (in.)	0.0039	0.0039	0.0039	0.0039	0.0039	0.0039
	69	Rotation at Left End, θ_a (rad)	0.0017	0.0127	0.0115	0.0018	0.0134	0.0121
	70	Rotation at Right End, θ_b (rad)	0.0130	0.0113	0.0060	0.0135	0.0119	0.0063
	71	Rotation Deflection, δ'' (in.)	0.166	0.270	0.196	0.172	0.284	0.206
	72	Net column Strip, δ_{cp} (in.)	0.170	0.274	0.200	0.176	0.288	0.210
	73	Net Middle Strip, δ_{sp} (in.)	0.170	0.274	0.200	0.176	0.288	0.210
	74	Central Deflection, Δ (in.)	**0.347**	**0.602**	**0.528**	**0.398**	**0.698**	**0.619**
	75	Long Term Deflection, Δ_{lt} (in.)	0.929	1.610	1.411	1.065	1.865	1.657
	76	Deflection Limit, L/480 (in.)	0.188	0.188	0.188	0.188	0.188	0.188
	77	Short-Term Check	NG	NG	NG	NG	NG	NG
	78	Long-Term Check	NG	NG	NG	NG	NG	NG

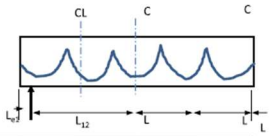

Lettered Column Lines

Bay Location	A/1-2	A/2-3	B/1-2	B/2-3
int/end	end	end	end	end
full/edge	edge	edge	full	full
f_{pc} (psi)	125	125	125	125
Unit F_e (lb/ft)	9000	9000	9000	9000
F_e (lb)	38250	38250	67500	67500
P_e/strand (lb)	26775	26775	26775	26775
# strands for F_e	2	2	3	3
# strands, n	4	4	4	4
cgs pier (in.)	2	2	2	2
cgs mid. (in.)	2	2	2	2
Unit $F_{e,actual}$ (lb/ft)	25200	25200	14280	14280
f_{pc} actual (psi)	350	350	198	198
a (in.)	0	0	0	0
w_{bal} (psf)	0	0	0	0
w_{net} (psf)	215	215	215	215

Numbered Column Lines

Bay Location	1/A-B	1/B-C	1/C-D	2/A-B	2/B-C	2/C-D
int/end	end	int	end	end	int	end
full/edge	edge	edge	edge	full	full	full
f_{pc} (psi)	125	125	125	125	125	125
Unit F_e (lb/ft)	9000	9000	9000	9000	9000	9000
F_e (lb)	38250	38250	38250	67500	67500	67500
P_e/strand (lb)	26775	26775	26775	26775	26775	26775
# strands for F_e	2	2	2	3	3	3
# strands, n	4	4	4	4	4	4
cgs pier (in.)	2	2	2	2	2	2
cgs mid. (in.)	2	2	2	2	2	2
Unit $F_{e,actual}$ (lb/ft)	25200	25200	25200	14280	14280	14280
f_{pc} actual (psi)	350	350	350	198	198	198
a (in.)	0	0	0	0	0	0
w_{bal} (psf)	0	0	0	0	0	0
w_{net} (psf)	215	215	215	215	215	215

	Lettered Column Lines				Numbered Column Lines			
	Edge Column	Edge Midspan	Full Column	Full Midspan	Edge Column	Edge Midspan	Full Column	Full Midspan
M_u (kip-ft)	-0.79	13.54	5.42	17.05	-1.85	13.79	-1.85	13.79
Required M_n (kip-ft)	-0.88	15.04	6.02	18.95	-2.06	15.32	-2.06	15.32
Φ (assumed)	0.9	0.9	0.9	0.9	0.9	0.9	0.9	0.9
Min. A_s (in^2)	0.405		0.405		0.405		0.405	
Bar Area (in^2)	0.2		0.2		0.2		0.2	
No. bars	3		3		3		3	
A_s/ft (in^2/ft)	0.141		0.080		0.141		0.080	
f_{ps} (psi)	187222	189444	188922	192843	187222	189444	188922	192843
ρ_{ps}	0.0060	0.0030	0.0034	0.0017	0.0060	0.0030	0.0034	0.0017
b (in.)	51	51	90	90	51	51	90	90
d (in.)	2	4	2	4	2	4	2	4
F_{ps}/ft (lb/ft)	26960	27280	15416	15736	26960	27280	15416	15736
F_s/ft (lb/ft)	8471		4800		8471		4800	
F_{total} (lb/ft)	35431	27280	20216	15736	35431	27280	20216	15736
a (in.)	0.868	0.669	0.495	0.386	0.868	0.669	0.495	0.386
M_n (k-ft)	19.65	35.42	22.14	37.44	19.65	35.42	22.14	37.44
β_1	0.85	0.85	0.85	0.85	0.85	0.85	0.85	0.85
c (in.)	1.022	0.787	0.583	0.454	1.022	0.787	0.583	0.454
e_t	0.0029	0.0123	0.0073	0.0234	0.0029	0.0123	0.0073	0.0234
Φ	0.722740957	0.9	0.9	0.9	0.722740957	0.9	0.9	0.9
ΦM_n (k-ft)	14.2	31.9	19.9	33.7	14.2	31.9	19.9	33.7
Check	OK	OK	OK	OK	OK	OK	OK	OK